Freiberg On-line
Geosciences Vol. 10

FOG is an electronic journal registered under ISSN 1434-7512.

Groundwater Modeling Taking Into Account Probabilistic Uncertainties

Wahyu Hardyanto

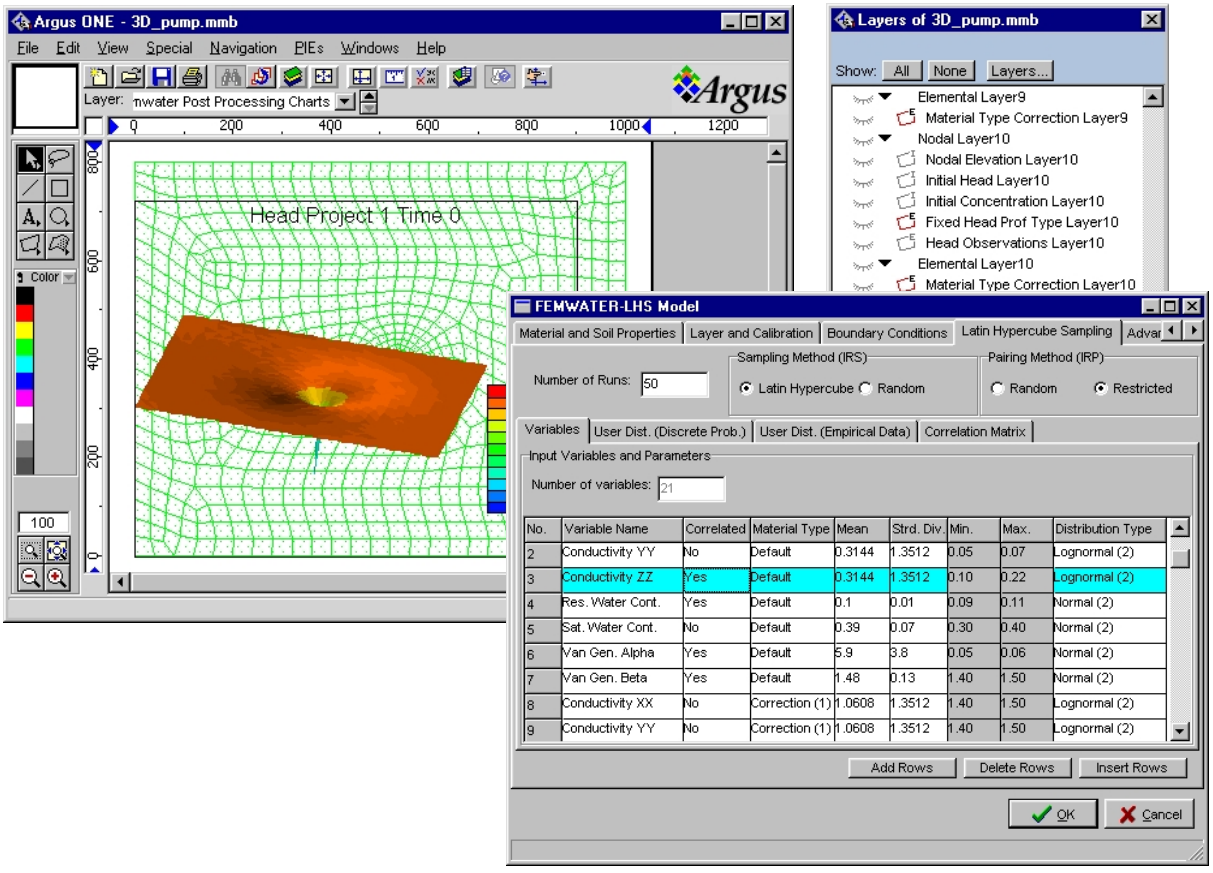

Institut für Geologie / Hydrogeologie
TU Bergakademie Freiberg

Table of contents

List of Symbols 5

Abstract 7

Acknowledgement 8

1. Introduction 9
   1.1 Objectives 13

2. Theory and Methods 14
   2.1 Latin Hypercube Sampling (LHS) 14
      2.1.1 Correlation Control 17
      2.1.2 Description of available parameter distributions 21
   2.2 The Governing Equation of Subsurface Flow 23
   2.3 The Governing Equations of Transport 26
   2.4 Numerical Formulation and Solution of the Equations 29
   2.5 Uncertainty Analysis 34
   2.6 Sensitivity Analysis 36
   2.7 Program Description 39
      2.7.1 General settings 40
         2.7.1.1 FEMWATER-LHS Type of Simulation Problem 41
         2.7.1.2 Model Title and Type 42
         2.7.1.3 Run Control Parameters 43
         2.7.1.4 Iteration Parameters 45
         2.7.1.5 Time Control 46
         2.7.1.6 Output Control 47
         2.7.1.7 Fluid Properties 47
         2.7.1.8 Material and Soil Properties 48
         2.7.1.9 Layer and Calibration 51
         2.7.1.10 Latin Hypercube Sampling 53
      2.7.2. Boundary Conditions 53
         2.7.2.1 Dirichlet Boundary Conditions 54
         2.7.2.2 Cauchy, Neuman and Variable Composite Boundary Conditions 55
         2.7.2.3 Distributed and Point Source/Sink Boundary Conditions 56

3. Verification and Applications 57
   3.1 Verification 57
      3.1.1 The Probabilistic Coverage Provided by LHS 57
      3.1.2 Two-Dimensional Drainage Problem 60
      3.1.3 Two-Dimensional Transport in a Rectangular Region 63
      3.1.4. Saltwater Intrusion in Confined Aquifer (Henry's Problem) 64
   3.2 Applications 67
      3.2.1 Application 1: Steady Drainage to Parallel Drains 72
         3.2.1.1 Problem Description 72
         3.2.1.2 Uncertainty Analysis for Application 1 73
         3.2.1.3 Sensitivity Analysis for Application 1 75
      3.2.2 Application 2: Transient Drainage 76

3.2.2.1 Problem Description 76
3.2.2.2 Uncertainty Analysis for Application 2 78
3.2.2.3 Sensitivity Analysis for Application 2 78
3.2.3 Application 3: 3-Dimensional Flow in an Unconfined Aquifer Subjected to Well Pumping 80
3.2.3.1 Problem Description 80
3.2.3.2 Uncertainty Analysis for Application 3 84
3.2.3.3 Sensitivity Analysis for Application 3 86
3.2.4 Application 4: Seawater Intrusion in Confined Aquifer 86
3.2.4.1 Problem Description 86
3.2.4.2 Uncertainty Analysis for Application 4 87
3.2.4.3 Sensitivity Analysis for Application 4 88

4. Summary and Conclusions 91

5. References 93

Appendix A: CD-ROM - System Requirements and Installation 97

Appendix B: Step-by-step Applications of the FEMWATER-LHS 98

List of Symbols

$[A]$	stiff matrix associated with the advection term;
$a_1, a_2, ..., a_8$	parameters used to describe concentration dependence of water density and dynamic viscosity (L^3/M);
$\{B\}$	load vectors from the boundary conditions;
B_c	Flux boundary;
B_d	Dirichlet boundary;
B_n	Gradient flux boundary;
B_v	variable boundary;
C	material concentration in aqueous phase (M/L^3);
$\{C\}$	a vector whose components are the concentration at all nodes;
C_d	prescribed concentration on the Dirichlet boundary B_d (M/L^3);
C_v	specified concentration on of water through the variable boundary B_v (M/L^3);
C_{in}	concentration in the source(M/L^3);
D	dispersion coefficient tensor (L^2/T);
$[D]$	stiff matrix associated with the dispersion term;
$\{dC/dt\}$	derivative of $\{C\}$ with respect to time;
$\{dH/dt\}$	column vectors containing the values of dH/dt;
$\{G\}$	load vectors from the gravity force;
g	acceleration of gravity (L/T^2);
H	pressure head (L);
$\{H\}$	column vectors containing the values of H at all nodes;
H_d	Dirichlet functional value (L);
h_m	minimum pressure (L) on the variable boundary;
h_p	ponding depth (L) on the variable boundary;
K	coefficient in the Langmuir or Freundlich nonlinear isotherm (L^3/M);
K	hydraulic conductivity tensor (L/T);
$[K]$	stiff matrix associated with all the first-order terms;
k	permeability tensor (L^2);
K_d	distribution coefficient (L^3/M);
k_r	relative permeability or relative hydraulic conductivity (L^2);
$\mathbf{k_s}$	saturated permeability tensor (L^2);
$[M]$	mass matrix resulting from the storage term;
$[M_1]$	mass matrices associated with the material derivative term;
$[M_2]$	mass matrix associated with the partial derivative term;
n	power index in the Freundlich nonlinear isotherm (dimensionless);
n	outward unit vector normal to the boundary;
$\{Q\}$	load vectors from the internal source/sink for flow module or load vector associated with all zero-order derivative terms for transport module;
q	source/sink (L^3/T per L) of water;
q_c	Flux value (L/T);
q_e	evaporation rate (L/T) on the variable boundary;
q_n	Gradient flux value (L/T);
q_p	throughfall of precipitation (L/T) on the variable boundary;
S	concentration in sorbed phase (M/M);
$[S]$	stiffness matrix resulting from the action of conductivity;
S_{max}	maximum concentration in the Langmuir nonlinear isotherm (M/M);
t	time (T);
(x_b,y_b,z_b)	spatial coordinate on the boundary;

z	elevation (L);
α	soil-specific coefficient (1/L);
α_L	longitudinal dispersivity (L);
α_T	lateral dispersivity (L);
α_m	molecular diffusion coefficient (L^2/T);
β, γ	soil-specific exponents (dimensionless);
δ	Kronecker delta tensor;
θ	moisture content (dimensionless);
θ_e	effective moisture content (dimensionless);
θ_s	saturation moisture content (dimensionless);
θ_r	residual moisture content (dimensionless);
λ	decay constant (1/T);
μ	dynamic viscosity of water at chemical concentration C (M/TL);
μ_0	reference dynamic viscosity (M/TL);
ρ	fluid density at chemical concentration C (M/L^3);
ρ_0	reference density (M/L^3);
ρ^*	density of injected fluid (M/L^3);
ρ_b	bulk density of the medium (M/L^3);
τ	tortuosity (L/T);

ABSTRACT

A 3-dimentional finite element groundwater model for density-dependent flow and transport through saturated-unsaturated porous media with stochastic approach (i.e. Latin Hypercube Sampling) FEMWATER-LHS has been developed. This code comes with an Argus ONE™ GUI (Argus Open Numerical Environments Graphical User Interfaces). The combined flow and transport can handle a wide range of real-world problems. The hybrid Lagrangian-Eulerian finite element method was incorporated in the transport module. Four problems were employed for verification by comparing numerical results from the model and from other models. The Latin Hypercube Sampling with the restricted pairing algorithm is used as a tool for sensitivity and uncertainty analysis. Sensitivity and uncertainty analysis are parts of model development, which should be performed within model calibration and before doing any prediction by modeling. To demonstrate the applicability of the model capabilities, the Latin Hypercube Sampling was performed for four applications, analyzing the sensitivity of different models output of FEMWATER-LHS, such as pressure head, flow rate through boundary condition and concentration. Based on this type of analysis the most important input parameters for a certain output can be determined. The analysis of uncertainty propagation associated with input parameters will result in estimation of cumulative distribution function of the model output.

Zusammenfassung

Auf Basis der Finite-Elemente-Methode wurde ein 3-D-Grundwassermodell weiter-entwickelt, das Dichteabhängigkeit berücksichtigt und für gesättigte und ungesättigte poröse Medien gilt. In das Transportmodul ist die Finite-Elemente-Methode mit dem hybriden Lagrange-Euler-Verfahren integriert. Für die Modellkalibrierung sowie die Sensitivitäts- und Unsicherheitsanalyse wurde ein probabilistischer Ansatz, das Latin-Hypercube-Sampling-Verfahren mit restriktem Paarungsalgorithmus, integriert. Die Stärke der Beziehung zwischen Parametern und Ergebnis (Wasserstände, Fließgeschwindigkeit Konzentrationsverteilung) wird durch die Koeffizienten der partiellen oder der Standard-Rangkorrelation ermittelt. Dies ermöglicht die Handhabung eines breiten Spektrums realer Probleme. Eine Verifizierung des Codes wurde erfolgreich an vier Beispielen gezeigt. Die Benutzerfreundlichkeit wurde durch die Entwicklung einer grafischen Oberfläche für Eingabe und Ausgabe garantiert.

ACKNOWLEDGEMENT

The author would like to thank Prof. Dr. habil B. Merkel, his supervisor for the advice, guidance, suggestions and encouragement during the period of this study.

I am grateful to the staff and colleagues of the Department of Hydrogeology, TU Bergakademie Freiberg for their help and contributions. My special appreciation go to Dr. V. Dunger, and Dr. P. Dietrich, Dr. C. Wolkerdorfer, Dr. A. Edet. I wish to also express my thanks to Mr. Qannam, Mr. Lange, Mr. Kolitsch, Mrs. Junghans, Mrs. Planer-Friedrich, Mr. Noubactep, Mr. Berrios, Mr. El Alfi, Mr. Al Mahamid and Mr. Eraifej for their support and faithful discussion during the period of this work.

Special thanks goes to Prof. F. Häfner and Dr. S. Wagner for the advice on the numerical solution of the flow and transport equations. I am also grateful to Prof. H. Schaeben and Dr. G. Meinrath, for the help in better understanding of probabilistic methods.

Argus Interware is acknowledged for providing expertise answers to all the questions posed during this work, the technical assistance provided by Mr. Margolin. The software described herein was developed using Argus ONE™ and Argus PIE technology.

The suggestions for made by Dr. Richard B. Winston (MODFLOW-GUI developer) from USGS (U.S. Geological Survey), especially for always giving prompt answer via email to my questions is highly appreciated. I would also like to thank all those who provided “bug-reports” or other advice while the revised FEMWATER-GUI was under development.

I would like to express my thanks to Messers Shortencarier and Helton from Sandia National Laboratories for providing some useful literature, the Latin Hypercube Sampling algorithms and program for the calculation of partial correlation and standardized regression coefficients.

I am very grateful to the Deutscher Akademischer Austauschdienst (DAAD) and Indonesia Government for financing my doctoral work and enabling me to continue my higher education at TU Bergakademie Freiberg in Germany.

Finally, a word of appreciation should go to my wife, my children and my parents for their support and patience during the period of my study in Germany. Without this support and understanding, it would have been impossible to do this thesis.

1. INTRODUCTION

The three-dimensional finite-element groundwater flow model for saturated-unsaturated media (3DFEMWATER) and the three-dimensional Lagrangian-Eulerian finite-element model of waste transport through saturated-unsaturated media (3DLEWASTE) were originally written for the U.S. Environmental Protection Agency (USEPA) by Dr. Gour-Tsyh (George) Yeh in 1992 at Pennsylvania State University. They are related numerical codes that can be used together to model flow and transport in three-dimensional, variably-saturated porous media under transient conditions with multiple distributed point sources and sinks. These two codes were combined and modified to simulate density-dependent flow field and distribution of contaminant in three-dimensional domain of subsurface media. This code will be referred as FEMWATER in the following. To ease the handling, FEMWATER was also integrated into the Department of Defence Groundwater Modeling System (GMS) with many numerous improvements. The entire program structure was changed to allow its integration into the GMS. This was a particularly onerous task in older implementation of the model since it suffered from the common limitations of older FORTRAN codes. Additional a series of new numerical solvers were added to replace the previously used block iterative solver. The density-driven (salinity) transport capability was added to allow salinity intrusion studies in coastal aquifers (Lin et al., 1997).

FEMWATER is used to build numerical models for density–dependent flow and transport through saturated-unsaturated porous media with the finite element method. The finite element method allows the analyst to specify different aquifer parameters for each element in the mesh, but a method is needed to obtain these parameters from a (usually) limited data set (e.g., the results of pumping test for a few wells). However, for real aquifers there is an uncertainty in the values and the distribution of the aquifer parameters (distribution and value of hydraulic conductivity and porosity). Values for parameters are not known exactly due to measurement errors and/or inherent spatial and temporal variability. In most cases the input parameters with the greatest uncertainty is the hydraulic conductivity, because it varies over a wide range for geologic materials. Measuring the hydraulic conductivity at a given location, the main uncertainty in this value at the location is due to errors in measuring techniques. However, uncertainties of the parameters are much higher by taking into account variations in space (and time). Therefore, it is more appropriate to express their value in terms of probability distribution rather than assign a single value and to use an uncertainty propagation

model to assess the effect of the variability on the groundwater flow and transport of contaminants.

Numerical groundwater models of real system are based on idealized models of hydrogeology and to fit data (hydraulic head, stream base flow, prior information, etc.) that are uncertain. The calibrated parameters and the predictions made by a groundwater model are also uncertain. The uncertainties are traditionally illustrated by sensitivity analysis where calibrated values of aquifer parameters (hydraulic conductivity, porosity, storage parameters) are changed one or few at a time. Calibration is done both by trial-and-error adjustment of parameters and inverse modeling. However, an infinite number of combinations of changes that account for the correlation among the calibrated parameters should be analyzed to quantify the uncertainty. Thus, calibration is difficult because values for aquifer parameters and hydrologic stresses are typically known at only a few nodes and even then, estimates are influenced by uncertainty. If the parameters used in the model are not consistent with the field-measurement heads, an incorrect description of the system will result.

Although it may be possible to estimate aquifer parameters using statistical methods (e.g., geostatistics) or by solving the inverse problem considerable uncertainty will remain and the effect of uncertainty in values of aquifer parameters on model results should be investigated in sensitivity analysis. According to Anderson and Woessner (1992), the purpose of the sensitivity analysis is to quantify the uncertainty in the calibrated models caused by uncertainty in estimating of aquifer parameters. During a sensitivity analysis, calibrated values for hydraulic conductivity, storage parameters, recharge, and boundary conditions are systematically changed within the previously established plausible range. Fig. 1.1 outlines the steps involved in groundwater model application.

Computer codes such as FEMWATER can be used with many input variables for modeling using numerical methods in a complex system. Time-consuming calculations and dependencies may exist among some of the input variables. The distribution function of these variables is frequently not well known. In addition, the relationships among the variables are usually complex, modeled only by systems of differential equations which are not mathematically tractable. The combination of many variables and the complex relationships among the variables results in a computer code that often requires several hours of CPU time to make a simulation run for a single input vector. For this situations, it is convenient to think the model as function $Y = f(x_1, ..., x_k, t)$ with independent variables $x_1, ..., x_k$ and possibly also

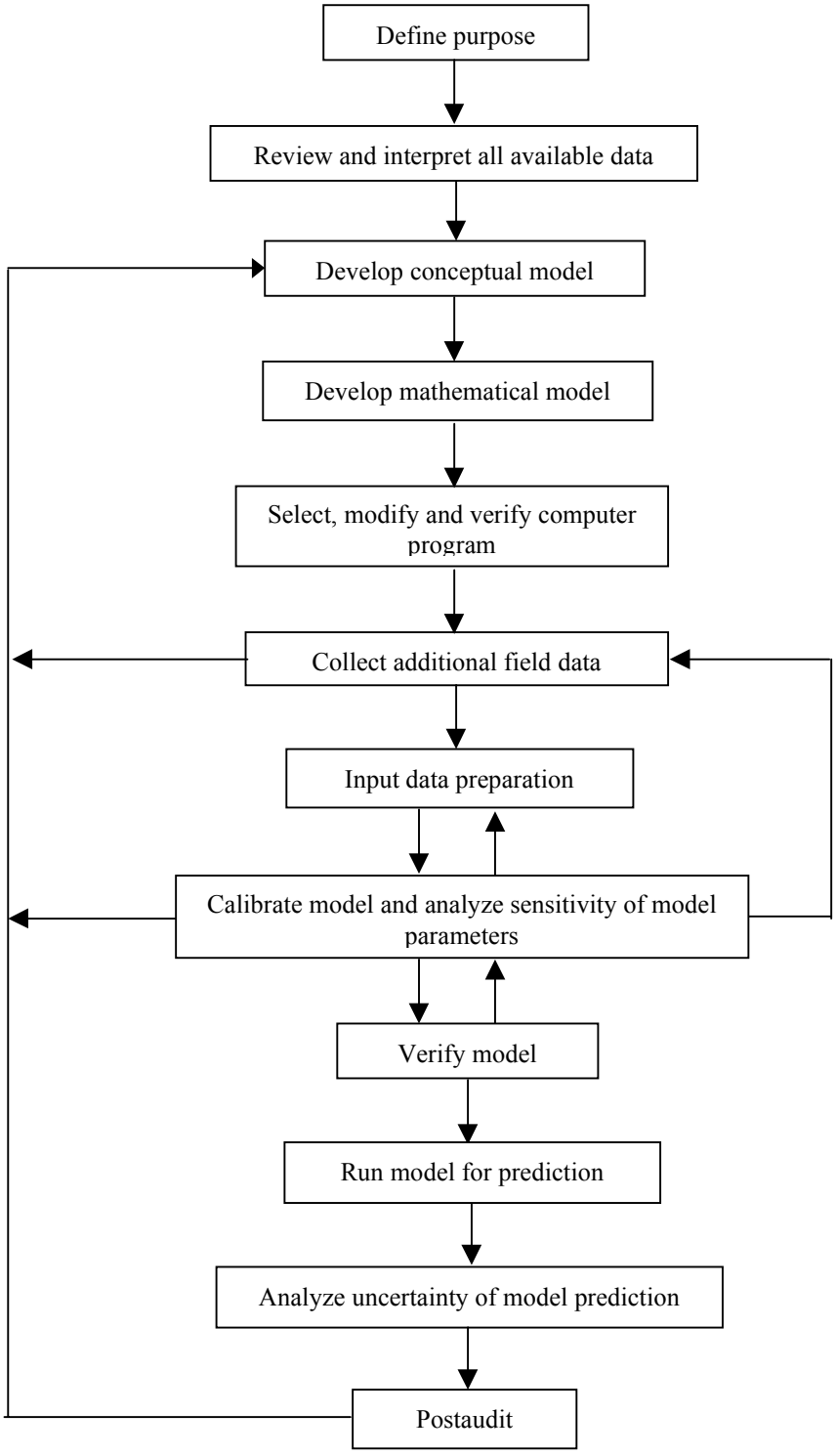

Fig. 1.1 Steps in groundwater model application.

of time. The variables $x_1, ..., x_k$ are hydraulic conductivity in the saturated and unsaturated zone, distribution coefficients for contaminants (Freundlich K or Langmuir K), bulk density, longitudinal and transverse dispersion, molecular diffusion coefficient, tortuosity, radioactive

decay, Freundlich n or Langmuir S_{max} or thermodynamical and kinetically parameters in case of multielement reactive transport modeling.

Uncertainty analysis involves the determination of the variation or imprecision in Y that results from the collective variation in the model variables $x_1, ..., x_k$. Sensitivity analysis involves the determination of change in the response of the model parameters and specification. Thus, sensitivity analysis is used to identify the main contributors to the variation or imprecision in Y. The analysis usually includes, but is not limited to the estimation of means, variances, and distribution functions of several output variables, an analysis of the model's sensitivity to the various input variables, the effect, that uncertainty regarding the distribution functions of the input variables has upon inferences pertaining to the output variables (Iman and Conover, 1980).

The easiest and the most efficient way for assessing output uncertainty of models with many parameters is the Latin Hypercube Sampling (LHS) (Iman et al., 1980). With the LHS strategy, the number of computer runs is given by a number of uncertainty-affected input variables, say in order of hundreds (Meinrath et al., 2000). Latin Hypercube Sampling as introduced by McKay, Conover, and Beckman (1979), appears to provide a satisfactory method for selecting input variables so that good estimators of means, variances, and distribution functions of the output variables may be obtained, providing the answer to part (i) of the desired analysis. The model's sensitivity to various input variables is then handled by partial rank correlation coefficients as described by Iman et al. (1985) and Helton (1993). This procedure satisfies part (ii) of the desired analysis. In order to handle part (iii) of the desired the application of Latin Hypercube Sampling was extended in this work.

Following this LHS algorithm Iman and Shortencarier (1984) at Sandia National Laboratories developed a LHS code in FORTRAN 77 which was intended to run on mainframe computer. For implementation of LHS in a finite element groundwater flow model (FEMWATER), the LHS code was modified and included to FEMWATER for Intel platforms under Windows™. This new code is named FEMWATER-LHS which comes with an Argus ONE™ GUI (Argus Open Numerical Environments Graphical User Interfaces). By means of this GUI the user can easily create meshes, edit parameters, and visualize simulation results.

1.1 Objectives

The main objectives of this work were:

- modify the three-dimensional finite-element model for density–dependent flow and transport (FEMWATER) through saturated-unsaturated porous media by combining of two previous codes: a groundwater flow model [3DFEMWATER, Yeh (1992)] and a subsurface contaminant transport model [3DLEWASTE, Yeh (1992)]. In this combined model, density-dependent effects are taken into consideration to account for saltwater intrusion in aquifers.

- include the Latin Hypercube Sampling to the finite element groundwater model with large uncertainties and varying degrees of complexity in order to highlight some of the problems areas that must be addressed in actual applications.

- develop the GUI (Preprocessor and Postprocessor Graphical User Interfaces) for preparing FEMWATER-LHS input data and viewing model output within Argus Open Numerical Environments (Argus ONE™).

2. THEORY AND METHODS

2.1 Latin Hypercube Sampling (LHS)

Latin Hypercube Sampling (LHS) is a concept similar to the Monte Carlo approach for addressing uncertainty. The Monte Carlo technique is based on simple random sampling (SRS) of the input variables and generally requires a large number of realizations (simulation) to be statistically meaningful. The LHS technique is a stratified sampling approach that allows efficient estimation of the statistics of the output and thus saving CPU-time. As an example, the effect of uncertainties in thermodynamic databases on prediction performances of reactive transport modeling of uranium (VI) was investigated with Monte Carlo approach using the transport code TReaC. The simulation for U-enriched water using 1d-sand column with 40 cm length and 70 cm^2 cross-section, required more than 120 hours (Nitzsche et al., 2000).

For notational convenience, assume that the model can be represented by a function of the form

$$Y = f(x_1, x_2, \ldots, x_n) = f(\mathbf{X}_i) \tag{2.1}$$

where Y is the output variable and $x_1, x_2, \ldots, x_n$ are the input variables of the model.

In practice, a simple random sampling involves two steps. The first step is to select a range and distribution for each sample element x_k. The second step is to samples from the range and distribution specified. Each sample element is selected independently of all other sample elements. The result of this step is a sequence of sample elements of the form

$$\mathbf{X}_i = [x_{i1}, x_{i2}, \ldots, x_{in}], \quad i = 1, 2, \ldots, m \tag{2.2}$$

where n is the number of input variables and m is the sample size. As illustrated in Fig. 2.1 for $m = 5$, $n = 2$, $x_1 = U$ and $x_2 = V$, the numbers *RU(1), RU(2), ..., RU(5)* are sampled from uniform distribution on [0,1] and in turn lead to sampled *U(1),U(2), ..., U(5)* from U based on CDF for U. Under the same conditions the numbers *RV(1),RV(2), ..., RV(5)* lead to sample *V(1),V(2), ..., V(5)* from V. The pairs

$$\mathbf{X}_i = [U(i), V(i)], \quad i = 1, 2, \ldots, m = 5 \tag{2.3}$$

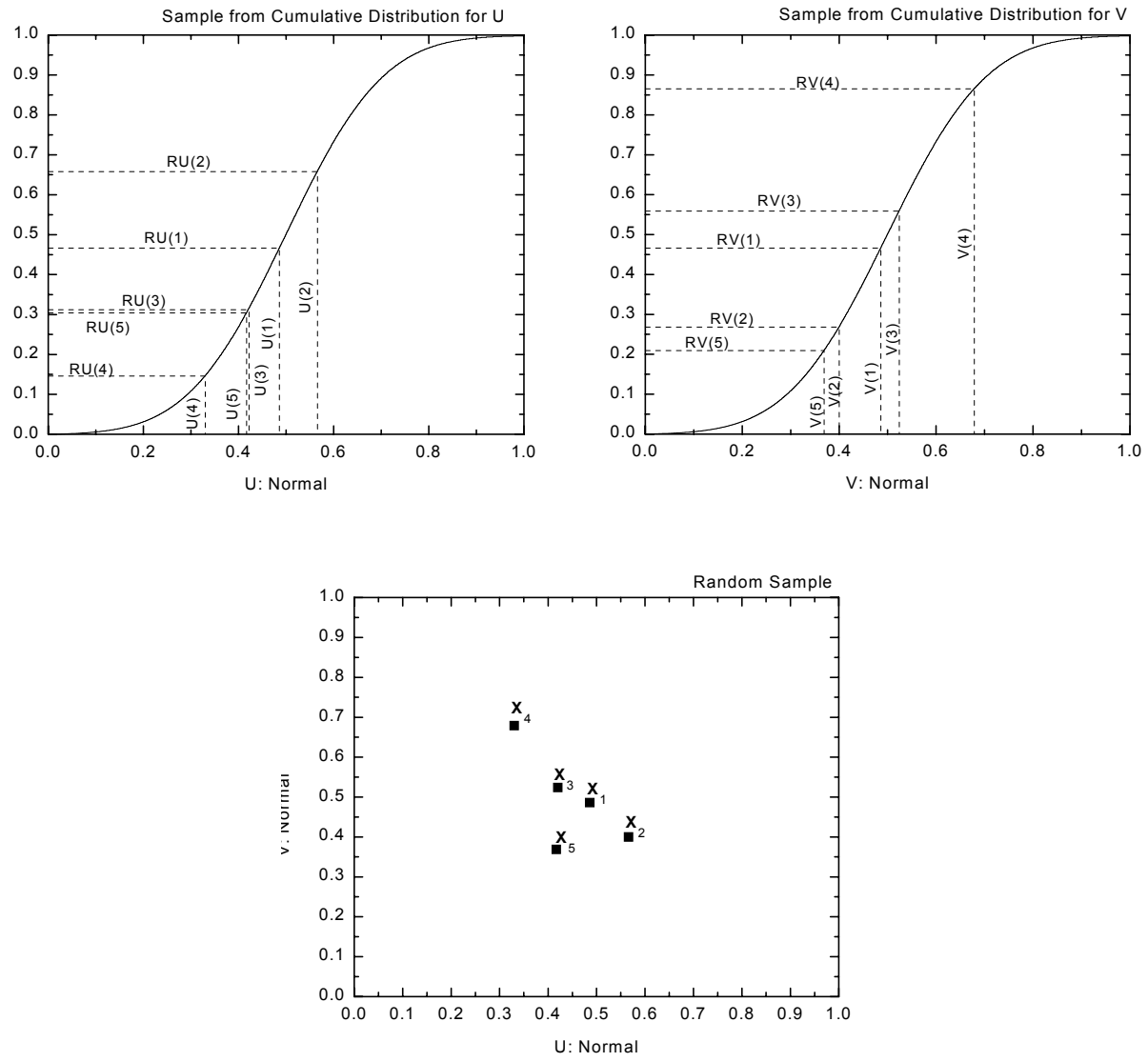

Fig. 2.1 Example of random sampling to generate a sample of $m = 5$ from $\mathbf{X} = [U,V]$, with U and V normal on [0,1].

then constitute a random sample from $\mathbf{X} = [U,V]$, where U and V both have normal distribution on [0,1] in this example.

The Latin Hypercube Sampling method divides distributions into regions of equal probability. A graph of the cumulative distribution function (CDF) is obtained by plotting the $P(X \le x)$ on vertical axis versus x on horizontal axis. The LHS is implemented by dividing the *vertical* axis of the graph into m nonoverlapping intervals of equal length, where m is the number of computer runs to be made. This forms the following m intervals on the vertical axis: $(0, 1/m)$, $(1/m, 2/m)$, ..., $((m\text{-}1)/m, 1)$. The intervals for $m = 5$ are illustrated in Fig. 2.2 in terms of both the density function and more easily used cumulative distribution function (CDF). A value is

randomly selected within each of these intervals. Each value that is selected is mapped through the inverse of the distribution function to produce an observation for the *i-th* input variable. Note that unlike simple Monte Carlo, this process guarantees a full coverage of range of each of the input variables. This process is repeated for all *m* input variables.

The generation of an LHS of size $m = 5$ from $\mathbf{X} = [U,V]$ is illustrated in Fig. 2.2 Initially, the ranges of U and V are subdivided into five intervals of equal probability, with this subdivision represented by the lines that originate at 0.2, 0.4, 0.6 and 0.8 on the ordinates of the two upper frames in Fig. 2.2, extend horizontally to CDFs, and dropping vertically to the abscissas to produce the 5 indicated intervals. Random values sampled *U(1),U(2), ..., U(5)* and *V(1),V(2), ..., V(5)* are then sampled from these intervals. The sampling of these random values is implemented by (a) sampling *RU(1)* and *RV(1)* from uniform distribution on [0,0.2], *RU(2)* and *RV(2)* from uniform distribution on [0.2, 0.4], and so on, and (b) the using the CDFs to identify (i.e. sample) the corresponding U and V values.

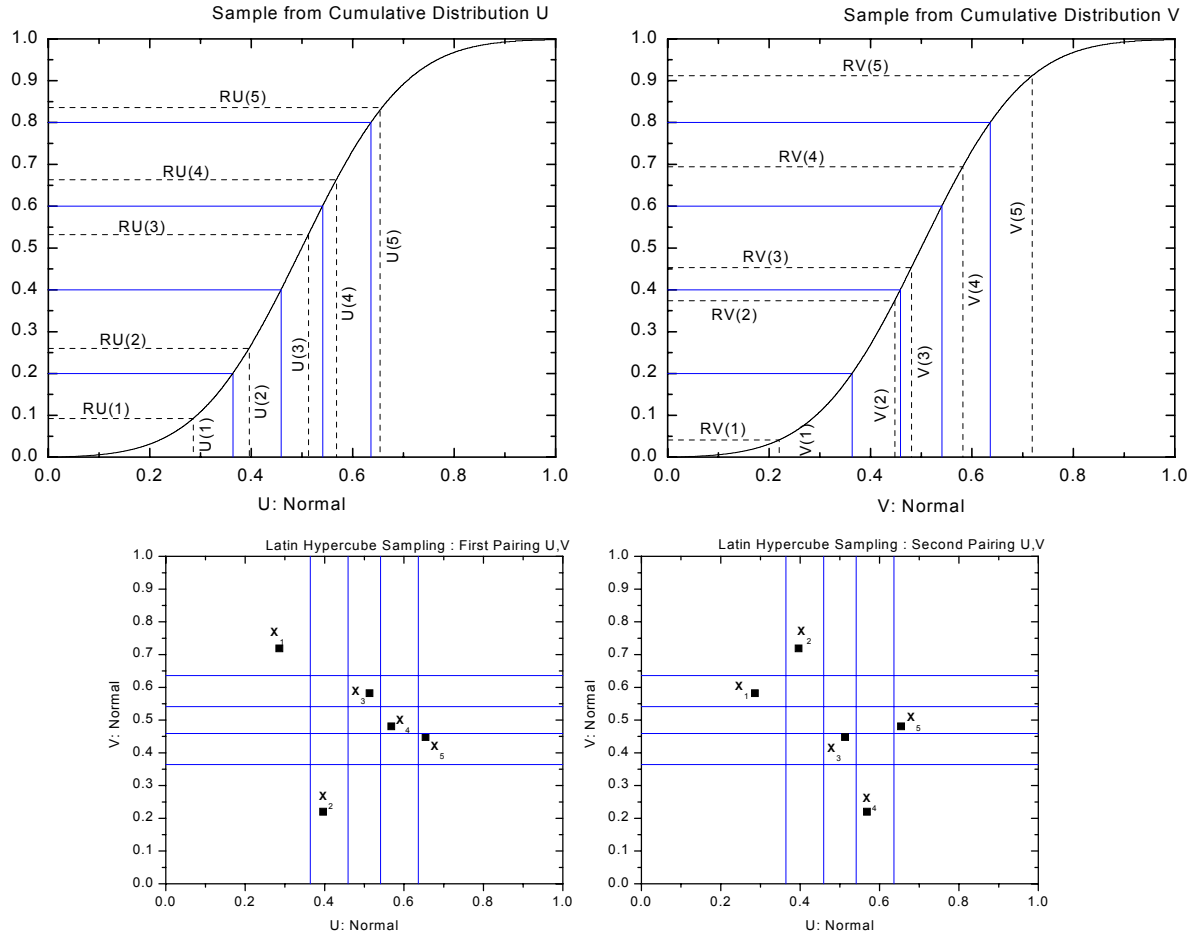

Fig. 2.2 Example of Latin hypercube sampling to generate a sample of $m = 5$ from $\mathbf{X} = [U,V]$, with U and V normal on [0,1].

The last step in generating the LHS is to place the m observations generated for input variable x_i into the *i-th* column of a $m \times n$ matrix **X** and random mixing is required, since, unlike simple random sampling, the observations in a LHS are not necessarily generated in random order. This mixing process serves to emulate the pairing of observations in a simple Monte Carlo process. This entire process is repeated for each of n input variables.

2.1.1 Correlation Control

In many cases some of the input variables are correlated due to various physical reasons. For example, there is a correlation between hydraulic conductivity, porosity and other soil properties. Thus control of correlation within a sample used in a Latin Hypercube Sampling analysis can be very important. If two or more variables are correlated, then it is necessary that the appropriate correlation structure is incorporated into the sample if meaningful results are to be obtained in subsequent uncertainty and sensitivity analysis. On the other hand, it is as well important that variables do not appear to be correlated when they are really independent.

It is often difficult to induce a desired correlation structure of a sample. Indeed, multivariate distributions can be incompatible with correlation parents that are proposed for them. Thus, it is possible to encounter analysis situations where the proposed variable distribution and the suggested correlations between the variables are inconsistent; in that case, it is not possible to have both the desired variable distributions and the requested correlations between the variables.

In response to this situation, Iman and Conover (1982) proposed a method for controlling the correlation structure in random and Latin hypercube samples based on rank correlation (i.e. on rank-transformed variables) rather than sample correlation (i.e. on the original data). If the input variables x_i are sorted from smallest to largest as $x_1, x_2, ..., x_n$ the corresponding ranks are *1, 2, ..., n*, with average ranks being used in the case of ties among the x_i. Spearman's rank correlation coefficient for the variables x_i and y_i for sample size n is computed as

$$r_R = \frac{\sum_{i=1}^{n} R_{x_i} R_{y_i} - C}{\sqrt{\left[\sum_{i=1}^{n} R_{x_i}^2 - C\right]\left[\sum_{i=1}^{n} R_{y_i}^2 - C\right]}} \tag{2.4}$$

where R_{x_i} is the rank of x_i, R_{y_i} is the rank of y_i, and $C = n(n+1)^2/4$. If there are no ties among the x_i and y_i, Eq. (2.4) can be reduced to

$$r_R = 1 - \frac{6\sum_{i=1}^{n}\left[R_{x_i} - R_{y_i}\right]^2}{n\left(n^2-1\right)} \tag{2.5}$$

The value of r_R in Eq. (2.4) and (2.5) is bounded between –1 and +1, and provides a measure of the strength of the monotonic relationship between x_i and y_i.

The following discussion provides an overview of Iman/Conover procedure for inducing a desired rank correlation structure on either a random or Latin hypercube sample (Helton, 1993). A more detailed discussion of the procedure is given in Iman and Conover (1982). The procedure begins with a sample of size m from the n input variables under consideration. This sample can be represented by the $m \times n$ matrix

$$\mathbf{X} = \begin{bmatrix} x_{11} & x_{12} & \cdots & x_{1n} \\ x_{21} & x_{22} & \cdots & x_{2n} \\ \vdots & \vdots & & \vdots \\ x_{m1} & x_{m2} & \cdots & x_{mn} \end{bmatrix} \tag{2.6}$$

where x_{ij} is the value for variable j in the sample element i. Thus, the rows of **X** correspond to sample elements, and the columns of **X** contain the sampled values for individual variables.

The procedure is based on rearranging the values in individual columns of **X** so that a desired rank correlation structure results between the individual variables. For convenience, let the desired correlation structure be represented by the $n \times n$ matrix

$$\mathbf{C} = \begin{bmatrix} c_{11} & c_{12} & \cdots & c_{1n} \\ c_{21} & c_{22} & \cdots & c_{2n} \\ \vdots & \vdots & & \vdots \\ c_{n1} & c_{n2} & \cdots & c_{nn} \end{bmatrix} \tag{2.7}$$

where c_{kl} is the desired rank correlation between variables x_k and x_l.

Although the procedure is based on rearranging the values in the individual columns of **X** to obtain a new matrix $\mathbf{X}^*$ that has a rank correlation structure close to that described by **C**, it is not possible to work directly with **X**. Rather, it is necessary to define a new matrix

$$\mathbf{S} = \begin{bmatrix} s_{11} & s_{12} & \cdots & s_{1n} \\ s_{21} & s_{22} & \cdots & s_{2n} \\ \vdots & \vdots & & \vdots \\ s_{m1} & s_{m2} & \cdots & s_{mn} \end{bmatrix} \tag{2.8}$$

that has the same dimensions as **X**, but is otherwise independent of **X**. Each column of **S** contains a random permutation of m van der Waerden scores (Conover, 1980) $\Phi^{-1}(i/m + 1)$, $i = 1,2, ..., m$, where Φ^{-1} is the inverse of the standard normal distribution.

The matrix **S** is then rearranged to obtain the correlation structure defined by **C**. This rearrangement is based on the Cholesky factorization of **C** by contracting a lower triangular matrix **P** such that

$$\mathbf{C} = \mathbf{P}\mathbf{P}^T \tag{2.9}$$

This rearrangement is possible because **C** is a symmetric, positive-definite matrix.

If the correlation matrix associated with **S** is the $n \times n$ identity matrix (i.e. if the correlations between the values in different columns of **S** are zero), then the correlation matrix for

$$\mathbf{S}^* = \mathbf{S}\mathbf{P}^T \tag{2.10}$$

is **C**. At this point, the success of the procedure depends on the following two conditions: that the correlation matrix associated with **S** being close to the $n \times n$ identity matrix; that the correlation matrix for $\mathbf{S}^*$ being approximately equal to the rank correlation matrix for $\mathbf{S}^*$.

If these two conditions hold, then the desired matrix **X*** can be obtained by simply rearranging the values in the individual columns of **X** in same rank order as the values in individual columns of **S***. This is the first time that the variables values contained in **X** enter into the correlation process. When **X*** is constructed in this manner, it will have the same rank correlation matrix as **S***. Thus, the rank correlation matrix for **X*** will approximate **C** to the same extent as the rank correlation matrix for **S*** does.

The condition that the correlation matrix associated with **S** being close to the identity matrix is now considered. For convenience, the correlation matrix for **S** will be represented by **E**. Unfortunately, **E** will not always be the identity matrix. However, it is possible to make correction for this. The starting point for this correction is the Cholesky factorization for **E**:

$$\mathbf{E} = \mathbf{Q}\mathbf{Q}^T \tag{2.11}$$

This factorization exists because **E** is a symmetric, positive-definite matrix. The matrix $\mathbf{S}^*$ define by

$$\mathbf{S}^* = \mathbf{S}(\mathbf{Q}^{-1})^T \mathbf{P}^T \tag{2.12}$$

has **C** as its correlation matrix. In essence, multiplication of **S** by $(\mathbf{Q}^{-1})^T$ transform **S** into a matrix whose associated correlation matrix is the $n \times n$ identity matrix. Then multiplication by $\mathbf{P}^T$ produces a matrix whose associated correlation matrix is **C**. As it is not possible to be sure that **E** will be an identity matrix, the matrix $\mathbf{S}^*$ used in the procedure to produce correlated input should be defined in the corrected form shown in Eq. (2.12) rather than in the uncorrected form shown in Eq. (2.10).

The condition that the correlation matrix for $\mathbf{S}^*$ is approximately equal to the rank correlation matrix for $\mathbf{S}^*$ depends on the choice of the scores used in the definition of **S**. On the basis of empirical investigation, Iman and Conover (1982) found that van der Waerden scores provided an effective means of defining **S**. These scores are incorporated into the rank correlation procedure in the widely used LHS program (Iman and Shortencarier, 1984). Other possibilities for defining these scores exist, but have not been extensively investigated. The user should examine the rank correlation matrix associated with $\mathbf{S}^*$ to ensure that it is close to the target correlation matrix **C**. If this is not the case, the construction procedure used to obtain $\mathbf{S}^*$ can be repeated until suitable approximation to **C** is obtained. Result given in Iman and Conover (1982) indicate the use of van der Waerden scores leads to rank correlation matrices for $\mathbf{S}^*$ that are close to the target matrix **C**.

This technique has a number of desirable properties:

(i) It is distribution free.

(ii) It can be used with any sampling scheme for which correlated input variables could logically be considered without destroying the intent of the sampling scheme. For

example, it can be used with either random sampling or LHS without altering the inherent nature of the sampling process.

(iii) Induces the pairwise rank correlation structure without disturbing the marginal distributions of the input variables (Iman, 1992).

The technique is implemented in the widely used LHS program (Iman and Shortencarier, 1984). This program generates both random and Latin Hypercube samples with user-specified rank correlations between variables. For integration of LHS in a finite element groundwater model (FEMWATER), this program was modified for Intel platforms. A portable Fortran random number generator algorithm has been used to generate uniform random numbers. This algorithms can be found in Bratley et al. (1987).

2.1.2 Description of available parameter distributions

In the FEMWATER-LHS program the user may select one of the following distributions: normal, lognormal, uniform, loguniform, triangular, user discrete probability, and empirical. The LHS shell has the ability to generate data from a number of these probability distributions. A representation of five of these distributions is provided in table 2.1.

Depending on the distribution selected, the user is required to input relevant parameter of the distribution. The first four distributions requires minimum and maximum values. For the normal distribution, the user must specify *A* and *B* to satisfy the following statements:

$$P(X < A) = 0.001 \quad \text{and} \quad P(X > B) = 0.001 \tag{2.13}$$

For the lognormal distribution, the user must specify $A > 0$ and $B > 0$ to satisfy the following statements:

$$P(Y < A) = 0.001 \quad \text{and} \quad P(Y > B) = 0.001 \tag{2.14}$$

However, for both normal and lognormal distribution it is also possible to directly specify the mean (μ) and the standard deviation (σ) of the distribution. For the uniform distribution, the

Table 2.1 Distributions, including equations for the density and distribution functions, expected value, variance for five distribution types.

Distribution Type	Density function	Distribution function	Expected value	Variance
Normal	$f(x)=\frac{1}{\sigma\sqrt{2\pi}}\exp\left\{\frac{-(x-\mu)^2}{2\sigma^2}\right\},\quad -\infty<x<\infty$	$F(x)=\int_{-\infty}^{x} f(t)dt,\ -\infty<x<\infty$	$E(X)=\mu=\frac{(A+B)}{2}$	$V(X)=\sigma^2=\left[\frac{(B-A)}{6.18}\right]^2$
Lognormal	$f(y)=\frac{1}{y\sigma\sqrt{2\pi}}\exp\left\{\frac{-(\ln y-\mu)^2}{2\sigma^2}\right\},\quad y>0$ $y=e^x$, if $x\sim N(\mu,\sigma^2)$	$F(y)=\int_{0}^{y} f(t)dt,\quad y>0$	$E(Y)=\exp\left(\frac{\mu+\sigma^2}{2}\right)$	$V(Y)=\exp(2\mu+\sigma^2)\left[\exp(\sigma^2)-1\right]$
Uniform	$f(x)=\frac{1}{(B-A)},\quad A\le x\le B$	$F(x)=\frac{(x-A)}{(B-A)},\quad A\le x\le B$	$E(X)=\frac{(A+B)}{2}$	$V(X)=\frac{(B-A)^2}{12}$
Loguniform	$f(x)=\frac{1}{(\ln B-\ln A)},\quad A<x<B$	$F(x)=\frac{(\ln x-\ln A)}{(\ln B-\ln A)},\quad A<x<B$	$E(X)=\frac{(B-A)}{(\ln B-\ln A)}$	$V(X)=\frac{(B-A)[(\ln B-\ln A)(B+A)-2(B-A)]}{[2(\ln B-\ln A)^2]}$
Triangular (a<b<c)	$f(x)=\frac{2(x-a)}{(c-a)(b-a)},\quad a\le x\le b$ $=\frac{2(c-x)}{(c-a)(c-b)},\quad b\le x\le c$	$F(X)=\frac{(x-a)^2}{(c-a)(b-a)},\ a\le x\le b$ $=\frac{b-a}{c-a}-\frac{(x+b-2c)(x-b)}{(c-a)(c-b)},\ b\le x\le c$	$E(X)=\frac{a+b+c}{3}$	$V(X)=\frac{a(a-b)+b(b-c)+c(c-a)}{18}$

user must specify the endpoints *A* and *B*. The loguniform distribution requires *A > 0* and *B > 0*. For the triangular distribution, the user is required to input *a, b* and *c* (*a < b < c*). For the discrete probability distribution, the user is required to input the data and the probability values. Finally, the empirical distribution requires some sample data points.

2.2 The Governing Equation of Subsurface Flow

The governing equation for unsaturated flow is basically the modified RICHARDS' equation, which describes the flow of variable-density fluid (Yeh et al., 1994; 1997) neglecting the flow of the second fluid (gas) in an unsaturated porous sediment:

$$\frac{\rho}{\rho_0}\frac{d\theta}{dH}\frac{\partial H}{\partial t} = \nabla\cdot\left[\mathbf{K}\cdot\left\{\nabla H + \frac{\rho}{\rho_0}\nabla z\right\}\right] + \frac{\rho^*}{\rho_0}q \tag{2.15}$$

where

H = pressure head

t = time

$\mathbf{K}$ = hydraulic conductivity tensor

z = elevation

q = source/sink

ρ = fluid density at chemical concentration C

ρ_0 = reference density

ρ^* = density of injected fluid

θ = moisture content

The hydraulic conductivity $\mathbf{K}$ is given by

$$\mathbf{K} = \frac{\rho g}{\mu}\mathbf{k} = \frac{(\rho/\rho_0)}{(\mu/\mu_0)}\frac{\rho_0 g}{\mu_0}\mathbf{k}_s k_r = \frac{\rho/\rho_0}{\mu/\mu_0}\mathbf{K}_{s0}k_r \tag{2.16a}$$

where

μ = dynamic viscosity of water at chemical concentration C

μ_0 = reference dynamic viscosity

g = gravity

$\mathbf{k}$ = permeability tensor

$\mathbf{k_s}$ = saturated permeability tensor

k_r = relative permeability or relative hydraulic conductivity

Note that hydraulic conductivity tensor **K**, has three diagonal components, K_{xx}, K_{yy}, K_{zz}, and three off-diagonal ones, K_{xy}, K_{xz}, and K_{yz}.

$$\mathbf{K} = \begin{bmatrix} K_{xx} & K_{xy} & K_{xz} \\ K_{xy} & K_{yy} & K_{yz} \\ K_{xz} & K_{yz} & K_{zz} \end{bmatrix} \tag{2.16b}$$

The reference value usually is taken at zero chemical concentration. The density and dynamic viscosity are functions of chemical concentration and assumed to have the following forms (Lin et al., 1997):

$$\frac{\rho}{\rho_0} = a_1 + a_2 C + a_3 C^2 + a_4 C^3 \tag{2.17a}$$

and

$$\frac{\mu}{\mu_0} = a_5 + a_6 C + a_7 C^2 + a_8 C^3 \tag{2.17b}$$

where

C is the chemical concentration; and a_1, a_2, ..., a_8 are parameters used to describe the concentration dependence of water density and dynamic viscosity.

The Darcy velocity is calculated as follows:

$$\mathbf{V} = -\mathbf{K} \cdot \left(\frac{\rho_0}{\rho} \nabla H + \nabla z \right) \tag{2.18}$$

The initial conditions for the flow equations include

$$H = H_i(x,y,z) \text{ in } R \tag{2.19}$$

where

R = region of interest

H_i = prescribed initial condition for the reference hydraulic head. The H_i can be obtained either by solving the steady-state version of equation (2.15) or, alternatively, by defining H_i through field measurements.

The boundary conditions for the flow equations are stated as follows.

Dirichlet Conditions:

$$H = H_d(x_b,y_b,z_b,t) \quad \text{on} \quad B_d \tag{2.20}$$

Neumann Conditions (gradient condition) :

$$-n \cdot \mathbf{K} \cdot \left(\frac{\rho_0}{\rho} \nabla H \right) = q_n(x_b,y_b,z_b,t) \quad \text{on} \quad B_n \tag{2.21}$$

Cauchy Conditions (flux condition) :

$$-n \cdot \mathbf{K} \cdot \left(\frac{\rho_0}{\rho} \nabla H + \nabla z \right) = q_c(x_b,y_b,z_b,t) \quad \text{on} \quad B_c \tag{2.22}$$

Variable Conditions - During Precipitation Period:

$$H = h_p(x_b,y_b,z_b,t) \quad \text{on} \quad B_v \tag{2.23a}$$

or

$$-n \cdot \mathbf{K} \cdot \left(\frac{\rho_0}{\rho} \nabla H + \nabla z \right) = q_p(x_b,y_b,z_b,t) \quad \text{on} \quad B_v \tag{2.23b}$$

Variable Conditions - During Non-precipitation period:

$$H = h_p(x_b,y_b,z_b,t) \quad \text{on} \quad B_v \tag{2.23c}$$

or

$$H = h_m(x_b,y_b,z_b,t) \quad \text{on} \quad B_v \tag{2.23d}$$

or

$$-n \cdot \mathbf{K} \cdot \left(\frac{\rho_0}{\rho} \nabla H + \nabla z \right) = q_e(x_b, y_b, z_b, t) \quad \text{on} \quad B_v \tag{2.23e}$$

where

(x_b, y_b, z_b) = spatial coordinate on the boundary

n = outward unit vector normal to the boundary

H_d = Dirichlet functional value

q_n = Gradient flux value

q_c = Flux value

B_d = Dirichlet boundary

B_n = Gradient flux boundary

B_c = Flux boundary

B_v = variable boundary

h_p = ponding depth

q_p = throughfall of precipitation on the variable boundary

h_m = minimum pressure on the variable boundary

q_e = evaporation rate on the variable boundary

Note that only one of Eqs. (2.23a) – (2.23e) is utilized at any point on the variable boundary at any time.

2.3 The Governing Equations of Transport

The governing equations for transport describe the transport of soluted constituents through groundwater systems. These equations are based on the laws of continuity of mass and flux. The major processes included are advection, dispersion/diffusion, decay, sorption, and biodegradation through both liquid and solid phases, as well as injection and withdrawal. Not included in the following equation are chemical reactions like dissolution and/or precipitation of minerals. Neither the complexity of system with more than one relevant species in the water is taken into account. Thus only very simple and well defined problems might be solved by this approach. The governing equations for this simple transport processes can be stated as

$$\theta \frac{\partial C}{\partial t} + \rho_b \frac{\partial S}{\partial t} + \mathbf{V} \cdot \nabla C = \nabla \cdot (\theta \, \mathbf{D} \cdot \nabla C) - \lambda (\theta C + \rho_b S) + q C_{in}$$

$$- \left(\frac{\rho^*}{\rho} q - \frac{\rho_0}{\rho} \mathbf{V} \cdot \nabla \left(\frac{\rho}{\rho_0} \right) \right) C \qquad (2.24)$$

where

$$S = K_d C \quad \text{for linear isotherm} \qquad (2.25a)$$

$$S = \frac{S_{\max} K C}{1 + K C} \quad \text{for Langmuir isotherm} \qquad (2.25a)$$

$$S = K C^n \quad \text{for Freundlich isotherm} \qquad (2.25c)$$

where

C = concentration in aqueous phase

ρ_b = bulk density of the medium

S = concentration in sorbed phase

D = dispersion coefficient tensor

λ = decay constant

C_{in} = concentration in the source

q = source rate of water

K_d = distribution coefficient

S_{max} = maximum concentration in the Langmuir nonlinear isotherm

K = coefficient in the Langmuir or Freundlich nonlinear isotherm

n = power index in the Freundlich nonlinear isotherm

The dispersion coefficient tensor is given by

$$\theta \, \mathbf{D} = \alpha_T |\mathbf{V}| \, \delta + (\alpha_L - \alpha_T) \mathbf{V}\mathbf{V} / |\mathbf{V}| + \theta \alpha_m \tau \, \delta \qquad (2.26)$$

where

|**V**| = magnitude of **V**

α_L = longitudinal dispersivity

α_T = lateral dispersivity

α_m = molecular diffusion coefficient

δ = Kronecker delta tensor

τ = tortuosity

To use the hybrid Langrangian-Eulerian approach,

$$\left(\theta + \rho_b \frac{dS}{dC}\right)\frac{D_{v_d} C}{Dt} = \nabla \cdot (\theta\, \mathbf{D} \cdot \nabla C) - \lambda(\theta C + \rho_b S) + qC_{in}$$

$$-\left(\frac{\rho^*}{\rho} q - \frac{\rho_0}{\rho}\mathbf{V} \cdot \nabla\left(\frac{\rho}{\rho_0}\right)\right) C \qquad (2.27a)$$

$$\mathbf{V}_d = \frac{\mathbf{V}}{\theta + \rho_b K_d} \quad \text{for Liniar isotherm model} \qquad (2.27b)$$

$$\theta \frac{D_{v_f} C}{Dt} + \rho_b \frac{dS}{dC}\frac{\partial C}{\partial t} = \nabla \cdot (\theta\, \mathbf{D} \cdot \nabla C) - \lambda(\theta C + \rho_b S) + qC_{in}$$

$$-\left(\frac{\rho^*}{\rho} q - \frac{\rho_0}{\rho}\mathbf{V} \cdot \nabla\left(\frac{\rho}{\rho_0}\right)\right) C \qquad (2.28a)$$

$$\mathbf{V}_f = \frac{\mathbf{V}}{\theta} \quad \text{for Freundlich and Langmuir models} \qquad (2.28b)$$

where $\mathbf{V}_d$ and $\mathbf{V}_f$ stands for retarded and fluid pore velocities, respectively, used for particle tracking; and $D_{vd}C/Dt$ and $D_{vf}C/Dt$ are material derivatives of C with respect to time using the retarded and fluid pore velocities, respectively.

The initial conditions for transport are

$$C = C_i(x, y, z) \text{ in } R \qquad (2.29)$$

where C_i is the initial concentration. The boundary conditions for transport include the following prescribed concentration (Dirichlet) boundary conditions:

$$C = C_d(x_b, y_b, z_b, t) \text{ on } B_d \qquad (2.30)$$

Neumann Boundary Conditions:

$$\mathbf{n}\cdot\left(-\theta\,\mathbf{D}\cdot\nabla C\right)=q_n\left(x_b,y_b,z_b,t\right)\ \text{ on }\ B_n \tag{2.31}$$

Cauchy Boundary Conditions:

$$\mathbf{n}\cdot\left(\mathbf{V}C-\theta\,\mathbf{D}\cdot\nabla C\right)=q_c\left(x_b,y_b,z_b,t\right)\ \text{ on }\ B_c \tag{2.32}$$

Variable Boundary Conditions:

$$\mathbf{n}\cdot\left(\mathbf{V}C-\theta\,\mathbf{D}\cdot\nabla C\right)=\mathbf{n}\cdot\mathbf{V}C_v\left(x_b,y_b,z_b,t\right)\ \text{ on }\ B_v\quad\text{if}\quad\mathbf{n}\cdot\mathbf{V}\le 0 \tag{2.33a}$$

$$\mathbf{n}\cdot\left(-\theta\,\mathbf{D}\cdot\nabla C\right)=0\ \text{ on }\ B_v\quad\text{if}\quad\mathbf{n}\cdot\mathbf{V}>0 \tag{2.33b}$$

where

C_d = prescribed concentration on the Dirichlet boundary B_d

C_v = specified concentration on of water through the variable boundary B_v

q_c = prescribed total flux through the Cauchy boundary B_c

q_n = prescribed gradient flux through the Neumann boundary B_n

2.4 Numerical Formulation and Solution of the Equations

The flow equation (2.15) is approximated in matrix form as

$$[M]\left\{\frac{dH}{dt}\right\}+[S]\{H\}=\{Q\}+\{G\}+\{B\} \tag{2.34}$$

where

$\{dH/dt\}$ = column vectors containing the values of dH/dt

$\{H\}$ = column vectors containing the values of H at all nodes

$[M]$ = mass matrix resulting from the storage term

$[S]$ = stiffness matrix resulting from the action of conductivity

$\{Q\}$ = load vectors from the internal source/sink

$\{G\}$ = load vectors from the gravity force

$\{B\}$ = load vectors from the boundary conditions

In performing the finite element discretization in space, quadrilateral elements are used. Finite difference method is applied to achieve temporal discretization. The detailed finite element formulation can be found elsewhere (Huyakorn and Pinder, 1983; Istok, 1989; Yeh, 1999).

The transport Eq. (2.24) is approximated as follows:

For the Conventional Finite-Element Approach

$$[M]\left\{\frac{dC}{dt}\right\}+([A]+[D]+[K])\{C\}=\{Q\}+\{B\} \tag{2.35}$$

For the Lagrangian-Eulerian approach with linear Isotherms

$$[M]\left\{\frac{D_{vd}C}{Dt}\right\}+([D]+[K])\{C\}=\{Q\}+\{B\} \tag{2.36}$$

For the Lagrangian-Eulerian approach with nonlinear isotherms

$$\left([M_1]\left\{\frac{D_{vf}C}{Dt}\right\}+[M_2]\left\{\frac{dC}{dt}\right\}\right)+([A]+[D]+[K])\{C\}=\{Q\}+\{B\} \tag{2.37}$$

where

$\{C\}$ = a vector whose components are the concentration at all nodes

$\{dC/dt\}$ = derivative of $\{C\}$ with respect to time

$[M]$, $[M_1]$ = mass matrices associated with the material derivative term

$[M_2]$ = mass matrix associated with the partial derivative term

$[D]$ = stiff matrix associated with the dispersion term

$[A]$ = stiff matrix associated with the advection term

$[K]$ = stiff matrix associated with all the first-order terms

$\{Q\}$ = load vector associated with all zero-order derivative terms

$\{B\}$ = load vector associated with boundary conditions

According to Yeh (2000), the Lagrangian-Eulerian approach based on the concept of "particle" are generally referred to as particle tracking methods. In particle tracking approaches, particles first are introduced in the domain (which is discretized with a fixed grid system). Each particle is associated with a spatial coordinate and a discrete quantity of mass. Thus, the number of particle and location of the particles introduced into the domain depend

on the initial concentration field, boundary conditions, and artificial sources/sinks. Second, these particles are moved forward with the flow (the flow should represent both advection and diffusion and is typically described in Eulerian frame). Third, whenever convenient, the number and location of the particles are processed back to concentrations at the fixed grid nodes as to give the instantaneous concentration field. Fourth, concentration changes at each node during the time interval resulting from bio-chemical reactions are computed. Finally, the mass associated with each particle is recomputed according to the new concentration fields. These procedures are repeated for each time step.

The detailed equations, matrices and vectors can be found in Yeh (1999, 2000). The two matrix system, in Eq. (2.34) and one of Eqs. (2.35) - (2.37), coupled of flow and transport equations, respectively, are linked by both density and discharges. Fig. 2.3 shows the structure of coupling used in FEMWATER-LHS for transient-state simulations. In figure 2.3, H^{k+1}, C^{k+1} represent the computed variables associated with subsurface flow and chemical transport, respectively. H^k and C^k are the present values of H and C respectively. The coupling in Fig. 2.3 mainly includes the following five steps for every time step:

(i) Compute the new value for subsurface flow. All the present iteration values are computed in the previous iteration.

(ii) Examine the convergence of subsurface flow by comparing the newly-computed value with the previous iteration value of subsurface flow.

(iii) Compute the new value for chemical transport. The newly-computed value of subsurface flow is used in this computation.

(iv) Examine the convergence of chemical transport by comparing the newly-computed and the previous iteration value of chemical transport.

(v) Determine if the next iteration is needed. If convergence has been reached for all the two modules, then the computation of the next time step is performed. Otherwise, the present iteration values are updated by relaxing the newly-computed and the previous iteration values. The coupling iteration continues after the updating.

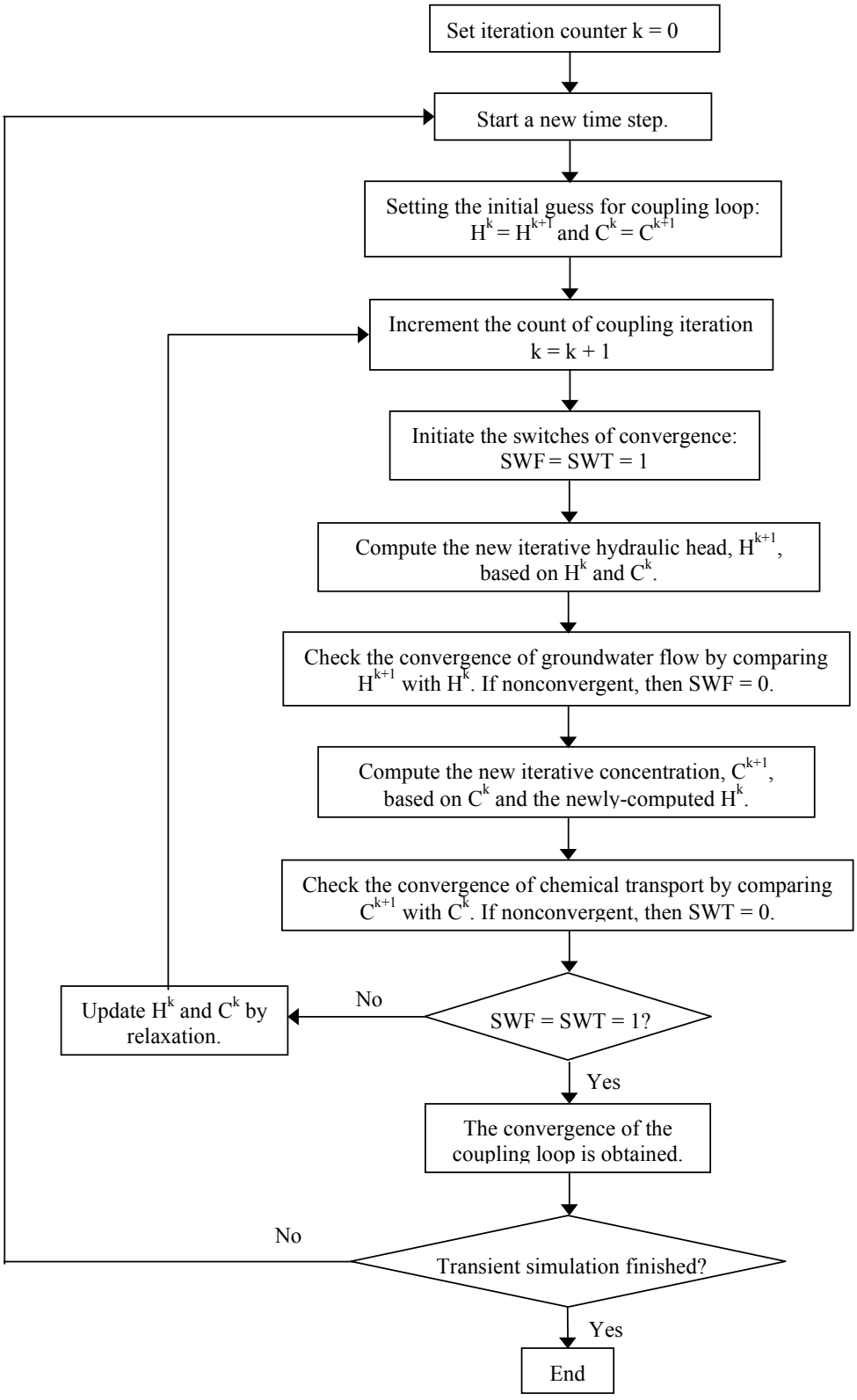

Fig. 2.3 General structure of coupling used in FEMWATER-LHS for transient simulations. H^{k+1}, H^k, C^{k+1} and C^k are the computed and present iterative values of the variables associated with flow and chemical transport respectively.

When the free convection resulting from the buoyancy-density difference between freshwater and saltwater becomes significant and makes the system nonlinear, the coupling of flow and transport is necessary. The nonlinearity of the system in FEMWATER-LHS is treated using Picard iteration and the generated set of linearized equations is solved using either a block iterative method or pointwise iterative matrix solver. The detail algorithms can be found elsewhere (Istok, 1989; Lin et al., 1997; Holzbecher, 1998; Yeh, 1999, 2000).

The Galerkin finite element method is employed to discretize the Richards' equation in the flow module, whereas the hybrid Lagrangian-Eulerian finite element method may be used to discretize the transport equation in the transport module. The following are the advantages of using the hybrid Lagrangian-Eulerian approach:

(i) Very large time step sizes can be used to subdue excessive numerical dispersion (Yeh et al., 1992);

(ii) numerical oscillation caused by the advection terms are entirely eradicated (Yeh, et al., 1995);

(iii) the mesh Peclet number can be anywhere in the range of zero to infinity (normally, the finite difference and conventional finite element methods have a heavy restriction on the mesh Peclet number that can be used) (Yeh et al., 1992).

(iv) additionally, the hybrid Lagrangian-Eulerian method will always be superior to and never worse than its corresponding upstream finite element method (Yeh et al., 1995).

Because of all the aforementioned advantages, the model FEMWATER is very suitable for simulating density-dependent flow and advection-dominant transport. A more satisfactorily solution over the full practical Peclet numbers with Lagrangian methods under finite difference is the method of characteristic (MOC) (Cheng et al., 1984; Kinzelbach, 1987; Häfner et al., 1992).

On the other side, the Front Limitation (FL) algorithm is suitable for the fast numerical solution of advection-dispersion problems. It solves the problem with the control volume method, and uses a split operator with an implicit dispersion and an explicit advection term as well as special front extrapolation technique. The algorithm does not show an upper Peclet number limit. Therefore, it is suitable for application in large scale groundwater pollution forecasting and for parameter identification in such models (Häfner et al., 1997).

Modeling unsaturated flow is more complex than modeling saturated flow for some reasons, unsaturated flow is basically a two fluid flow: gas and water. This is highly complicated, however, even using the simplified approach of RICHARDS (neglecting the gas flow) is still not as easy as saturated flow due to unlinearity of the equation system. RICHARDS equation (Eq. 2.15) requires that the modeler specify the relationship between unsaturated hydraulic conductivity and pressure head (**K** vs. *H*) as well as the soil moisture characteristic curve, which defines the relationship between moisture content and tension (θ vs. *H*). This another simplification is not taken into account the hysteresis between wetting and dewatering of unsaturated media. Thus, there are many uncertainties associated with the development and application of the model (Anderson and Woessner, 1992). Understanding of these uncertainties and their causes is required to correctly interpret model predictions. A very efficient way for a sensitivity and uncertainty analysis of models with many parameters is the Latin hypercube sampling (LHS) procedure (Iman, 1992). For this purpose, FEMWATER was modified to include LHS. With the combination of LHS and FEMWATER (FEMWATER-LHS), one is able to simulate probability distributions of various model outputs.

2.5 Uncertainty analysis

If a sample has been generated, the next step is the propagation of the sample through the analysis. Each element of the sample is transferred to the model in a subroutine, and the corresponding model predictions are saved for use in uncertainty and sensitivity analysis.

In uncertainty analysis associated with Latin Hypercube Sampling, it is desired to estimate the means and the variance for the output. The means and the variance for *Y* can be estimated by

$$E(Y) = \sum_{i=1}^{m} \frac{Y_i}{m} \tag{2.38}$$

and

$$V(Y) = \sum_{i=1}^{m} \frac{[y_i - E(Y)]^2}{(m-1)} \tag{2.39}$$

respectively.

In practice, the distributions of the output variables considered in performance assessment are often highly skewed. Due to the disproportionate impact of large but unlikely values, the estimates for the means and variance associated with such distributions tend to be unstable. Unstable means there is large amount of variation among estimates obtained from independently generated samples. Further, when skewed distributions are under consideration, means and variances give a poor characterization for distribution shape. Basically, means and variances do not contain enough information to characterize highly skewed distributions adequately. Therefore, an estimate of the cumulative distribution function (CDF) gives a better characterization of the uncertainty in an output variable than a mean and a variance (Helton, 1993; Meinrath et al. 2000). Cumulative distribution functions can be estimated from the step function *F*. This function is defined by

$$F(Y) = \begin{cases} 0 & \text{if } Y < Y_1 \\ i/m & \text{if } Y_i \le Y < Y_{i+1}, \quad i = 1,2,\ldots,m-1 \\ 1 & \text{if } Y_m \le Y \end{cases} \tag{2.40}$$

where it is assumed that the Y_i have been ordered $Y_i \le Y_{i+1}$.

Since the first stage of the uncertainty analysis involves some screening of the model variables, the estimated cumulative distribution function can be used as a summary tool in this part of analysis without an undue concern about its probabilistic interpretation (Iman and Helton, 1988). LHS is based on a probabilistic input selection technique. When an output variable *Y* is graphed as an empirical cumulative frequency distribution, an estimate of the CDF is obtained directly.

Fig. 2.4 shows an example of estimated cumulative distribution function. The horizontal axis represents the values for the output variable *Y*, and the vertical axis represents cumulative probability, which is the probability of obtaining a value equal to or less than the probability associated with the individual sample elements. If Latin Hypercube sampling was being used, each observation would be assigned a weight that equal the probability of the stratum from which it was obtained divided by the number of observations from the stratum.

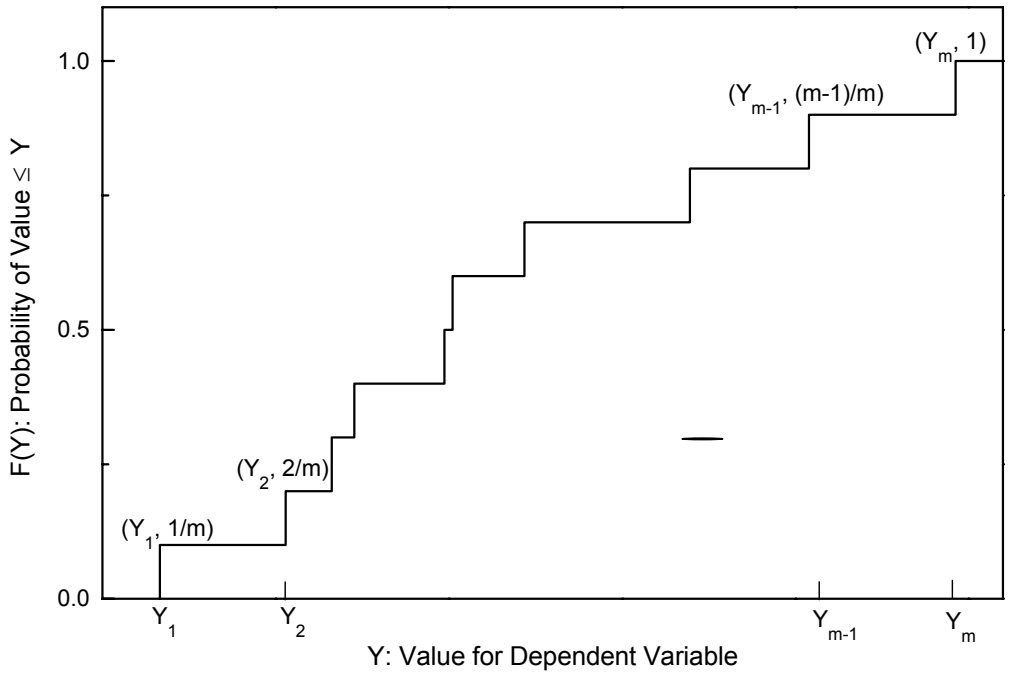

Fig. 2.4 Example of an estimated distribution function.

2.6 Sensitivity analysis

The generation of scatterplots is undoubtedly the simplest sensitivity analysis technique. This approach consists of generating plots of the points (x_{ij}, Y_i), i = 1,2, ..., m, for each input variable x_j.

Sometimes scatterplots alone will completely reveal the relationships between model input and model predictions. This is often the case when only one or two inputs dominate the outcome of the analysis. Further, scatterplots often reveal nonlinear relationships, thresholds and variable interactions that facilitate the understanding of model behavior and the planning of more sophisticated sensitivity studies. The examination of scatterplots is always a good starting point in Monte Carlo sensitivity study. The examination of such plots when Latin Hypercube Sampling is used can be particularly revealing due to the full stratification over range of each input variables (Helton, 1993).

Many of the FEMWATER-LHS output variables are functions of time or location. A useful way to present sensitivity results is with plots of partial correlation coefficients or standard regression coefficients.

Sensitivity analysis in conjunction with Monte Carlo sampling is closely related to the construction of regression models which approximate the behavior calculated by the computer model. Eqs. (2.1) and (2.2) show after making m runs of the model, that the multivariate observations (x_{i1}, ...x_{in}, Y_i); i = 1, 2, ..., m can be used to construct an approximate regression model of the form

$$\hat{Y} = b_0 + \sum_j^n b_j x_j \tag{2.41}$$

where x_j are the input variables. The constant b_o and the regression coefficient b_j are obtained by usual methods of least squares. The ordinary regression coefficients are the partial derivatives of the regression model with respect to the input variables. However, these ordinary regression coefficients are likely influenced by the units in which the variables are measured (i.e. cm hr^{-1}, dm day^{-1}, m day^{-1}, etc.). Therefore, they do not provide a very reliable measure of the relative importance of the input variables. This problem can be eliminated by standardizing all variables used in the regression model by means of Eq. (2.42)

$$x^* = (x - \bar{x})/s_x \tag{2.42}$$

where $\bar{x}$ and s_x are the mean and standard deviation, respectively. Eq. (2.41) can be rewritten in the following standardized form:

$$Y^* = \sum_j^n b_j^* x_j^* \tag{2.43}$$

The coefficients in this standardized model are called standardized regression coefficients. Such coefficients are useful since they can be used to provide a direct measure of the relative importance of the input variables (Iman et al., 1985).

The partial correlation coefficient differs from a simple correlation coefficient in as much that it measures the degree of linear relationship between the x_j and Y after making an adjustment to remove the linear effect of all of remaining variables. The actual calculation involves

finding the inverse of correlation matrix C between the individual x_j's and Y based on m computer runs. The inverse matrix can be written as follows:

$$C^{-1} = \begin{bmatrix} 1/\left(1-R_{x_1}^2\right) & c_{12} & \cdots & c_{1k} & -b_1/\left(1-R_y^2\right) \\ c_{21} & 1/\left(1-R_{x_2}^2\right) & \cdots & c_{2k} & -b_2/\left(1-R_y^2\right) \\ \cdots & \cdots & \cdots & \cdots & \cdots \\ c_{k1} & c_{k1} & \cdots & 1/\left(1-R_{x_k}^2\right) & -b_k/\left(1-R_y^2\right) \\ -b_1/\left(1-R_y^2\right) & -b_2/\left(1-R_y^2\right) & \cdots & -b_k/\left(1-R_y^2\right) & 1/\left(1-R_y^2\right) \end{bmatrix} \tag{2.44}$$

The value b_j in C^{-1} is the standardized regression coefficient; the value R_y^2 is the coefficient of determination from regressing Y on $x_1, x_2, ..., x_k$, and the value $R_{x_j}^2$ is the coefficient of determination from regressing x_j on $Y, x_1, x_2, ..., x_{j-1}, ..., x_k$.

The partial correlation coefficient for x_j and Y is obtained directly from C^{-1} as

$$P_{x_j y} = \frac{-c_{jy}}{\left(c_{jj}c_{yy}\right)^{1/2}} \tag{2.45}$$

Therefore, the partial correlation coefficient can be written as

$$P_{x_j y} = \frac{b_j/\left(1-R_y^2\right)}{\left\{\left[1/\left(1-R_{x_j}^2\right)\right]\left[1/\left(1-R_y^2\right)\right]\right\}^{1/2}} = b_j\sqrt{\frac{1-R_{x_j}^2}{1-R_y^2}} \tag{2.46}$$

Eq. (2.46) shows the close relationship between $P_{x_j y}$ and b_j ; however, it is important to recognize that they yield different types of information. Standardized regression coefficients are from a conditional univariate distribution, while partial correlation coefficients stem from a conditional bivariate distribution.

When the relationship between x_j and Y is basically nonlinear but monotonic, it is often more revealing to calculate standardized regression coefficients and partial correlation coefficients on variable ranks than on the actual values for the variables. Such coefficient are known as standardized rank regression coefficients (SRRC) and partial rank correlation coefficients (PRCC). Specifically, the smallest value of each variable x_j is assigned the rank 1, the next smallest value is assigned rank 2, and so on up to the largest value which is assigned the rank m, where m denotes the number of observations or the number of computer runs. If ties are

found among the x_j, then average tied ranks is used for the range of x_j. The standardized regression coefficient and/or partial correlation coefficient are calculated on these ranks. This transformation converts the sensitivity measure from one linearity between x_j and Y to one of monotonicity between x_j and Y. A computer program (Iman et al., 1985) for performing such calculations has been developed at Sandia National Laboratories.

2.7 Program description

The FEMWATER-LHS can be used to simulate saturated-unsaturated flow and contaminant transport including density driven flow. This program is also capable of performing sensitivity and uncertainty analysis (hydraulic conductivity, porosity, water content, etc.). Therefore, the uncertainty and sensitivity associated with the predictions have to be quantified. Consequently, this program provide this capability by utilizing Latin Hypercube simulation techniques. For a better performance, FEMWATER-LHS source code has been compiled with 32 bit compiler (GNU Fortran g77 v05.5.25 for Win32).

FEMWATER-LHS can be run in LHS mode so that probabilistic estimates of the material properties parameters of the saturated-unsaturated zone from the source area can be made.

A schematic representation for the uncertainty and sensitivity analysis is given in Fig. 2.5. The analysis involves the following steps:

1. Mesh generation, setting the input parameters and importing data from GIS (Geographical Information System). There are some file format that can be imported, such as simple TEXT, DXF (AutoCAD format), Images (GIF, TIFF, Xbitmap, MacPaint, Windows DIB, Sun Raster or Nexpert Objects Images format), and Shape (ArcView™ format) files

2. Obtaining random samples from the probability distributions of the inputs

3. Performing FEMWATER-LHS for the combination of sampled inputs

4. Performing CALSTATS and PCCSRCP for the calculation of the cumulative distributions, means, variance and partial correlation coefficients or standard regression coefficients

5. Statistical analysis of the model outputs, see Section 2.5 and 2.6.

It should be noted that BIN2ASC is a program running behind the FEMWATER-LHS for

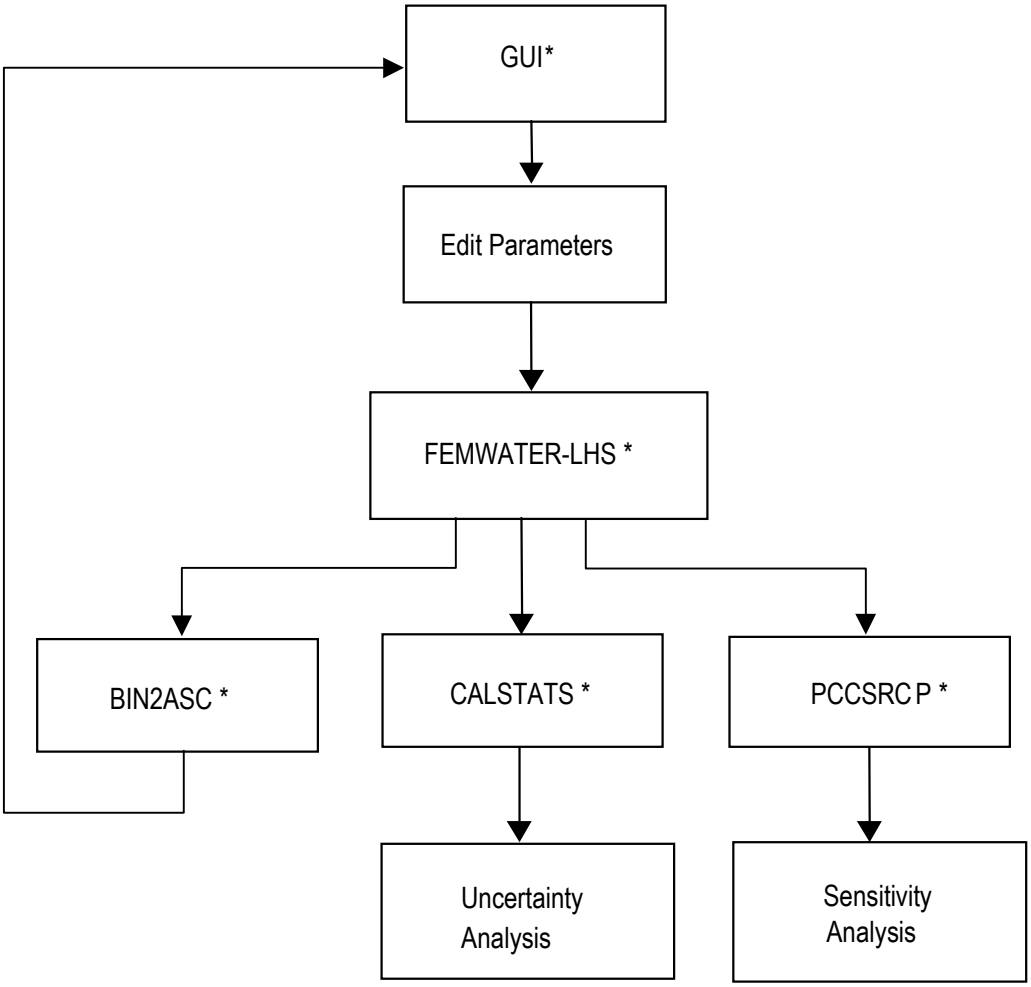

Fig. 2.5 Schematic representation of example analysis. (*): programs.

visualizing the results in deterministic mode.

2.7.1 General settings

Numerical models like FEMWATER-LHS can not be regarded as representations of the real world because the complexity of natural hydrogeologic systems can never be captured in the discretized parameters of a numerical model. Instead, numerical modeling should be understood as a means of testing hydrologic hypotheses based on model parameters that best represent measured phenomena. However, testing hydrogeologic hypotheses often becomes

time consuming because numerical models require complex data. To facilitate the modeling process, graphical-user interfaces (GUI's) are needed to handle geospatial information and simulation control parameters, as well as visualize the simulated results. For this purpose, a FEMWATER-GUI has been developed using Borland Delphi™ Professional 4.0. This GUI for FEMWATER-LHS was developed using commercially available software developed by Argus Interware. The Argus Interware product, known as Argus Open Numerical Environment (Argus ONE™), is a model-independent, programmable system with Geographic-Information-System-like (GIS-like) functionality that includes automated griding and meshing capabilities for synthesizing geospatial information and linking it with finite difference and finite element discretizations techniques. This GUI's must be used in conjunction with the Argus ONE commercial package. Together, these codes provide a convenient graphical pre- and post-processor, that significantly reduce the time and effort required for use of FEMWATER-LHS as hydrogeologic tool.

The FEMWATER-GUI dialog boxes are used to enter simulation control parameters and other nonspatial information. To enter project information for a FEMWATER-LHS simulation, the FEMWATER-GUI is launched from the **PIEs** menu by choosing **New FEMWATER Project**. The information in these dialog boxes is synthesized to build the structure of geospatial information layers needed for the FEMWATER-LHS simulation. In the following, the selected parameters in each of the dialog boxes are described. A complete description of the parameters is contained in 3DFEMWATER/3DLEWASTE reference manual (Yeh et al., 1993), FEMWATER (GMS version) reference manual (Lin et al., 1997), and the user's guide for LHS program (Iman et al., 1984). However, a step-by-step applications of FEMWATER-LHS is given in Appendix B. In most cases, the default values are appropriate.

2.7.1.1 FEMWATER-LHS Type of Simulation Problem

The *FEMWATER-LHS Type of Simulation Problem* dialog (Fig. 2.6) allows the user to choose the type of simulation problem to be solved with FEMWATER-LHS.

If the user exits this window, the FEMWATER-LHS interface will have been configured, and the problem type cannot be changed without starting over with a **PIEs|New FEMWATER Project**.

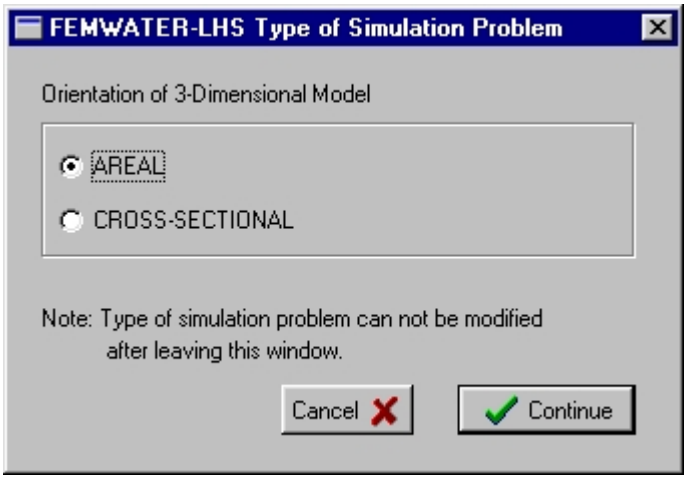

Fig. 2.6 Type of Simulation Problem dialog.

2.7.1.2 Model Title and Type

The *Model Title and Type* dialog (Fig. 2.7) allows the user to choose the type of model and simulation to be solved with FEMWATER-LHS, and enter the information related to the description of the simulation.

Type of Model (KMOD)

Two options are available for designating the type of models to be performed by FEMWATER-LHS:

1. Perform a flow model only

2. Perform a coupled flow and transport model

With a couple flow and transport simulation, either density-dependent flow or density independent flow can be simulated. This option is controlled by entering the appropriate parameters defining the relationship between concentration and density and concentration and viscosity. This parameters are entered in *Fluid Properties* dialog described in Section 2.7.1.7.

Type of Simulation (LHSON)

Two options are available for designating the type of simulations to be performed by FEMWATER-LHS:

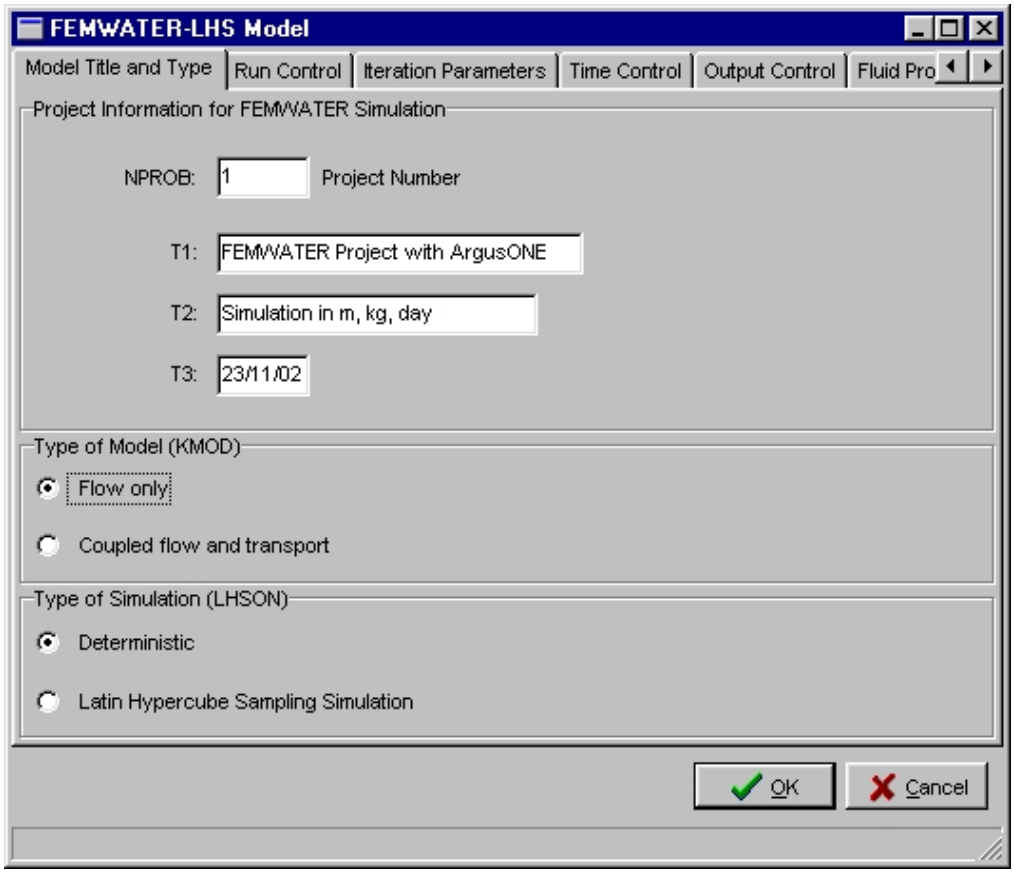

Fig. 2.7 Model Title and Type dialog.

1. Perform a deterministic simulation

2. Perform a Latin Hypercube Sampling Simulation

   This option implies that the appropriate parameters describing the LHS variables must be entered by the user. These parameters are entered in the *Latin Hypercube Sampling* dialog described in Section 2.7.1.10.

2.7.1.3 Run Control Parameters

The *Run Control* dialog is shown in Fig. 2.8 This dialog used to enter a set of general analysis options.

Steady State vs. Transient (KSS/KSST)

FEMWATER-LHS can be run in either a steady state or transient mode. The steady state mode is only allowed when *Flow only* has been selected.

Element Tracking and Particle Tracking Pattern (IDETQ)

The *Element Tracking* edit box and *Element Tracking and Particle Tracking Pattern (IDETQ)* check box are used to edit parameters relating to how the particle tracking is carried out by FEMWATER-LHS during the transport phase. Particle tracking, as its name implies, is a means of using numerical results to track fictitious individual particles across a numerical model mesh, approximating the advection of the contaminant front. In order to accurately track particles over large elements with large velocity gradients, it is sometimes necessary to subdivide the individual elements into smaller subelements.

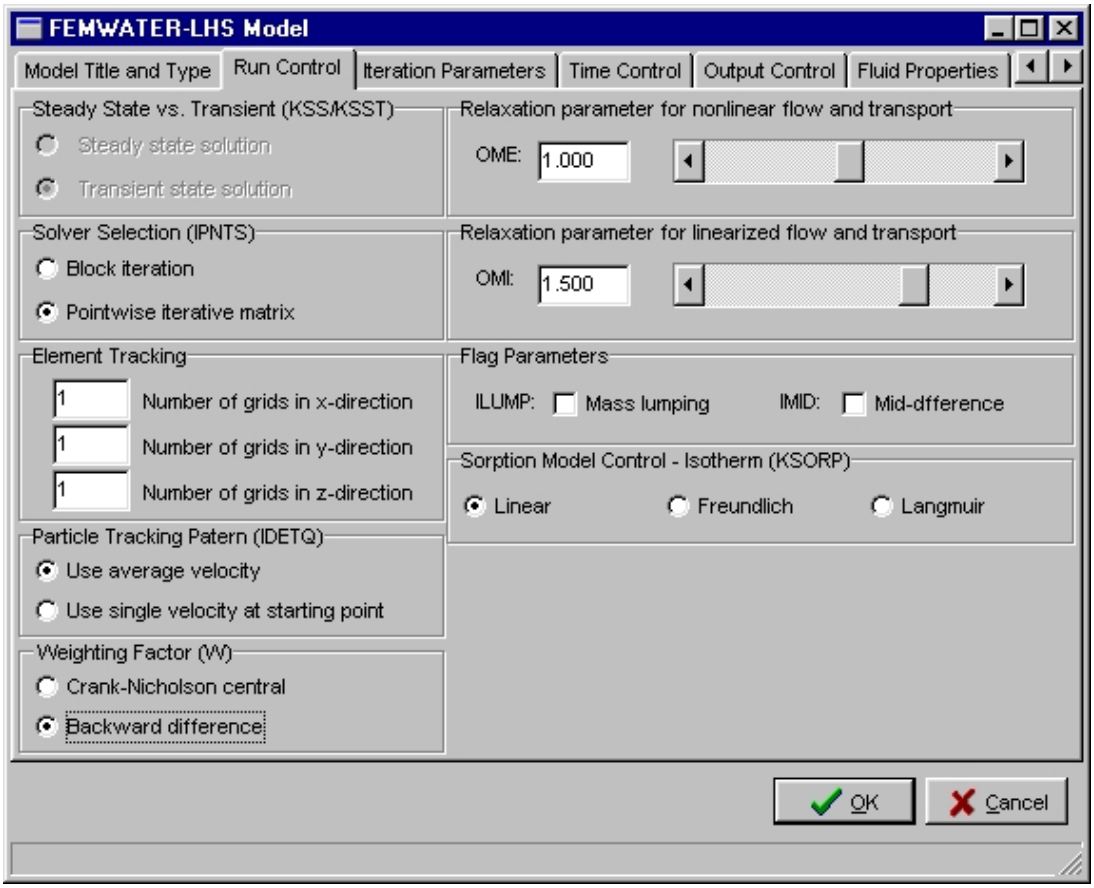

Fig. 2.8 Run Control dialog.

Solver Selection (IPNTS)

Two solvers are provided in FEMWATER-LHS:

1. Block iterative solver. As a general rule, subregions comprised of vertical or sub-vertical nodal slices provide the smallest half-bandwidth and will perform well in the block

iterative method, although this may not always be the case. For some problems, horizontal slicing may be advantageous. The block iterative logic contains a relaxation factor which can be used to over-relax the solution and help accelerate the rate of convergence (Yeh et al.,1993).

2. Pointwise iterative matrix solver. The Point iterative matrix solver employs the basic successive iterative method to solve the matrix equation, including the Gauss-Seidel method, successive under relaxation, and successive over relaxation. When the resulting matrix is diagonally dominant, the pointwise iterative solver provides a convergent solution. This solver is preferred because it is more robust than the other solvers (Lin et al., 1997).

2.7.1.4 Iteration Parameters

The *Iteration Parameters* dialog shown in Fig. 2.9 is used to enter the iteration parameters for each simulation type (flow only or coupled flow and transport).

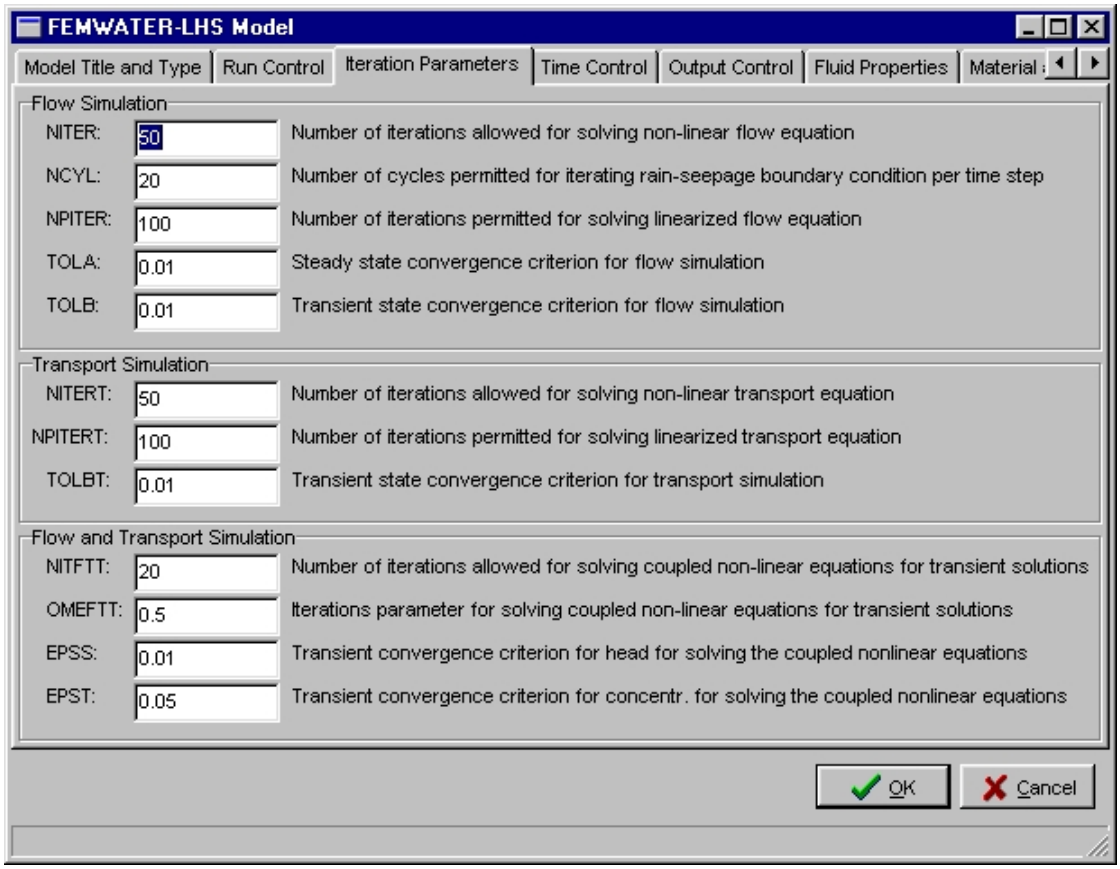

Fig. 2.9 Iteration Parameters dialog.

2.7.1.5 Time Control

The *Time Control* dialog is used to enter the data used by FEMATER-LHS to describe the time of simulation. For a constant time-step size, the number of time steps, NTI is obtained by dividing the simulation time by the time-step size, DELT. If the time-step size is variable, this number is can be computed by NTI = I1 + 1 + I2 + 1, where I1 is the largest integer not exceeding Log(DELMAX/DELT)/Log(1+CHNG), I2 is the largest integer not exceeding (RTIME-DELT*((1+ CHNG)**(I1+1)-1)/CHNG)/DELMAX, RTIME is the real simulation time, DELMAX is the maximum time-step size, DELT is the time-step size used for the first time-step computation if the variable CHNG is not equal to 0.0, and CHNG specifies how much of an increase one would like to make to the time-step size for each subsequent time step. If a steady state solution is desired, NTI should be set equal to zero. The dialog is shown in Fig. 2.10.

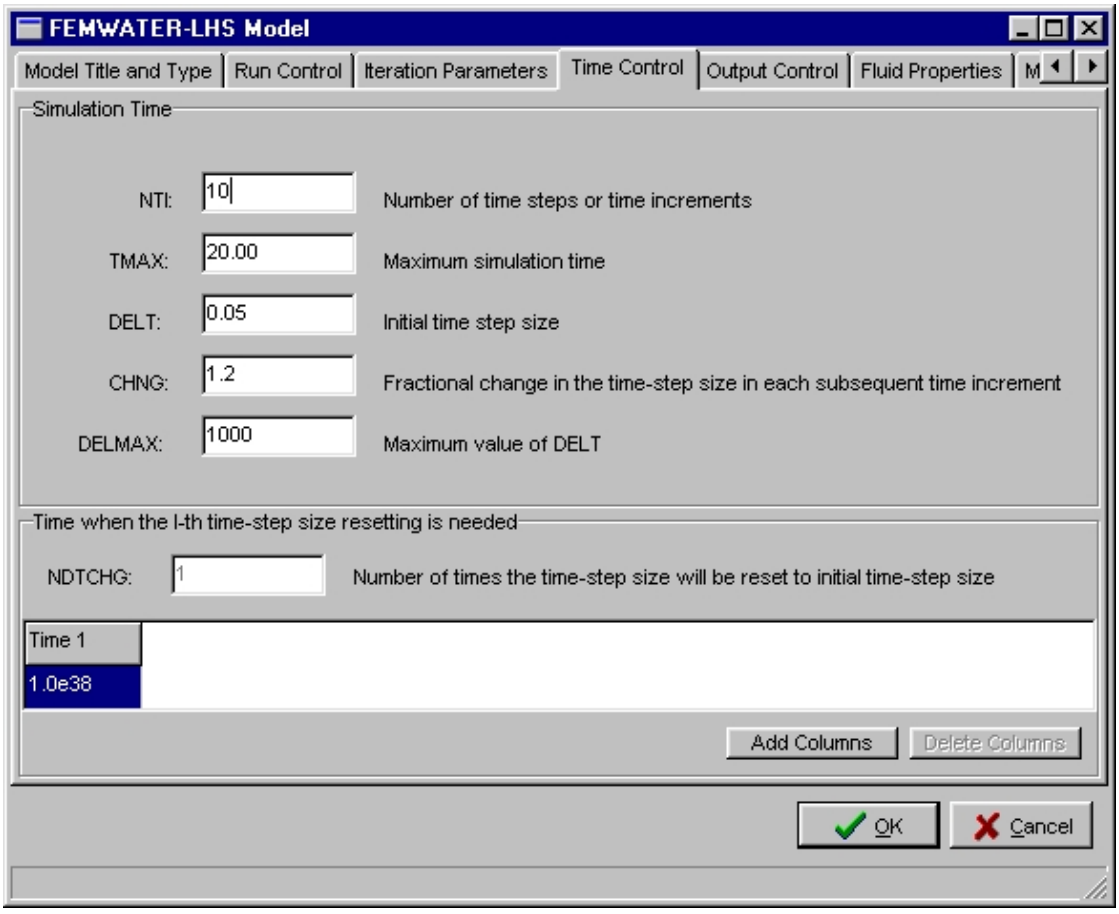

Fig. 2.10 Time Control dialog.

2.7.1.6 Output Control

The *Output Control* dialog is used to select parameters defining what type of output will be printed from FEMATER-LHS. The dialog is shown in Fig. 2.11.

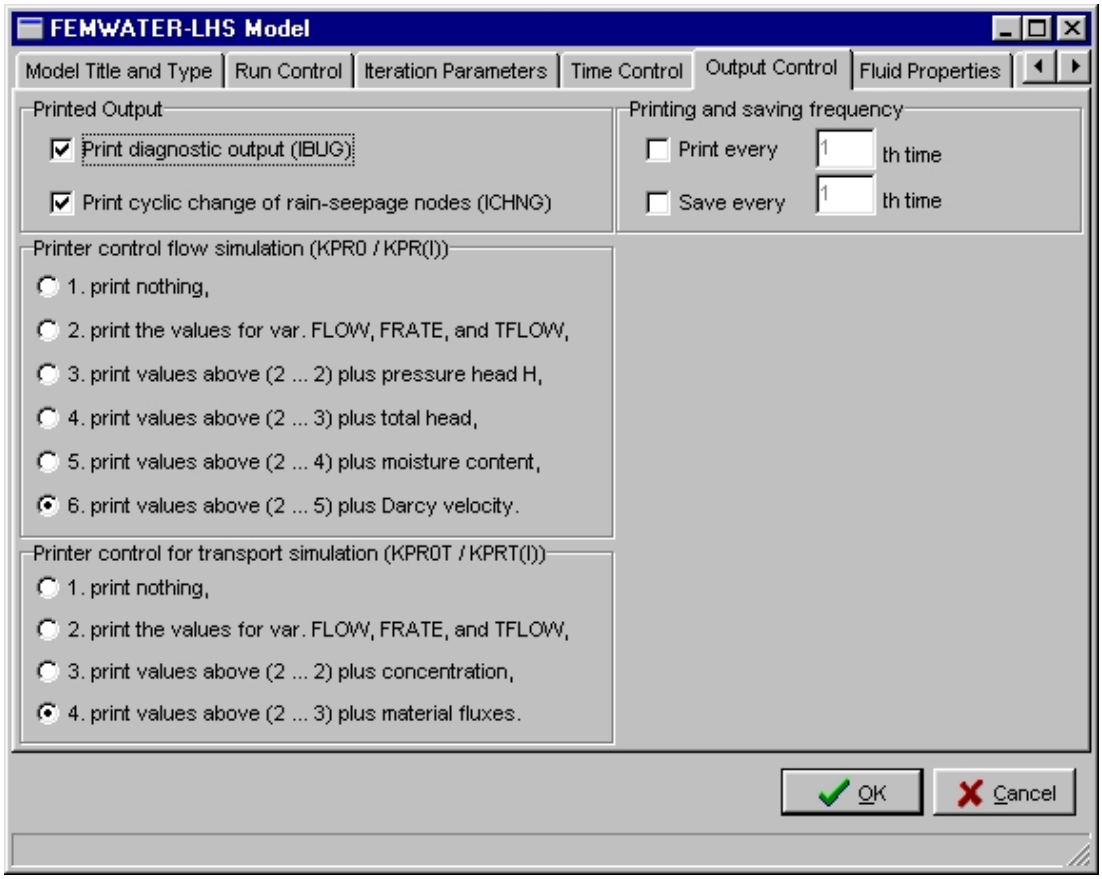

Fig. 2.11 Output Control dialog.

2.7.1.7 Fluid Properties

The *Fluid Properties* dialog is used to specify the acceleration of gravity and the density, viscosity of fluid. Specifying the acceleration of gravity allows the user to use any desired units for the fluid properties, soil properties, and all other parameters input to FEMWATER-LHS. All parameters should be consistent with the units of the specified acceleration of gravity (e.g. GRAV = 7.316×10^{10} m day^{-2}, VISC = 1.1232×10^{4} kg m^{-1} day^{-1}) and RHO = 1.0×10^{3} kg m^{-3}).

For a density-driven flow and transport simulation, the relationships between concentration, density and viscosity must be defined. The relationships used by FEMWATER-LHS are Eqs.

(2.17a) and (2.17b). Thus, values of coefficients a_1, ..., a_8 must be specified by the user. The dialog is shown in Fig. 2.12.

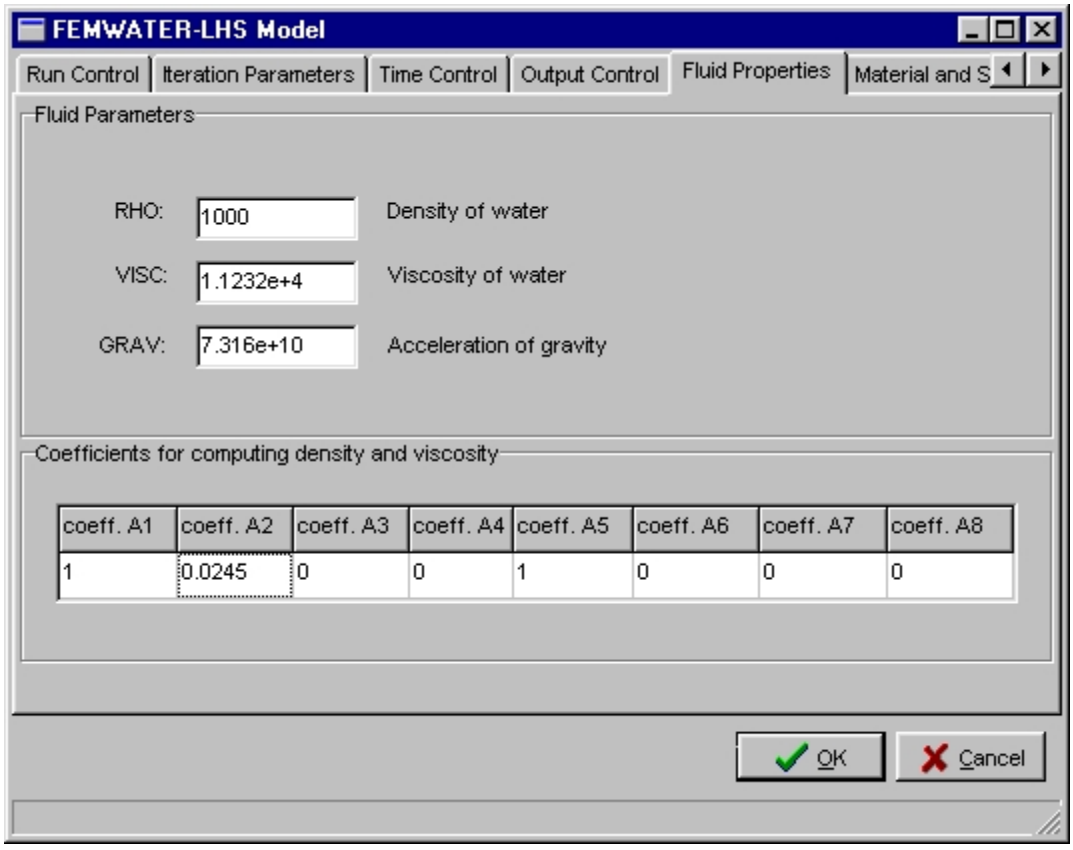

Fig. 2.12 Fluid Properties dialog.

2.7.1.8 Material and Soil Properties

Conductivity/Permeability (KCP)

Hydraulic conductivity is the coefficient of proportionality which appears in Darcy's Law. For three-dimensional flow in an anisotropic medium, hydraulic conductivity varies with direction at any point in space and is expressed as a symmetric second-rank tensor (Eq. 2.16b). Permeability is equal to hydraulic conductivity multiplied by a scalar value, as is seen in Eq. (2.16a).

Material and Soil tabs

As a quadrilateral finite element mesh is generated, a default material is defined and each element (quasi-3D element) in the mesh has a default material type associated with it. The dialog is shown in Fig. 2.13. The first two tabs in the dialog are follows:

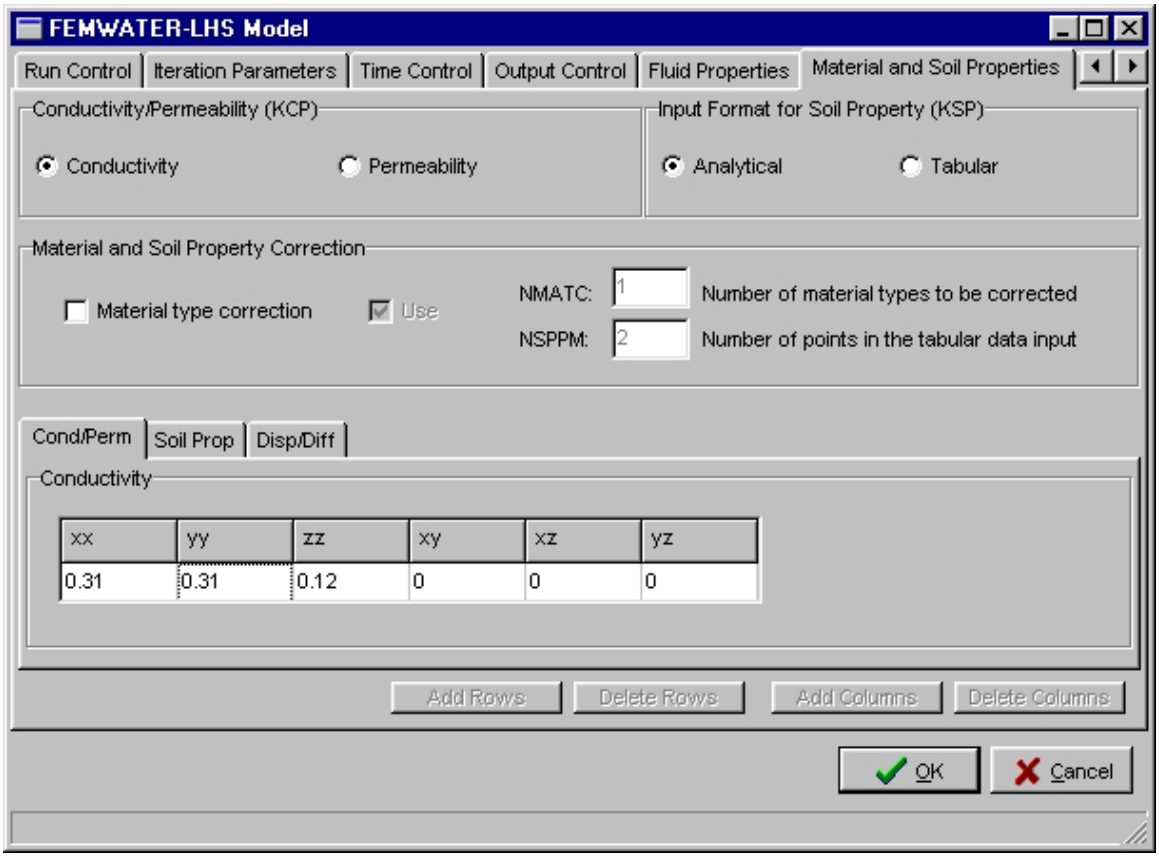

Fig. 2.13 Material and Soil Properties dialog; Cond/Perm

1. Hydraulic Conductivity or Permeability (*Cond/Perm*)

   The hydraulic conductivity or permeability tensor for the default material is entered in the tabular format (Fig. 2.13). Since the tensor is symmetry, only 6 of the 9 terms are needed (K_{xx}, K_{yy}, K_{zz}, $K_{xy} = K_{yx}$, $K_{xz} = K_{zx}$ and $K_{yz} = K_{zy}$).

2. Soil Property Parameters (*Soil Prop*)

   Analytical equations developed by van Genuchten (1980) are used in the code to describe the relationship between pressure head (H) and moisture content (θ) and the relationship between relative hydraulic conductivity (K) and moisture content (θ) (see Eq. 3.5 through 3.9). In order to solve these equations, five parameters must be entered in the tabular for the default material type: residual moisture content (θ_r), saturated moisture content or porosity (θ_s), air entry pressure head (h), and two soil-specific empirical parameters, α and β.

If the *Coupled flow and transport* model in *Model Title and Type* dialog is selected, the *Disp/Diff* tab in the *Material and Soil Properties* dialog is visible. The transport parameters (i.e. distribution coefficient (K_d), bulk density (ρ_b), longitudinal (α_L) and transverse (α_T) dispersion, molecular diffusion coefficient (α_m), tortuosity (τ), radioactive decay (λ) and Freundlich n or Langmuir S_{max} (K)) associated with the default material are displayed in the dialog and can be edited.

Material and Soil Property Correction

To make the *Correction Cond/Perm*, *Correction Soil Prop* and *Correction Disp/Diff* tabs visible and enter the available data of the material correction properties the *Material types correction* check box must be checked (Fig. 2.14). This also offers the ability to add rows for more correction material types. Each of these material correction types can be assigned to a element within elemental layer, the element should be selected with the *Close Contour* or *Open Contour* tool. An example about the spatial differences for the correction material types

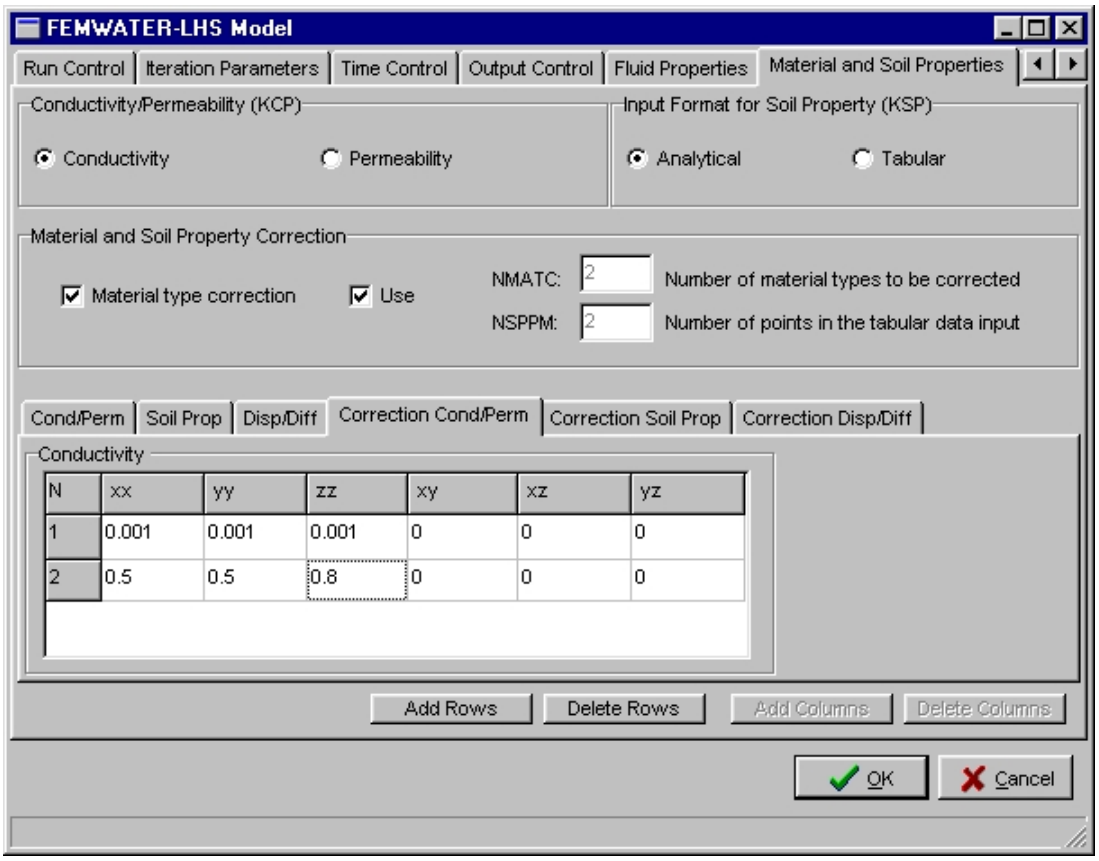

Fig. 2.14 Material and Soil Properties dialog; Correction Cond/Perm

shown in Fig. 2.15. This figure shows three types of the material: the default material, material correction type 1 and 2.

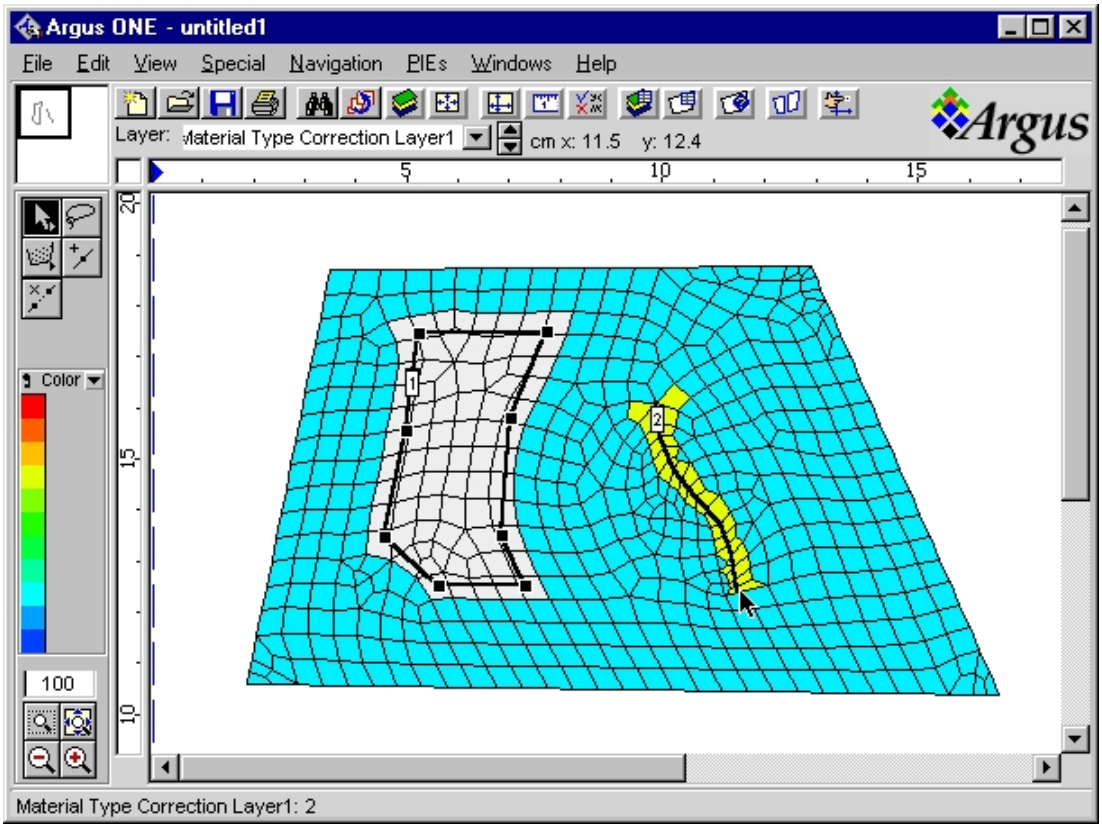

Fig. 2.15 Mesh representation of the material correction types within elemental layer.

2.7.1.9 Layer and Calibration

The *Layer and Calibration* dialog is used to add or delete the number of nodal layers or elemental layers. A simple areal model layers that represent a quasi-three-dimensional are illustrated in Fig. 2.16. This figure represent 2 elemental layers and 3 nodal layers with several elements and nodes for each layer. The dialog is shown in Fig. 2.17.

To add a layer, the cursor is moved to the table listing the layers and a layer is select by clicking on it. Clicking the **Add** button adds a layer below the highlighted layer. This provides a quasi-three-dimensional finite element mesh, that means extrude two-dimensional finite elements as prisms.

To delete a layer from the list, the cursor is moved to the table listing the layers. Clicking the row in the table highlights and then clicking the **Delete** button removes the layer from the list.

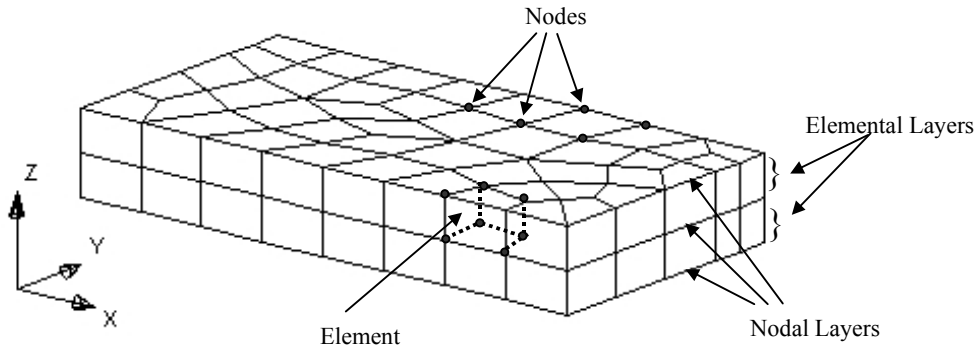

Fig. 2.16 Schematic diagram of a quasi-three-dimensional model.

The remaining layers are renumbered. It is important to note that deleting a layer will delete the geospatial information layers and all information in those layers. This information will be deleted once the **OK** button is clicked; clicking the **Cancel** button will cancel changes made in the dialog.

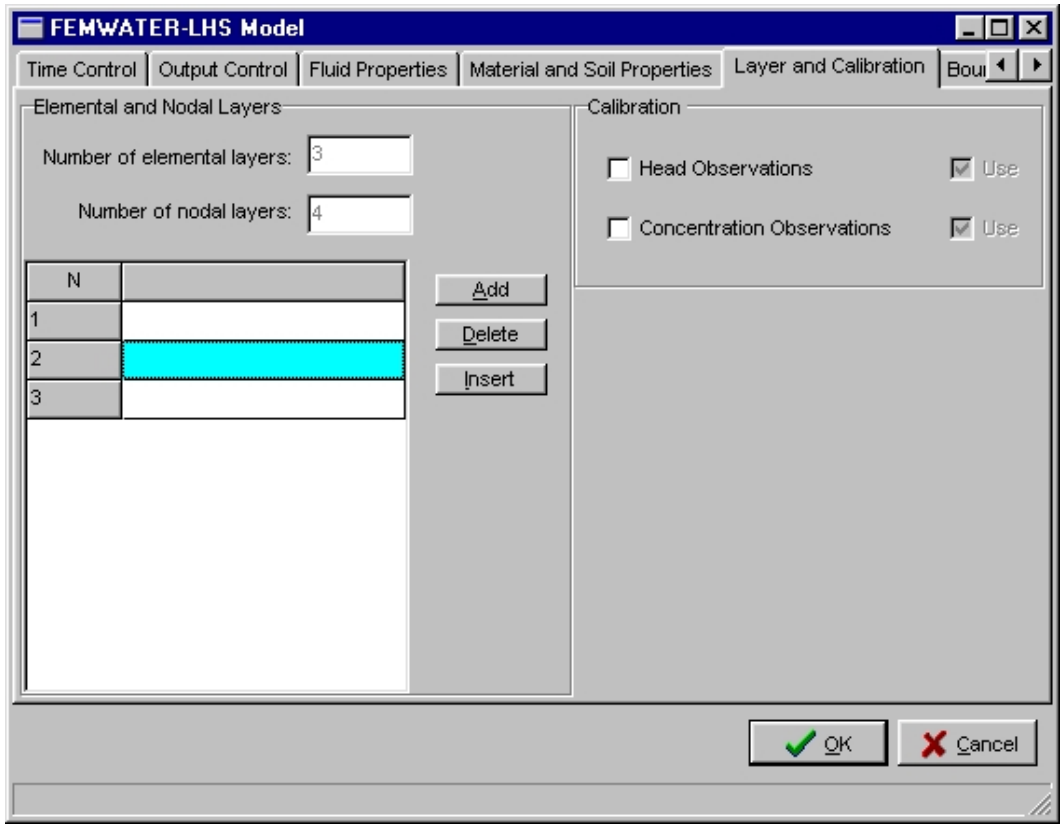

Fig. 2.17 Layer and Calibration dialog.

If the *Head Observations* and/or *Concentration Observations* check box is checked, then it is enable to create and specify some observation points for head and/or concentration in the model to be used in the model calibration.

2.7.1.10 Latin Hypercube Sampling

The *Latin Hypercube Sampling* dialog (Fig. 2.18) allows the user to select distributions for key parameters from a variety of distributions; normal and lognormal, uniform, triangular, discrete probability and empirical. The user may also specify correlations between the input parameters. The model then executes a prespecified number of runs.

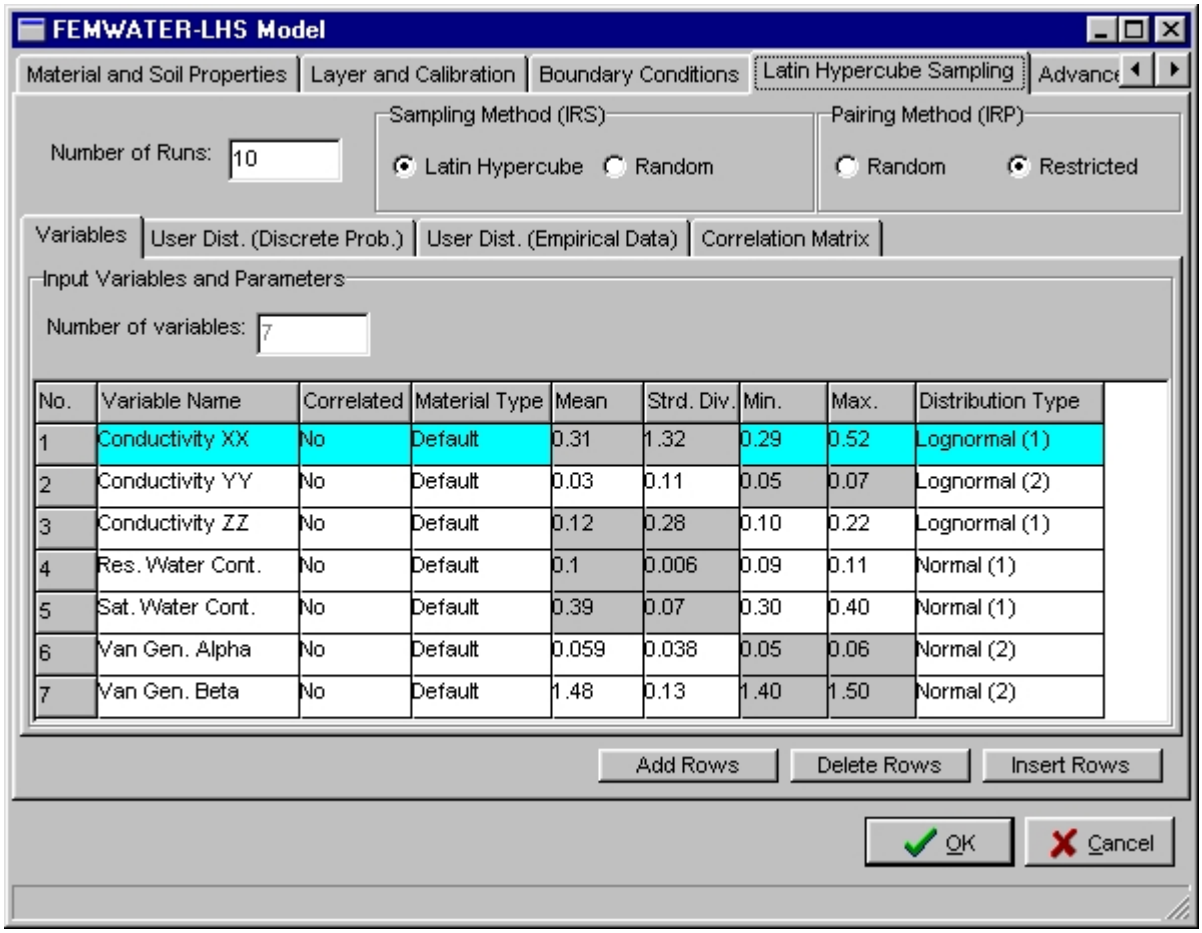

Fig. 2.18 Latin Hypercube Sampling dialog.

2.7.2. Boundary Conditions

A set of boundary conditions must also be defined on the *Boundary Condition* dialog in order to complete the input required by FEMWATER-LHS.

A set of rules or guidelines for determining the appropriate set of boundary conditions for particular problem is presented in the 3DFEMWATER/3DLEWASTE Reference Manual (Yeh et al., 1993).

2.7.2.1 Dirichlet Boundary Conditions

The dialog that appears depends on whether *Flow only* or *Coupled flow and transport* model is selected in *Model Title and Type* dialog. If the *Coupled flow and transport* is selected, the dialog shown in Fig. 2.19 appears.

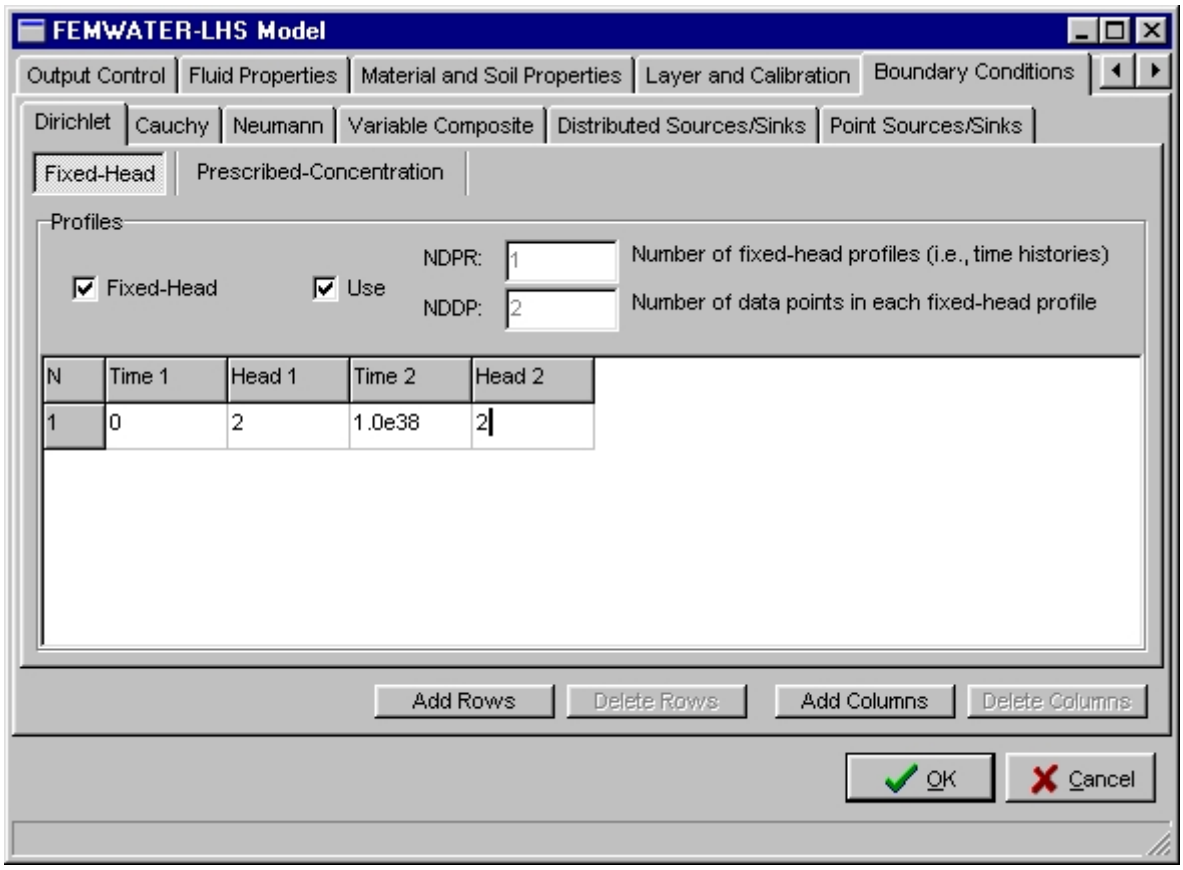

Fig. 2.19 Boundary Conditions dialog; Dirichlet.

Fixed head boundary conditions in FEMWATER-LHS are assigned as total head. FEMWATER-LHS converts the total head to pressure heads internally. Heads can be specified as a constant value (unlimited time) or allowed to vary with time (transient value) at several nodes.

To enter the available data of the total head the *Fixed-Head* check box must be checked. This also offers the ability to add rows for more Dirichlet boundary condition types and add columns for more time-dependent values.

The concentration can also be specified as either a constant or transient value. In that case the **Fixed-Head** button has to be cleared. If a concentration is defined via Dirichlet boundary condition this means a fixed concentration at the certain node and it does not represent the concentration of the incoming fluid. For more details read Appendix B.

2.7.2.2 Cauchy, Neuman and Variable Composite Boundary Conditions

If the *Cauchy*, *Neuman* or *Variable Composite* tab is clicked, the dialog shown is identically with Fig. 2.19. *Cauchy*, *Neuman* and Variable Composite Boundary Conditions are flux-type boundary conditions. Both flux and concentration can be assigned independently. In both cases, the type must be designated as either *Cauchy*, *Variable Composite* or *Neuman*. The value can be defined as a constant or transient value. For more details read Appendix B.

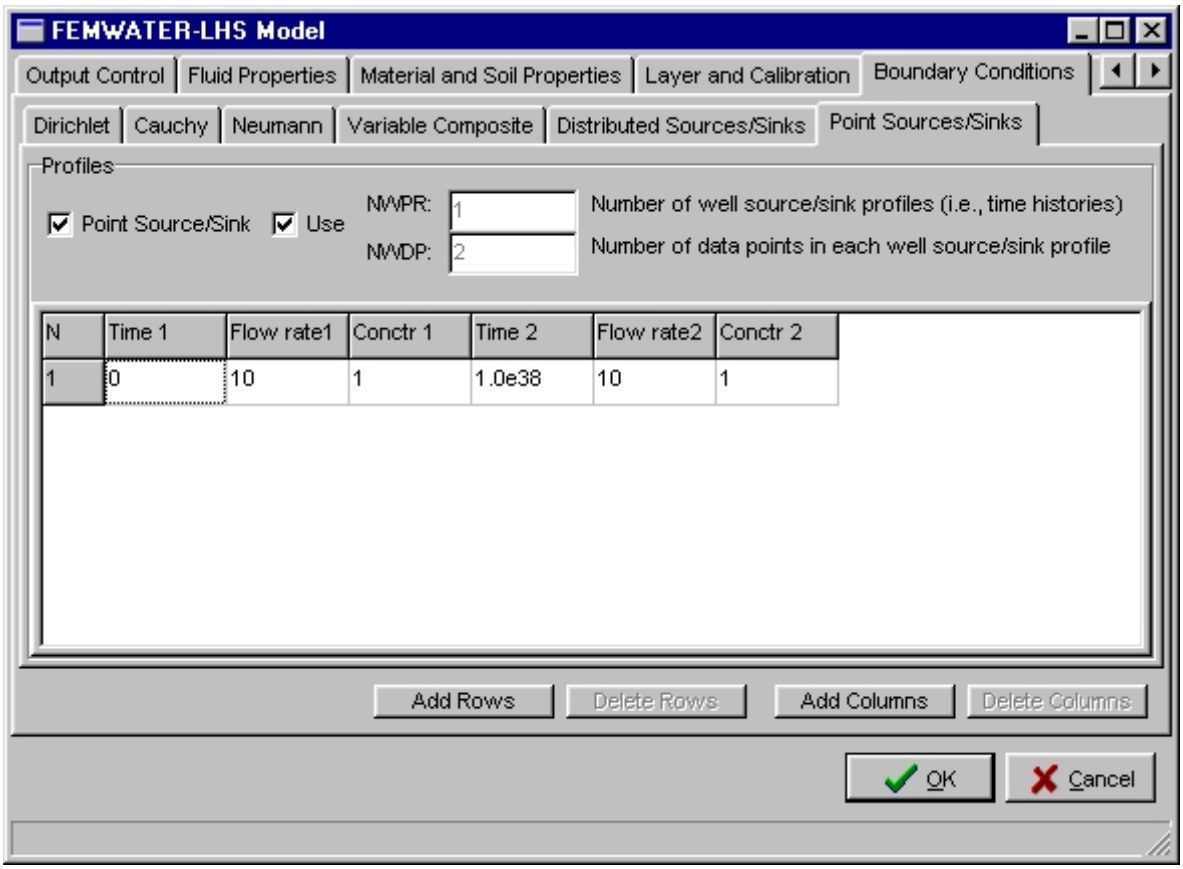

Fig. 2.20 Boundary Conditions dialog; Point Sources/Sinks.

2.7.2.3 Distributed and Point Source/Sink Boundary Conditions

The *Distributed* and *Point Source/Sink Boundary Conditions* commands are used to assign a flux rate to the node. The *Distributed Source/Sink* option is typically used to assign flux rate per unit volume for each distributed source element. This option allows a user modeling a large area to approximate the influence of several wells within one element. The *Point Source/Sink* option is generally used to assign flux rates to interior nodes to simulate injection or extraction wells. If the *Distributed Source/Sink* or *Point Source/Sink* tab is activated, the dialog shown is identically with Fig. 2.20.

Both a flow rate and a concentration may be specified at a source/sink element or node. The values can be constant or transient. For more details read Appendix B.

3. VERIFICATION AND APPLICATIONS

3.1 Verification

To test the consistency of the revised LHS program, an illustrative example reported by Iman (1992) is presented. This example shows the LHS capabilities to generate samples and the probabilistic coverage. To verify FEMWATER-LHS, three illustrative examples reported by Yeh (1999) and Yeh (2000) are presented. Example 1 is a drainage problem in a parallel plate. Example 2 is a two-dimensional transport in a rectangular region. Example 3 is Henry's saltwater intrusion problem.

3.1.1 The Probabilistic Coverage Provided by LHS

Assume U and V are input variables for the LHS program being uniformly distributed random variables on the interval (0,1). Table 3.1 gives the values for two random samples of size m = 10 that have been selected from this distribution as output from the program, with U denoting the first sample and V denoting the second sample. The values in Table 3.1 are paired in random order in which they were produced by the random sampling process for each sample.

Table 3.1 Two random samples of size m = 10 for a random variable uniformly distributed on [0,1].

Observation Number	U	V
1	0.305	0.704
2	0.558	0.716
3	0.268	0.346
4	0.21	0.91
5	0.466	0.933
6	0.146	0.157
7	0.311	0.191
8	0.865	0.499
9	0.466	0.367
10	0.658	0.0933
Sample Mean	0.425	0.492
Sample Variance	0.049	0.095

In Fig. 3.1*a* shows a scatterplot of the ten pairs of observations in Table 3.1. No observations were selected for U in the 1st, 8th and 10th intervals, and no observations were selected for V in the 2nd,7th and 9th intervals. Figure 3*b* repeats the scatterplot of the points in Table 3.1 with a rectangle added to the plot to indicate the probabilistic coverage of the UV input space. Using the maximum and minimum values for U and V from Table 3.1, the probabilistic coverage is calculated to be

$P(0.146 \le U \le 0.865) \times P(0.0933 \le V \le 0.933) \times 100\% = 60\%$

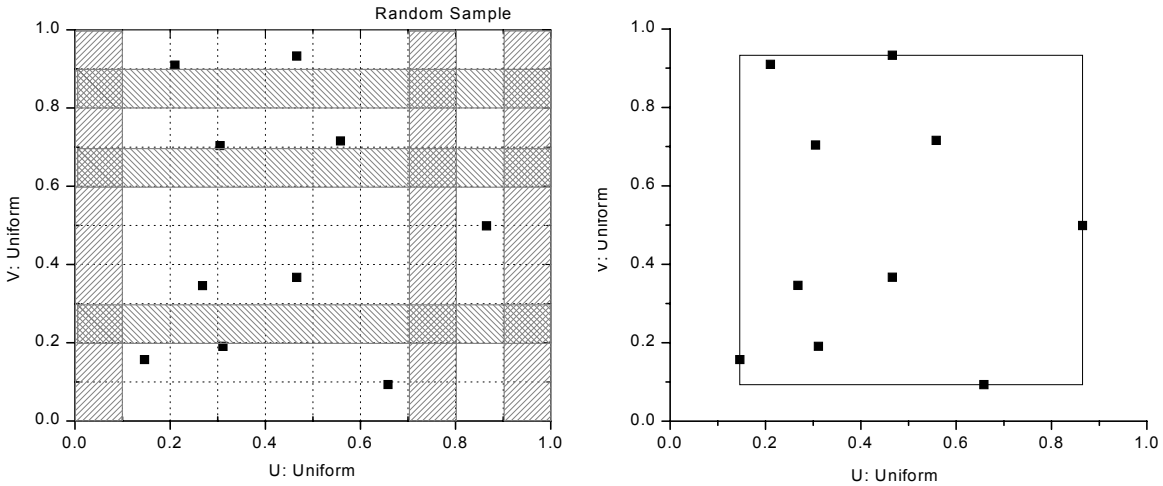

(a) (b)

Fig. 3.1 A scatterplot (a) and probabilistic coverage (b) of the input space for two random samples in Table 3.1.

The selection process was repeated for two LHS's of size m = 10 with the same random seed used to generate the two random samples shown in Table 3.1. These value are given in Table 3.2. The values in Table 3.2 were randomly paired after they were generated. Fig. 3.2*a* gives a scatterplot of the pairs of observations in Table 3.2.

It is obvious that exactly one observation occurs in each of the 10 intervals on both the U and V axes. In fact, this is the nature of the LHS process, no matter how the equal-probable intervals for each input variable are. Fig. 3.2*b* repeats the scatterplot of the points in Table 3.2 with a rectangle added to the plot to indicate the probabilistic coverage of the UV input space.

Table 3.2 Two Latin hypercube samples of size $m = 10$ for a random variable uniformly distributed on [0,1].

Observation Number	U	V
1	0.331	0.619
2	0.727	0.791
3	0.266	0.393
4	0.13	0.85
5	0.521	0.916
6	0.0466	0.109
7	0.415	0.27
8	0.956	0.535
9	0.687	0.472
10	0.847	0.0367
Sample Mean	0.493	0.499
Sample Variance	0.094	0.092

Using the maximum and minimum values from Table 3.2 the probabilistic coverage is calculated to be

$P(0.0466 \le U \le 0.956) \times P(0.0367 \le V \le 0.916) \times 100\% = 80\%$

The probabilistic coverage of UV input space provided by LHS (80%) is greater than the

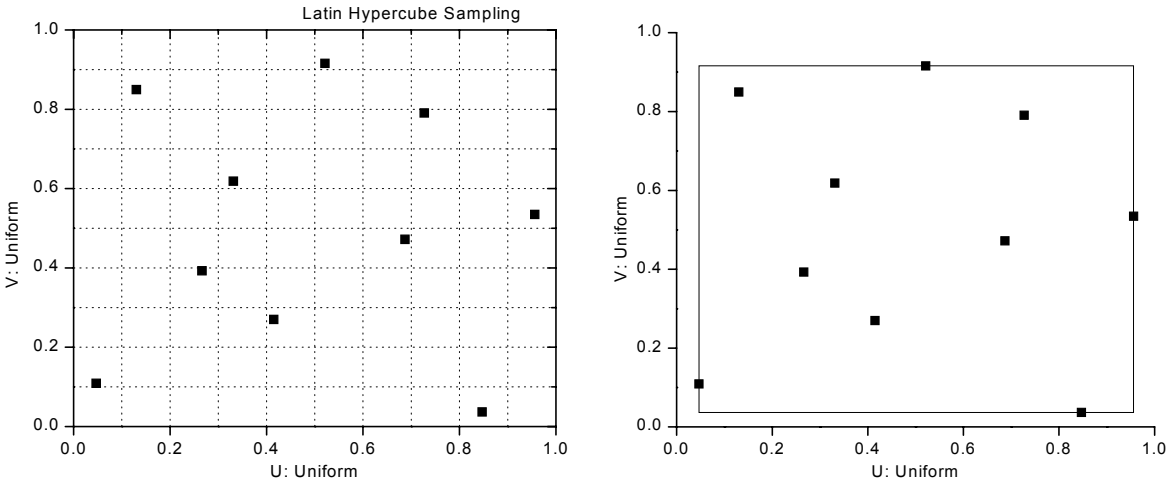

(a) (b)

Fig. 3.2 A scatterplot (a) and probabilistic coverage (b) of the input space for two LHS's in Table 3.2.

probabilistic coverage provided by random sampling (60%) in this example. However, is this observed difference in probabilistic coverage a change in general? Iman (1992) has shown that the expected coverage for two variables under random sampling is given as

$$\left(\frac{m-1}{m+1}\right)\times 100\% \tag{3.1}$$

The expected coverage for two variables under LHS is given as

$$\left(\frac{m-1}{m}\right)\times 100\% \tag{3.2}$$

When m = 10, Eq. (3.1) gives 66.9%, thus the observed probabilistic coverage of 60% for the samples in Table 1 is close to the expected coverage. For LHS, Eq. (3.2) gives 81% coverage, thus no significant difference to the observed probabilistic coverage of 80% for the samples in Table 3.2. can be seen.

Since therefor for $m \geq 2$ the expression in Eq. (3.2) is always greater that the expression in Eq. (3.1), LHS can be expected to provide better probabilistic coverage of input space than a simple random sample.

3.1.2 Two-Dimensional Drainage Problem

This example was chosen to test the scheme for handling infiltration boundary condition under steady state flow condition. This problem is presented by Huyakorn et al. (1986) and Yeh (1999). The region of interest is bounded on the left and right by parallel drains fully penetrating the medium, on the bottom by an impervious aquifuge, and on the top by an air-soil interface (Fig. 3.3). The case considered in this work corresponds to a situation where it is necessary to apply the atmospheric pressure head constraint to avoid surface ponding. The distance between the two drains is 20 m (Fig. 3.3). The medium is assumed to have a saturated hydraulic conductivity of 0.01 m/d, a porosity of 0.25, and a field capacity of 0.05. The unsaturated characteristic hydraulic properties of the medium are given as

$$\theta = \theta_s + (\theta_s - \theta_r)\frac{A}{A + |h - h_a|^B} \tag{3.3}$$

and

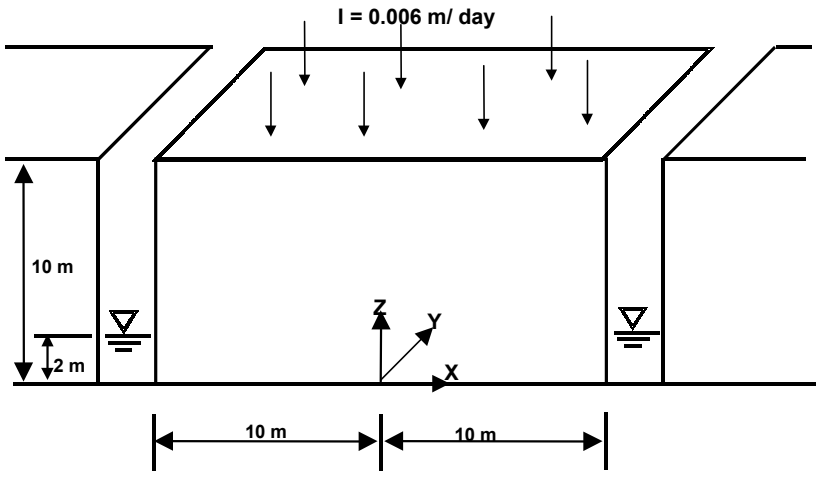

Fig. 3.3 Problem definition for two-dimensional steady-state flow to parallel drains (Yeh, 1999).

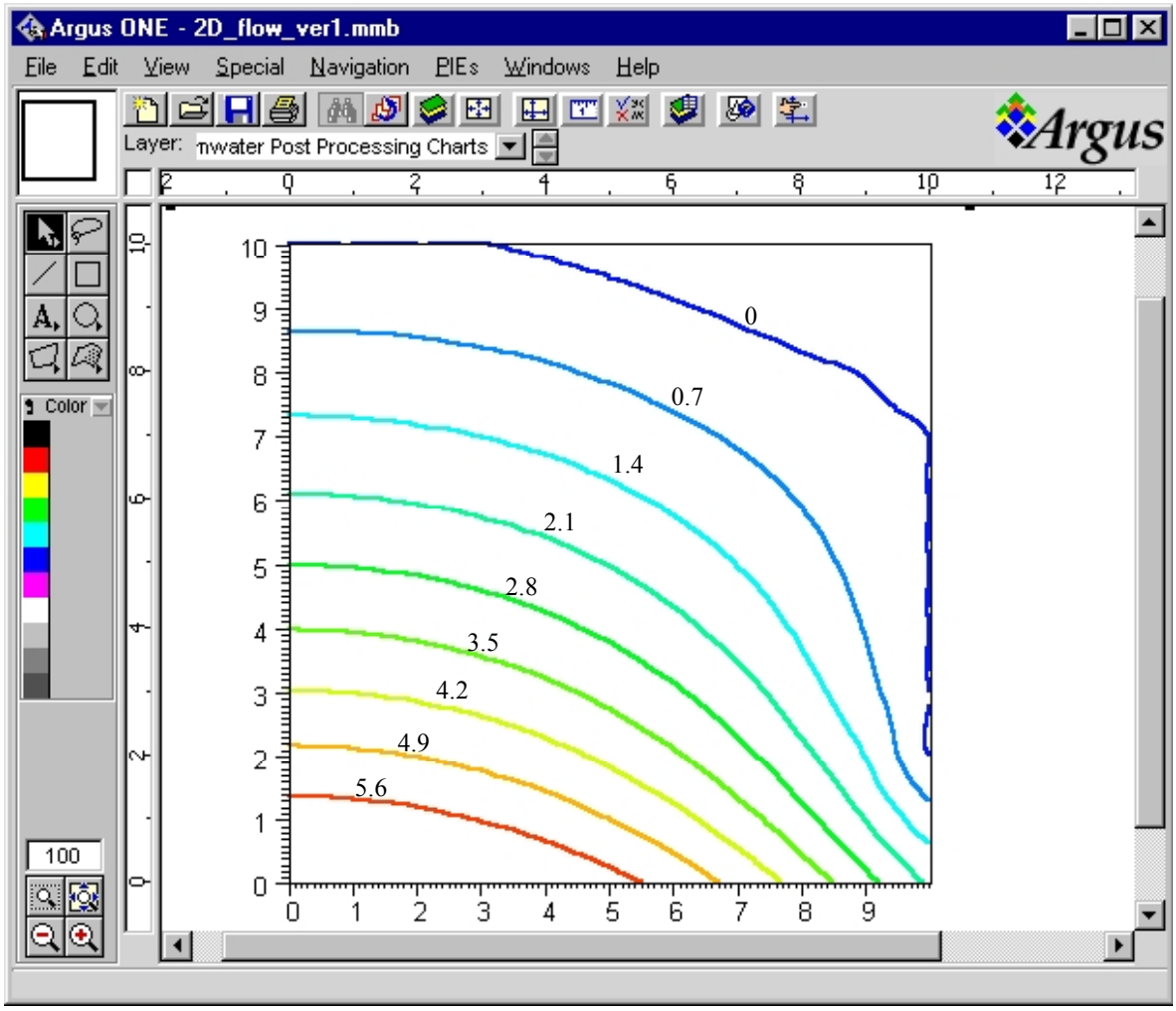

Fig. 3.4 Simulated Steady-State Water Table and Pressure Head for Two-dimensional Drainage Problem with FEMWATER-LHS. Zero potential line shows an artefact due to the spline interpolation algorithm.

$$K_r = \left(\frac{\theta - \theta_r}{\theta_s - \theta_r} \right)^n \tag{3.4}$$

where h_a, A, and B are the parameters used to compute the water content and n is the parameter to compute the relative hydraulic conductivity.

Because of the symmetry, the region for numerical simulation is taken as $0 < x < 10$ m and $0 < z < 10$ m, and 10 m along the y-direction. The boundary conditions are: no flux is imposed on the left ($x = 0$), front ($y = 0$), back ($y = 10$), and bottom ($z = 0$) sides of the region; pressure head is assumed to vary from zero at the water surface ($z = 2$) to 2 m at the bottom ($z = 0$) on the right side ($x = 10$); and variable conditions are used elsewhere. Depth of the pond is

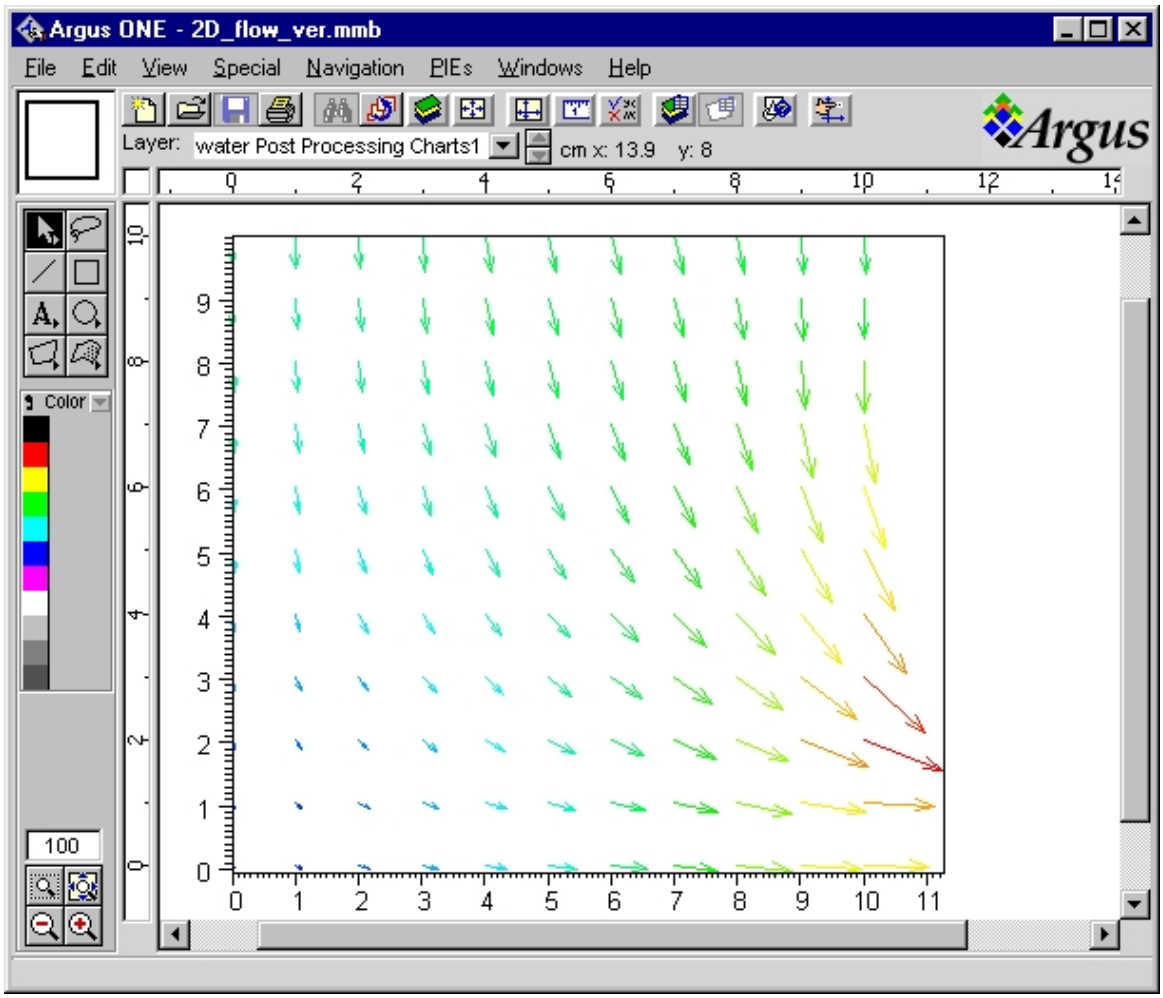

Fig. 3.5 The velocity field for Two-dimensional Drainage Problem.

assumed to be zero meter on the whole variable boundary. Atmospheric infiltration conditions on the top side of the variable boundary are assumed equal to 0.006 m/d and seepage face conditions on the right side above the water surface boundary are equal zero. Steady state is assumed.

The pressure head tolerance is 2×10^{-3} m for nonlinear and is 10^{-3} m for block or point-wise iteration. The relaxation factors for both the nonlinear iteration and block or point-wise iteration are equal to 0.5. The pressure heads and the velocity field simulated with FEMWATER-LHS are plotted in Fig. 3.4 and Fig.3.5. Numerical predictions of these pressure heads are in good agreement with those given by Huyakorn (1986) and Yeh (1999).

3.1.3 Two-Dimensional Transport in a Rectangular Region

As second test case a two-dimensional transport problem in a rectangular region with 540.0 cm length, 270.0 cm width, and 1.0 cm thickness (Fig. 3.6) was used. Initially, the concentration is zero g/cm^3 throughout the region of interest. A concentration of 1.0 g/cm^3 is maintained at x = 0.0 cm and 180.0 cm < y < 270.0 cm by applying a Dirichlet boundary condition. A concentration of 0.0 g/cm^3 is maintained at x = 0.0 cm and 0.0 cm < y < 90.0 cm and 180.0 cm < y < 270.0 cm. A natural condition is imposed at x = 540.0 cm using a variable boundary condition. A uniform material with a bulk density of 1.2 g/cm^3, a longitudinal dispersivity of 10.0 cm, and a lateral dispersivity of 1.0 cm is assumed and no adsorption or decay is taken into account. A specific discharge (Darcy velocity) of 2.0 cm/d and a moisture content of 0.2 is assumed.

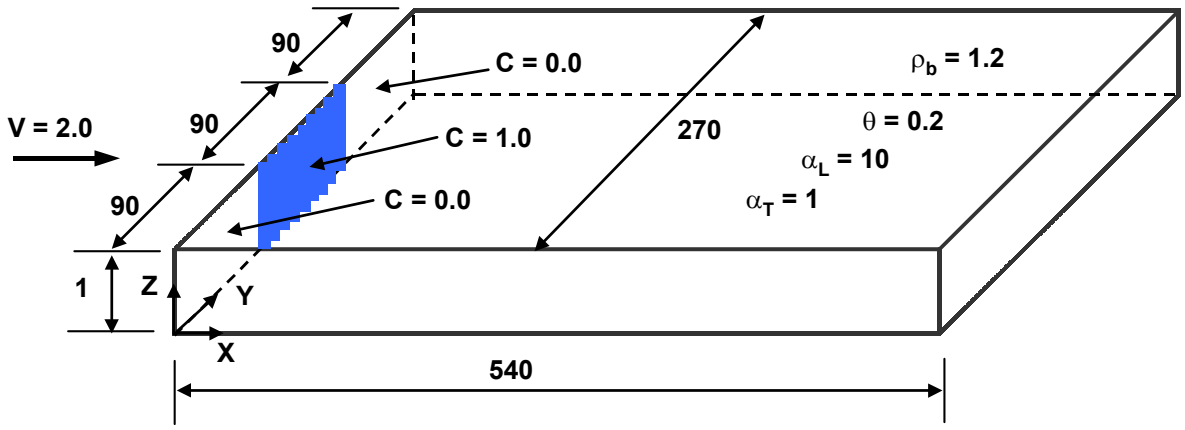

Fig. 3.6 Two-dimensional transient transport in a rectangular region (Yeh, 2000).

Fig. 3.7 depicts the concentration contours at the simulation times of 4.5 days and 45 days (the 40%, 50% and 60% concentration contours at various times) illustrating how the

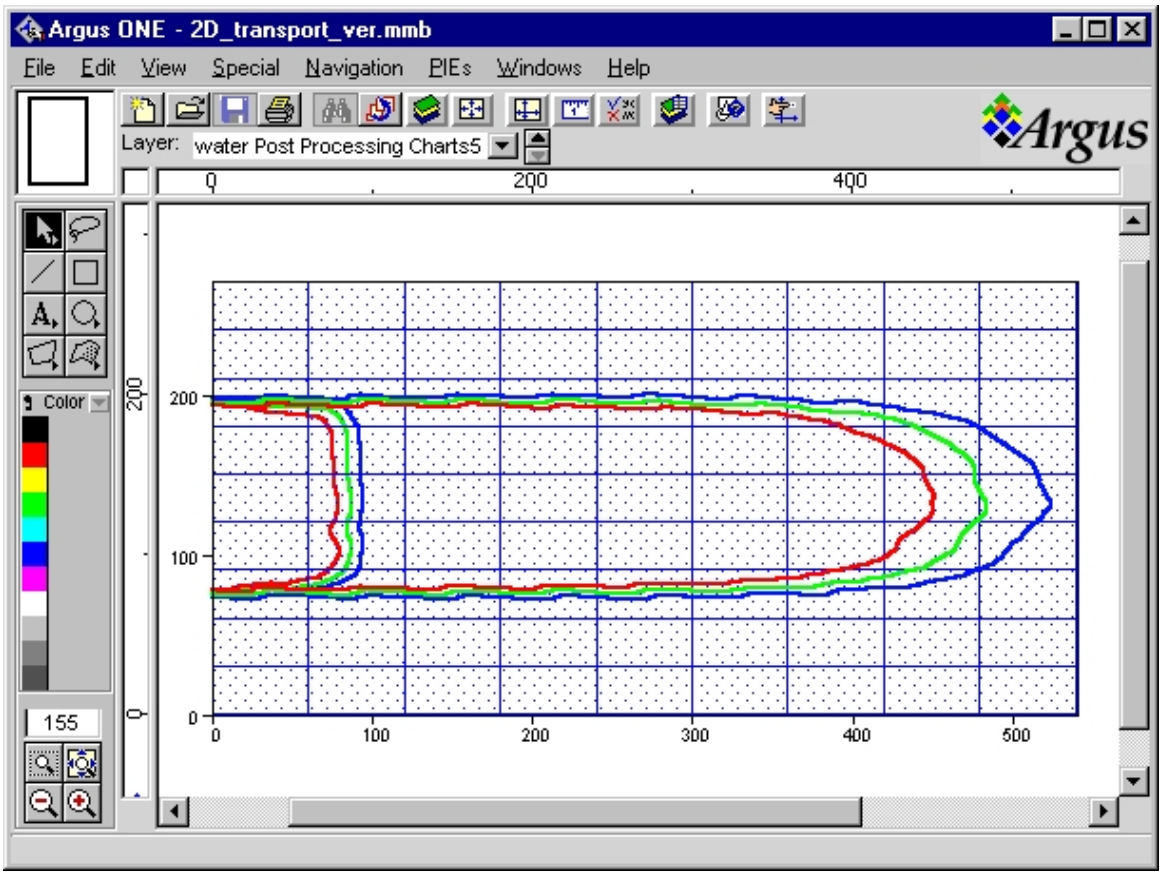

Fig. 3.7 Contours of 40%, 50% and 60% Concentration at t = 4.5 and t = 45.

pollutant moves through the medium with time.

The results are in good agreement with numerical simulation using 3DLEWASTE (Yeh, 2000) and the same set of data and boundary conditions.

3.1.4. Saltwater Intrusion in Confined Aquifer (Henry's Problem)

This example is widely known as Henry's saltwater intrusion problem (Henry, 1964): A confined aquifer is discharging fresh water horizontally into the open sea. The idealized aquifer for the simulation of Henry's problem is shown in Fig. 3.8 The boundary conditions for flow consist of impermeable boundaries along the top and the bottom. Fresh water enters the aquifer on the left face, and the coastal side corresponds to the right face. For the upper

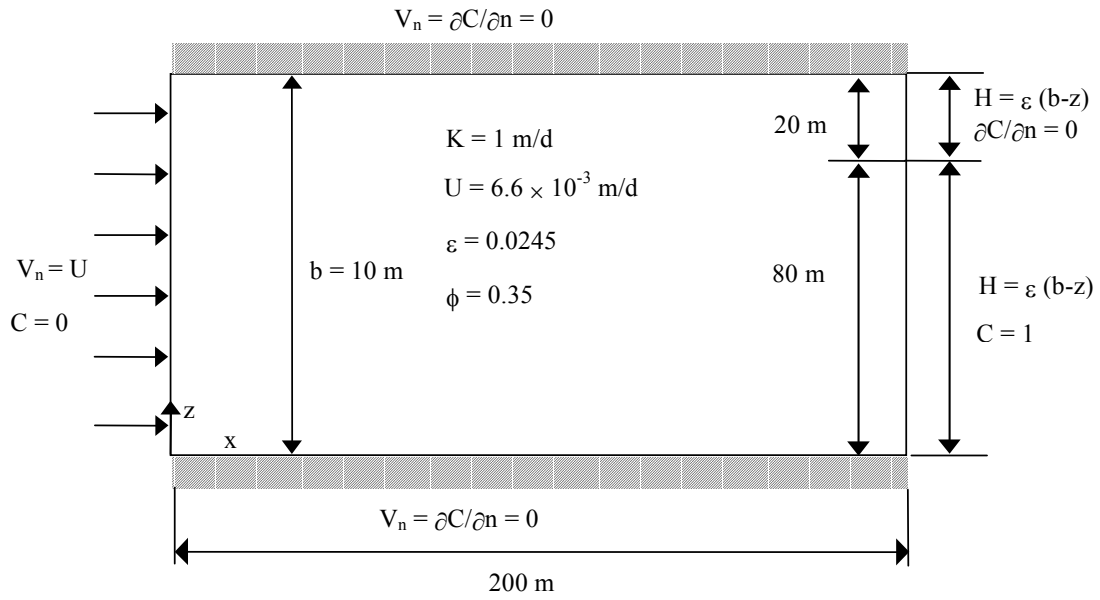

Fig. 3.8 Definition of the Henry problem (Huyakorn et al., 1987).

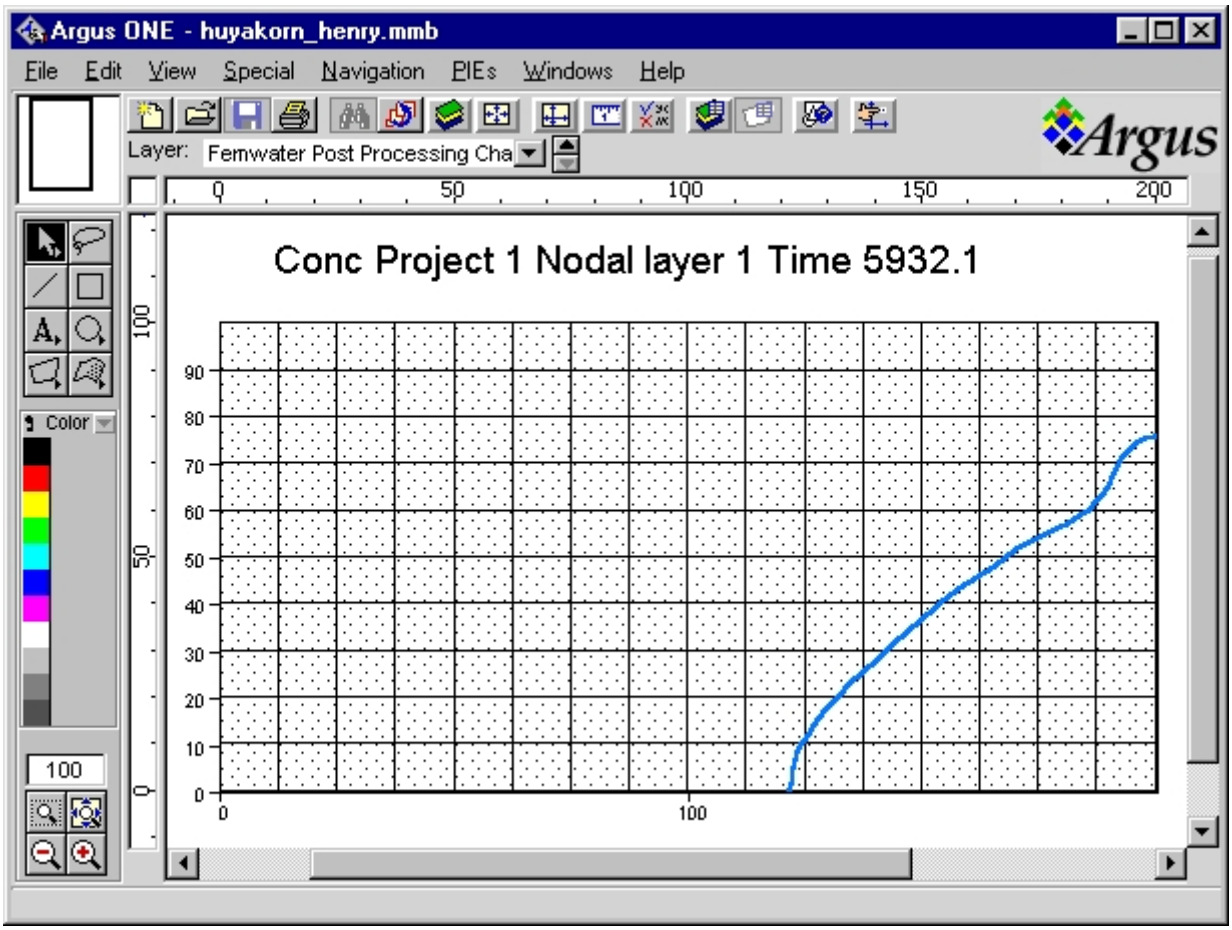

Fig. 3.9 The 0.5 concentration contours at the simulation time of 5932.1 days.

part ($80 \leq z \leq 100$ m) of the coastal interface, variable boundary conditions are used to permit convective salt transport in both direction depending of flow direction.

Both the longitudinal and lateral dispersivities are set to zero, only a molecular diffusion coefficient of 6.6×10^{-2} m^2/d is assumed. The relationship between fluid density and concentration (under isothermal condition) is expressed as

$$\frac{\rho}{\rho_0} = a_1 + a_2 C + a_3 C^2 + a_4 C^3$$

where a_3 and a_4 are set to zero; $a_1 = 1$ and $a_2 = 0.0245$, ρ is the density of water at saltwater concentration C, and ρ_0 is the density of water at zero concentration. Other parameters for the problem are the velocity $U = 6.6 \times 10^{-3}$ m/d, the hydraulic conductivity K = 1 m/d, and the porosity $\phi = 0.35$.

The region of interest was discretized into 187 nodes and 160 rectangular elements. A transient simulation based on assumption of zero initial concentration and hydrostatic pressure head 0 m (the total head datum is set at z = 100 m) was performed. An initial time step of 6 days was used with a time multiplier of 1.17169 until a maximum time step of 600 days is reached. 15 time-steps are performed in this simulation. Fig. 3.9 shows a plot of the position of the 0.5 isochlor after 6000 days. The results also match very well with numerical simulation by Huyakorn et al. (1987).

3.2 APPLICATIONS

As discussed in the last section FEMWATER-LHS has been verified with a variety of designed examples. Verification of these examples are employed to determine the correctness of algorithm and the numerical formulation. Therefore, the verification examples are usually simplified in deterministic mode only (see the last three examples in Section 3.1).

In order to demonstrate the capability of FEMWATER-LHS in handling real three-dimensional problems for the portion of the uncertainty and sensitivity analysis utilizing a LHS, four simulations are presented in the following chapters. The first three simulations are involved with soil hydraulic parameters in the groundwater flow in variably saturated porous media under various boundary conditions. Therefore, the distribution of hydraulic conductivity as well as the soil hydraulic parameters are required. Carsel and Parrish (1988)

Table 3.3 Descriptive statistics for saturated hydraulic conductivity (cm hr^{-1}).
Source: Carsel and Parrish (1988).

	Hydraulic Conductivity (K_s)*			
Soil Type	$\bar{x}$	s	CV	n
Clay**	0.2	0.42	210.3	114
Clay Loam	0.26	0.7	267.2	345
Loam	1.04	1.82	174.6	735
Loamy Sand	14.59	11.36	77.9	315
Silt	0.25	0.33	129.9	88
Silt Loam	0.45	1.23	275.1	1093
Silty Clay	0.02	0.11	453.3	126
Silty Clay Loam	0.07	0.19	288.7	592
Sand	29.7	15.6	52.4	246
Sandy Clay	0.12	0.28	234.1	46
Sandy Clay Loam	1.31	2.74	208.6	214
Sandy Loam	4.42	5.63	127	1183

* n = Sample size, $\bar{x}$ = Mean, s = Standard deviation, CV = Coefficient of variation (percent)
** Agricultural soil, less than 60 percent clay

gives an overview of the probability distributions of the soil hydraulic parameters for different USDA soil types (texture). These distributions were used for the simulations. Table 3.3 gives representative hydraulic conductivity values for various soil types. The most likely shape for the distribution is lognormal. The fourth simulation involved saltwater intrusion problem of density-dependent groundwater flow and salt transport on coastal aquifers under saturated flow conditions. The step-by-step procedures to perform these simulations are described in Appendix B.

The FEMWATER-LHS code allows the user to define the analytic expressions using the van Genuchten functions (1980) or sets of paired values of relative hydraulic conductivity versus moisture content and moisture content versus pressure head given in lookup table format. The van Genuchten relationships in FEMWATER-LHS are as follows:

Table 3.4 Descriptive statistics for saturation water content (θ_s) and residual water content (θ_r). Source: Carsel and Parrish, 1988.

soil type	saturation water content (θ_s)*				residual water content (θ_r)*			
	$\bar{x}$	s	CV	n	$\bar{x}$	s	CV	n
Clay**	0.38	0.09	24.1	400	0.068	0.034	49.9	353
Clay Loam	0.41	0.09	22.4	364	0.095	0.010	10.1	363
Loam	0.43	0.10	22.1	735	0.078	0.013	16.5	735
Loamy Sand	0.41	0.09	21.6	315	0.057	0.015	25.7	315
Silt	0.46	0.11	17.4	82	0.034	0.010	29.8	82
Silt Loam	0.45	0.08	18.7	1093	0.067	0.015	21.6	1093
Silty Clay	0.36	0.07	19.6	374	0.070	0.023	33.5	371
Silty Clay Loam	0.43	0.07	17.2	641	0.089	0.009	10.6	641
Sand	0.43	0.06	15.1	246	0.045	0.010	22.3	246
Sandy Clay	0.38	0.05	13.7	46	0.100	0.013	12.9	46
Sandy Clay Loam	0.39	0.07	17.5	214	0.100	0.006	6.0	214
Sandy Loam	0.41	0.09	21.0	1183	0.065	0.017	26.6	1183

* n = Sample size, $\bar{x}$ = Mean, s = Standard deviation, CV = Coefficient of variation (percent)
** Agricultural soil, less than 60 percent clay

$$K_r = \theta_e^{0.5}\left[1-\left(1-\theta_e^{1/\gamma}\right)^{\gamma}\right]^2 \tag{3.5}$$

and

$$\theta_e = \left[1+\left(|\alpha h|\right)^{\beta}\right]^{-\gamma} \qquad \text{for } h<0 \tag{3.6}$$

$$\theta_e = 1 \qquad \text{for } h \geq 0 \tag{3.7}$$

where

$$\theta = \theta_r + \theta_e\left(\theta_s - \theta_r\right) \tag{3.8}$$

$$\gamma = 1-\frac{1}{\beta} \tag{3.9}$$

and

θ = moisture content (dimensionless)

θ_e = effective moisture content (dimensionless)

θ_s = saturation moisture content (dimensionless)

θ_r = residual moisture content (dimensionless)

β, γ = soil-specific exponents (dimensionless)

α = soil-specific coefficient (1/L)

To provide a linkage for the soil parameters to widely known or easily obtainable soils data (such as soil texture), Carsel and Parrish (1988) fitted these analytic functions to data from soils all over the United States and tabulated corresponding parameter values by texture. These are show in Table 3.4. The required parameters are α , β, and γ of the van Genuchten functions (Eq. 3.5). Mean values of these parameters are shown along with CVs for each by soil texture. Others parameters required are the saturation moisture content (θ_s) and residual moisture content (θ_r). Values of these parameters are given in Table 3.5 along with their respective CVs. In addition, Table 3.6 gives the correlations between these parameters by soil texture classification.

Table 3.5 Descriptive statistics for van Genuchten water retention model parameters, α, β, γ.
Source: Carsel and Parrish, 1988.

	Parameter α (cm^{-1})*				Parameter β*				Parameter γ*			
Soil Type	$\bar{x}$	s	CV	n	$\bar{x}$	s	CV	n	$\bar{x}$	s	CV	n
Clay**	0.008	0.012	160.3	400	1.09	0.09	7.9	400	0.08	0.07	82.7	400
Clay Loam	0.019	0.015	77.9	363	1.31	0.09	7.2	364	0.24	0.06	23.5	364
Loam	0.036	0.021	57.1	735	1.56	0.11	7.3	735	0.36	0.05	13.5	735
Loamy Sand	0.124	0.043	35.2	315	2.28	0.27	12	315	0.56	0.04	7.7	315
Silt	0.016	0.007	45	88	1.37	0.05	3.3	88	0.27	0.02	8.6	88
Silt Loam	0.02	0.012	64.7	1093	1.41	0.12	8.5	1093	0.29	0.06	19.9	1093
Silty Clay	0.005	0.005	113.6	126	1.09	0.06	5	374	0.09	0.05	51.7	374
Silty Clay Loam	0.01	0.006	61.5	641	1.23	0.06	5	641	0.19	0.04	21.5	641
Sand	0.145	0.029	20.3	246	2.68	0.29	20.3	246	0.62	0.04	6.3	246
Sandy Clay	0.027	0.017	61.7	46	1.23	0.1	7.9	46	0.18	0.06	34.7	46
Sandy Clay Loam	0.059	0.038	64.6	214	1.48	0.13	8.7	214	0.32	0.06	53	214
Sandy Loam	0.075	0.037	49.4	1183	1.89	0.17	9.2	1183	0.47	0.05	10.1	1183

* n = Sample size, $\bar{x}$ = Mean, s = Standard deviation, CV = Coefficient of variation (percent)
** Agricultural soil, less than 60 percent clay

Table 3.6 Pearson product moment correlation among input variables, n = Sample size.
Source: Carsel and Parrish, 1988.

	K_s	θ_r	α	β
		Silt (n = 61)		
K_s	1			
θ_r	**-0.204**	1		
α	**0.984**	**-0.200**	1	
β	**0.466**	**-0.610**	**0.551**	1
		Clay (n= 95)		
K_s	1			
θ_r	**0.972**	1		
α	**0.948**	**0.890**	1	
β	**0.908**	**0.819**	**0.910**	1
		Silty Clay (n = 123)		
K_s	1			
θ_r	**0.949**	1		
α	**0.974**	**0.964**	1	
β	**0.908**	**0.794**	**0.889**	1

Table 3.6 Pearson product moment correlation among input variables, n = Sample size. Source: Carsel and Parrish, 1988 (continued).

	K_s	θ_r	α	β
		Sandy Clay (n = 46)		
K_s	1			
θ_r	**0.939**	1		
α	**0.957**	**0.937**	1	
β	**0.972**	**0.928**	**0.932**	1
		Sand (n= 237)		
K_s	1			
θ_r	**-0.515**	1		
α	**0.743**	**0.119**	1	
β	**0.843**	**-0.858**	**0.298**	1
		SandyLoam(n=1145)		
K_s	1			
θ_r	**-0.273**	1		
α	**0.856**	**0.151**	1	
β	**0.686**	**-0.796**	**0.354**	1
		Loamy Sand(n= 313)		
K_s	1			
θ_r	**-0.359**	1		
α	**0.986**	**-0.301**	1	
β	**0.730**	**-0.590**	**0.354**	1
		Silt Loam (n= 1072)		
K_s	1			
θ_r	**-0.359**	1		
α	**0.986**	**-0.301**	1	
β	**0.730**	**-0.590**	**0.775**	1
		Silty Clay Loam (n= 591)		
K_s	1			
θ_r	**0.724**	1		
α	**0.986**	**0.777**	1	
β	**0.918**	**0.549**	**0.911**	1
		Clay Loam (n= 328)		
K_s	1			
θ_r	**0.790**	1		
α	**0.979**	**0.836**	1	
β	**0.936**	**0.577**	**0.909**	1
		Sandy Clay Loam (n= 212)		
K_s	1			
θ_r	**0.261**	1		
α	**0.952**	**0.392**	1	
β	**0.909**	**-0.113**	**0.787**	1
		Loam (n= 664)		
K_s	1			
θ_r	**0.204**	1		
α	**0.982**	**-0.086**	1	
β	**0.632**	**-0.748**	**0.591**	1

In Table 3.6 six appear (boldface) entries below the matrix diagonal in each case. In most cases, correlations were significant for van Genuchten parameters. For example, correlations generally were greater than 0.7 for between K_s and α. The implication is that an assumption of independence in Monte Carlo or LHS simulation is not plausible.

3.2.1 Application 1: Steady Drainage to Parallel Drains

3.2.1.1 Problem Description

Geometry and boundary conditions of the problem are similar to the first verification example in Section 3.1.2. However, in this example, the simulated domain is composed of two materials (i.e. material 1 = Silty Clay Loam and material 2 = Silt) as shown in Fig. 3.10. Characterizations of input variables (hydraulic parameters) can take a number of forms

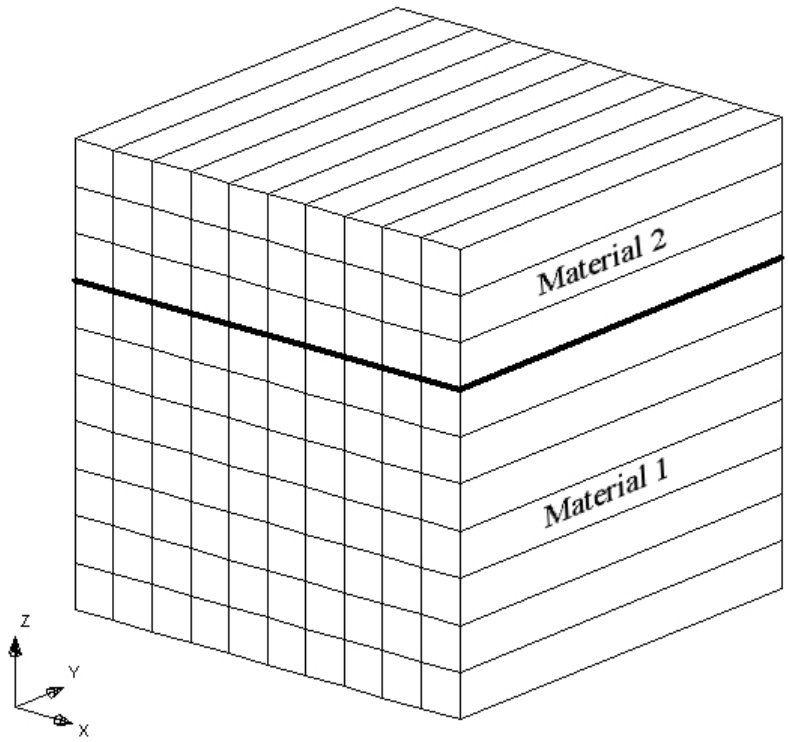

Fig. 3.10 A two-material simulated domain in application 1.

ranging from bounding values to a complete probability distribution (density function). The input variables for which probability distributions of material parameters were assigned for the simulation of subsurface flow are shown in Table 3.7. Therefore, the input variables to the model involves 12 variables that describe parameters of two materials. In this case, these

Table 3.7 Parameter distributions used in application 1.

Input Var.	Parameter	Mat.*	Distribution	Mean	Std. Dev.
x_1	Saturated K_{xx} [m day^{-1}]	1	Lognormal	0.0168	0.0456
x_2	Saturated K_{zz} [m day^{-1}]	1	Lognormal	0.0168	0.0456
x_3	Res. Water Content (θ_r)	1	Normal	0.089	0.01
x_4	Sat. Water Content (θ_s)	1	Normal	0.43	0.07
x_5	Van Genuchten α [m^{-1}]	1	Normal	1	0.6
x_6	Van Genuchten β	1	Normal	1.23	0.06
x_7	Saturated K_{xx} [m day^{-1}]	2	Lognormal	0.06	0.0792
x_8	Saturated K_{zz} [m day^{-1}]	2	Lognormal	0.06	0.0792
x_9	Res. Water Content (θ_r)	2	Normal	0.034	0.01
x_{10}	Sat. Water Content (θ_s)	2	Normal	0.46	0.11
x_{11}	Van Genuchten α [m^{-1}]	2	Normal	1.6	0.7
x_{12}	Van Genuchten β	2	Normal	1.37	0.05

* Material type (1 = Silt Clay Loam and 2 = Silt)

variables are assumed to be independently from each other. All soil hydraulic parameter distributions were taken from Carsel and Parrish (1988) for appropriate soil types (silty clay loam for material 1 and silt for material 2). These parameter distributions are listed in Table 3.3 - 3.5. Equations (3.5) - (3.9) are assumed to described the soil parameters of the two medias.

3.2.1.2 Uncertainty Analysis for Application 1

The purpose of the analysis presented is to evaluate the uncertainties in the model output (i.e. pressure head in spatial and temporal variability) which results from the uncertainty in model input variables (i.e. hydraulic conductivity and soil parameters). The model provides multivariate output for groundwater flow in unsaturated zone: (i) steady-state pressure head, (ii) Darcy velocity, (iii) moisture content and (iv) total flow and total flow rates through various types of boundaries. The following output variables are considered in this analysis: Y_1 and Y_2 are pressure head at $(x, z) = (2,3)$ and $(4,5)$ respectively.

For this part of the analysis utilizing a LHS, 50 computer runs were made. In the first case, the restricted pairing procedure of Iman and Conover (1982) was utilized with the LHS, which kept all off-diagonal rank correlation close to zero.

Results of the estimates based on a LHS utilizing restricted pairing with m = 50. For ease in comparing these estimates, an estimate based on a random sample with m = 500 has also been included in Fig. 3.11. Further, the CDFs (Cumulative Distribution Functions) estimated by random sampling simulation are

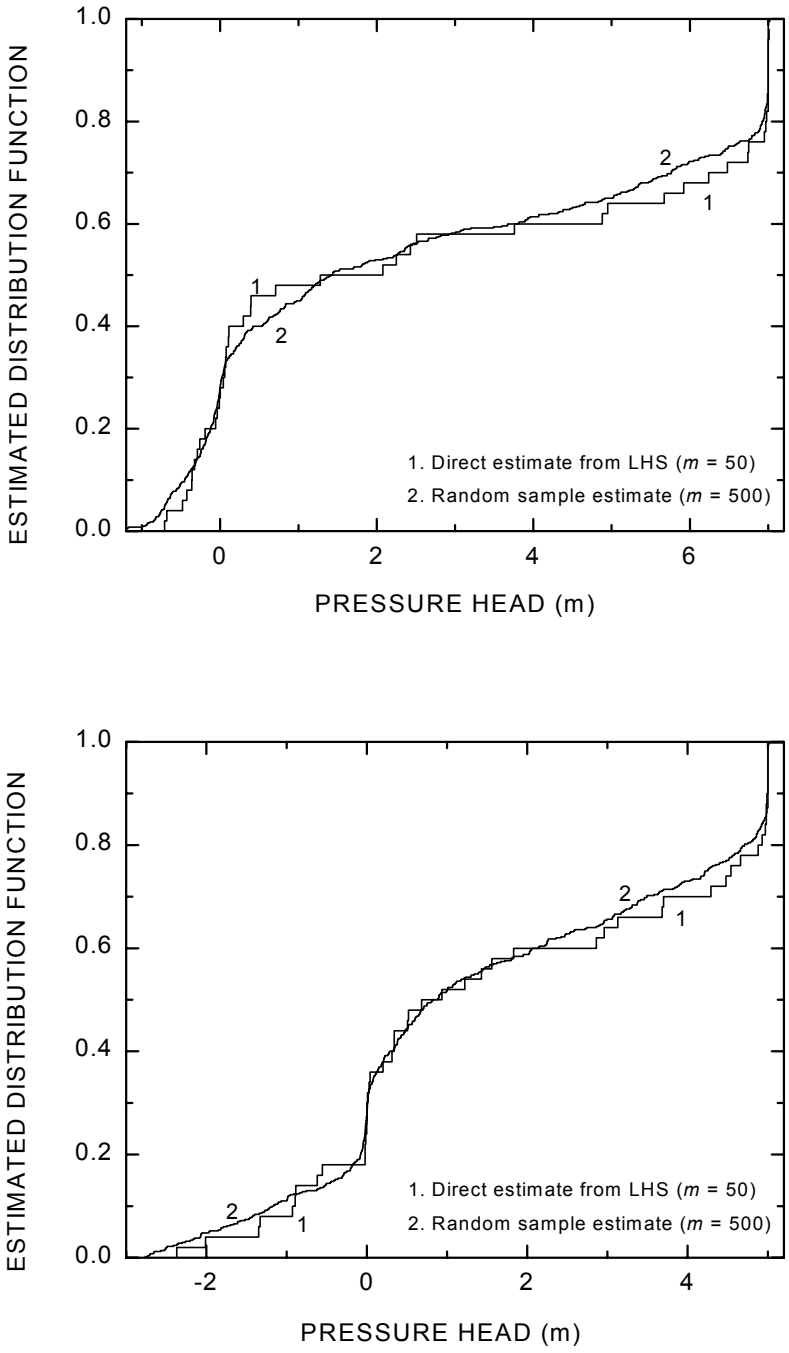

Fig. 3.11 Estimates of CDF's (Cumulative Distribution Functions) for Y_1 and Y_2 in application 1.

considered to be the "correct" CDFs. The results in Fig. 3.11 show that the LHS estimate is in close agreement with the random sample estimate for both output variables Y_1 and Y_2.

3.2.1.3 Sensitivity Analysis for Application 1

Statistically sensitivity measures as calculated by the program for calculation of partial correlation and standardized regression coefficient (Iman et al., 1985) are presented in Table

Table 3.8 Statistical sensitivity measures for Y_1 and Y_2.

Output variable	Parameter	Rank	PCC	Rank	SRC	Rank	PRCC	Rank	SRRC
Y_1	Saturated K_{xx} Mat. 1	1	-0.185	1	-0.194	1	**-0.854**	1	-0.804
	Saturated K_{zz} Mat. 1	12	0.018	12	0.017	2	0.594	2	0.342
	Res. Water Content Mat. 2	2	-0.169	2	-0.176	3	-0.132	3	-0.063
	Van Genuchten α Mat. 1	9	-0.054	9	-0.053	4	0.101	4	0.048
	Van Genuchten β Mat. 2	5	0.09	4	0.096	5	-0.085	5	-0.043
	Saturated K_{zz} Mat. 2	4	-0.093	5	-0.092	6	-0.074	6	-0.035
	Van Genuchten β Mat. 1	8	-0.056	8	-0.056	7	-0.073	7	-0.034
	Res. Water Content Mat. 1	11	-0.036	11	-0.035	8	-0.073	8	-0.034
	Sat. Water Content Mat. 2	3	-0.115	3	-0.12	9	-0.062	9	-0.03
	Van Genuchten α Mat. 2	10	0.05	10	0.05	10	-0.036	10	-0.017
	Sat. Water Content Mat. 1	6	-0.077	6	-0.076	11	0.029	11	0.014
	Saturated K_{xx} Mat. 2	7	-0.075	7	-0.076	12	0.016	12	0.007
	Model R^2		0.117		0.117		0.798		0.798
Y_2	Saturated K_{xx} Mat. 1	2	-0.18	2	-0.19	1	**-0.841**	1	-0.807
	Saturated K_{zz} Mat. 1	8	-0.038	9	-0.037	2	0.538	2	0.313
	Sat. Water Content Mat. 2	1	-0.187	1	-0.199	3	-0.203	3	-0.106
	Res. Water Content Mat. 1	9	0.036	10	0.036	4	0.142	4	0.071
	Van Genuchten α Mat. 1	12	0.003	12	0.003	5	0.107	5	0.053
	Van Genuchten β Mat. 2	4	0.087	4	0.093	6	-0.092	6	-0.05
	Sat. Water Content Mat. 1	6	-0.057	6	-0.056	7	0.09	7	0.046
	Van Genuchten α Mat. 2	11	0.029	11	0.028	8	-0.07	8	-0.035
	Saturated K_{zz} Mat. 2	5	-0.065	5	-0.065	9	0.06	9	0.03
	Saturated K_{xx} Mat. 2	7	-0.051	7	-0.051	10	-0.02	10	-0.01
	Res. Water Content Mat. 2	3	-0.161	3	-0.168	11	-0.011	11	-0.005
	Van Genuchten β Mat. 1	10	-0.036	8	-0.037	12	0.009	12	0.005
	Model R^2		0.111		0.111		0.773		0.773

P(R)CC: Partial (Rank) Correlation Coefficient
S(R)RC: Standard (Rank) Regression Coefficient

3.8. The results were calculated using the steady-state pressure heads Y_1 and Y_2. The parameters are ordered in Table 3.8 by the magnitude of the partial rank correlation coefficient (PRCC). The PRCC could reasonably be expected to represent best the importance of parameters because of the nonlinearities and parameter correlations in the simulation. As for this case, however, the statistical correlation measures do not provide a definitive ranking of the importance of parameters. All of the four statistical correlation measures show input variable x_1 (saturated hydraulic conductivity K_{xx} for material 1) to be the most important parameter for both output variables Y_1 and Y_2. The input variable x_1 is highly ranked by each of the statistical correlation measures and appears to have the greatest impact on both output variables Y_1 and Y_2. For this application it appears that, the statistical correlation measures are useful in determining the relative importance of parameters. The dependence of pressure head Y_1 and Y_2 on the saturated hydraulic saturated hydraulic conductivity K_{xx} x_1 is obviously.

3.2.2 Application 2: Transient Drainage

3.2.2.1 Problem Description

This application is presented for a transient flow situation involving a seepage face. Geometry of flow region and boundary conditions used in the simulation are also described in Section 3.1.2. This simulation is restricted to only one soil type, namely the Silt Loam soil. The probability distributions of the soil hydraulic parameters used in this simulation are given in Table 3.9. These soil hydraulic parameter distributions were taken from Carsel and Parrish (1988). The unsaturated characteristic hydraulic parameters of the medium are given as Eqs. (3.5) to (3.9).

Table 3.9 Parameter distributions used in application 2.

Input Var.	Parameter	Distribution	Mean	Std. Dev.
x_1	Saturated K_{xx} [m day^{-1}]	Lognormal	0.0168	0.0456
x_2	Saturated K_{zz} [m day^{-1}]	Lognormal	0.0168	0.0456
x_3	Res. Water Content (θ_r)	Normal	0.089	0.01
x_4	Sat. Water Content (θ_s)	Normal	0.43	0.07
x_5	Van Genuchten α [m^{-1}]	Normal	1	0.6
x_6	Van Genuchten β	Normal	1.23	0.06

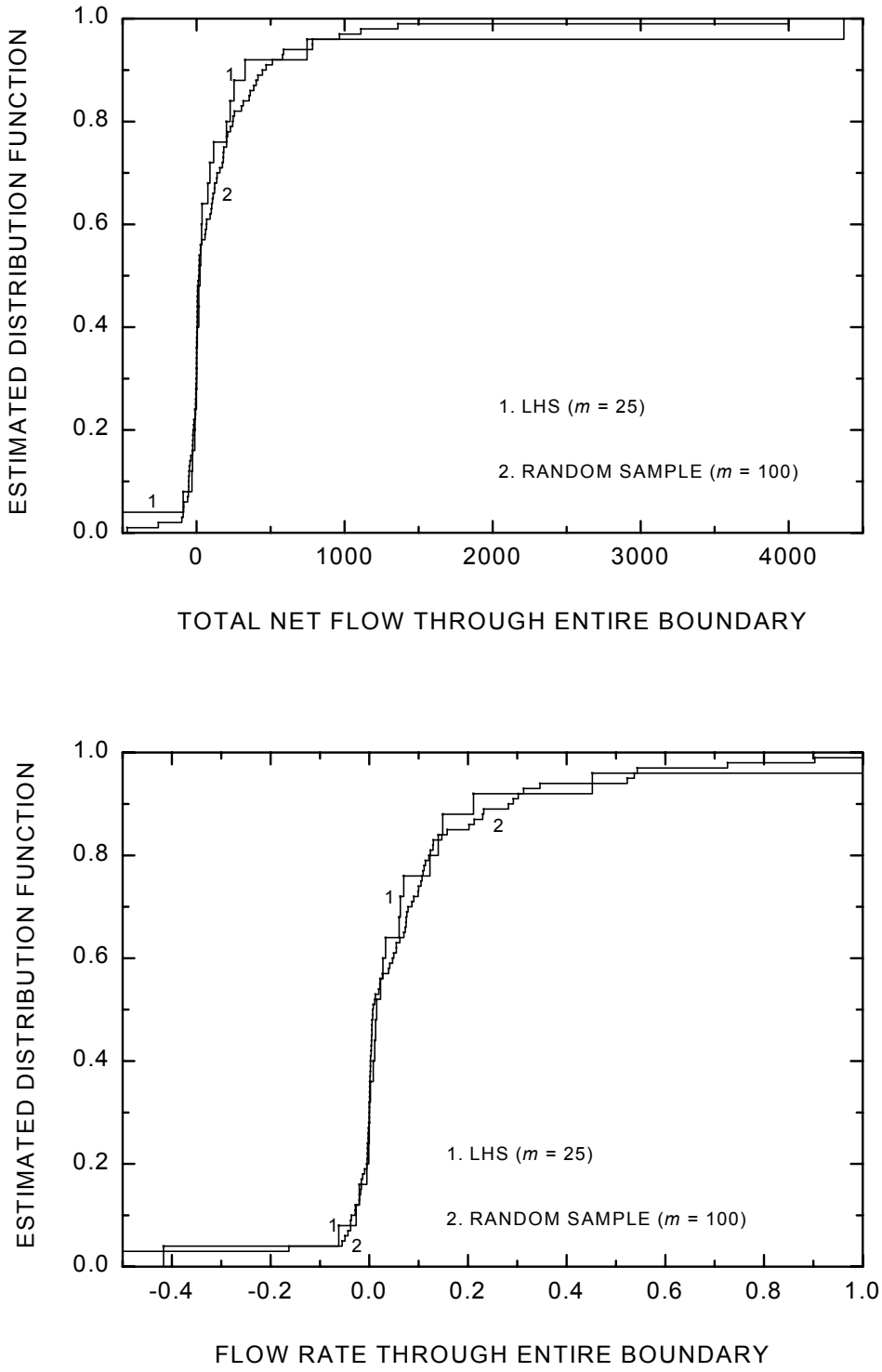

Fig. 3.12 A comparison of two estimates of the CDF's (Cumulative Distribution Functions) for Y_1 (total net flow through entire boundary over time) and Y_2 (flow rate through entire boundary at day 510.25) in application 2.

In this case the initial conditions used were the steady state solution resulting from zero flux on the top. The transient simulation was performed for 50 time steps. The initial time step size is 0.25 day and each subsequent time step size is increased with a multiplier of 2.0 with the maximum time step size of less than or equal to 32 days. The pressure head tolerance for nonlinear iteration was 2×10^{-3} m. The relaxation factor for the nonlinear iteration was set equal to 0.5.

3.2.2.2 Uncertainty Analysis for Application 2.

The output from this simulation is multivariate as was the case with the previous application. For this analysis, three output variables were selected for consideration: total net flow (Y_1), flow rate (Y_2) through entire boundary and pressure head at (x,z) = (4,2) (Y_3). The variable Y_1 is integrated over time (1470.25 day), while Y_2 is examined only at one day (510.25). However, Y_3 is examined at multiple time steps later in the next section when illustrating graphs of sensitivity measures over time.

Estimates of the CDF's of the output variables Y_1 and Y_2 obtained directly from the LHS and indirectly by using Monte Carlo simulation appear in Fig. 3.12. As a check on the adequacy of these estimates a estimate based on simple random of size 100 has been included in these figures. Results in Fig. 3.12 show a good agreement between the LHS estimates (m = 25) and the random sample estimate (m = 100) for both output variables Y_1 and Y_2.

3.2.2.3 Sensitivity Analysis for Application 2

When output is time dependent, the relative important of the input variables may change with time. To illustrate this, the output Y_3 was recorded at 50 time steps. A statistical sensitivity measure can be calculated for each input variable versus each output variable at each of these 50 time steps. The influence of a particular input variable x_j on a particular output variable Y is easily summarized by plotting the measure of sensitivity on the vertical axis versus time on the horizontal axis. The statistical sensitivity measures to demonstrate the value of such plots are the standardized regression coefficient (SRC) and the partial correlation coefficient (PCC). As discussed in Section 2.6, when the relationship between x_j and Y is basically nonlinear but monotone, each individual variables x_j and Y can be replaced by their corresponding ranks from 1 to m and either sensitivity measures can be computed on these ranks. This transformation converts the sensitivity measure from linearity between x_j and Y to

one of monotonicity between x_j and Y. The result of this transformation is referred to as either the standardized rank regression coefficient (SRCC) or the partial rank correlation coefficient (PRCC).

Fig. 3.13 displays two sets of graphs of the two sensitivity measures. The upper set (Fig.

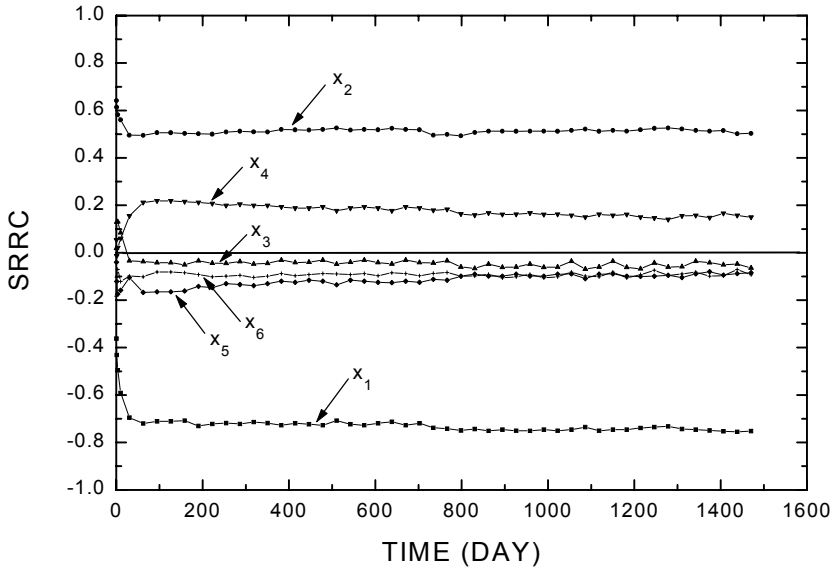

Fig. 3.13a

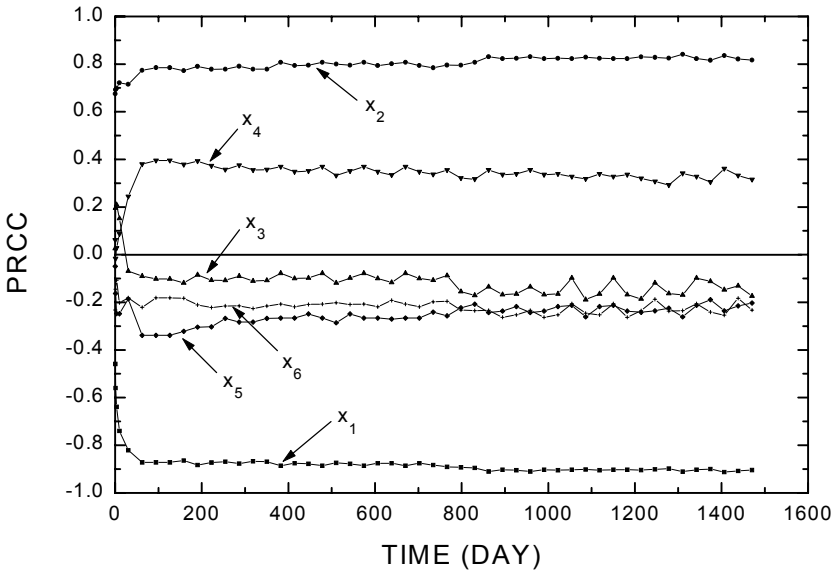

Fig. 3.13b Standardized rank regression coefficients and partial rank correlation coefficients for Y_3 in application 2. $x_1 = K_{xx}$; $x_2 = K_{zz}$; x_3 = Res. Water Content; x_4 = Sat. Water Content; x_5 = van Genuchten α ; x_6 = van Genuchten β.

3.13*a*) contains standardized rank regression coefficients plotted as a function of time. The lower set (Fig. 3.13*b*) contains partial rank correlation coefficient as a function of time. For both sets graphs, the dependent variables are the output Y_3 at 50 time steps. Each graph displays the values of the standardized rank regression coefficient or partial rank correlation coefficient relating these pressure heads to single input variable as a function of time. Although having different numerical values, both measures exhibit the same pattern of sensitivity. Fig. 3.13 shows clearly that the output is highly sensitive to the influence of the input variables but its sensitivity to time is very low.

3.2.3 Application 3: 3-Dimensional Flow in an Unconfined Aquifer Subjected to Well Pumping

3.2.3.1 Problem Description

This example was selected to demonstrate the three-dimensional application of the code with the commonly encountered problem of groundwater flow and contaminant transport in an unconfined aquifer downstream of a landfill and being subject to well pumping.

In this application, both saturated and unsaturated zone are considered. The region of interest is bounded on the left and right by hydraulically connected rivers; on the front, back, and bottom by impervious confining beds; and on the top by an air-soil interface (Fig. 3.14). Initially, the water table was assumed to be located 60 m above the base of aquifer. The water level in the well was then lowered to a height of 30 m above the base, and this height was maintained until a steady state condition is reached. A pressure head boundary was assumed hydrostatic on two vertical planes located at $x = 0$ and $0 < z < 60$, and $x = 1000$ and $0 < z < 60$, respectively. A no-flow condition was assumed at all other boundaries. A steady state analysis of the stated flow problem was performed. Values of the media parameters and probability distributions used in this analysis are shown in Table 3.10. Soil parameters were taken from the recommended distributions presented in Carsel and Parrish (1988).

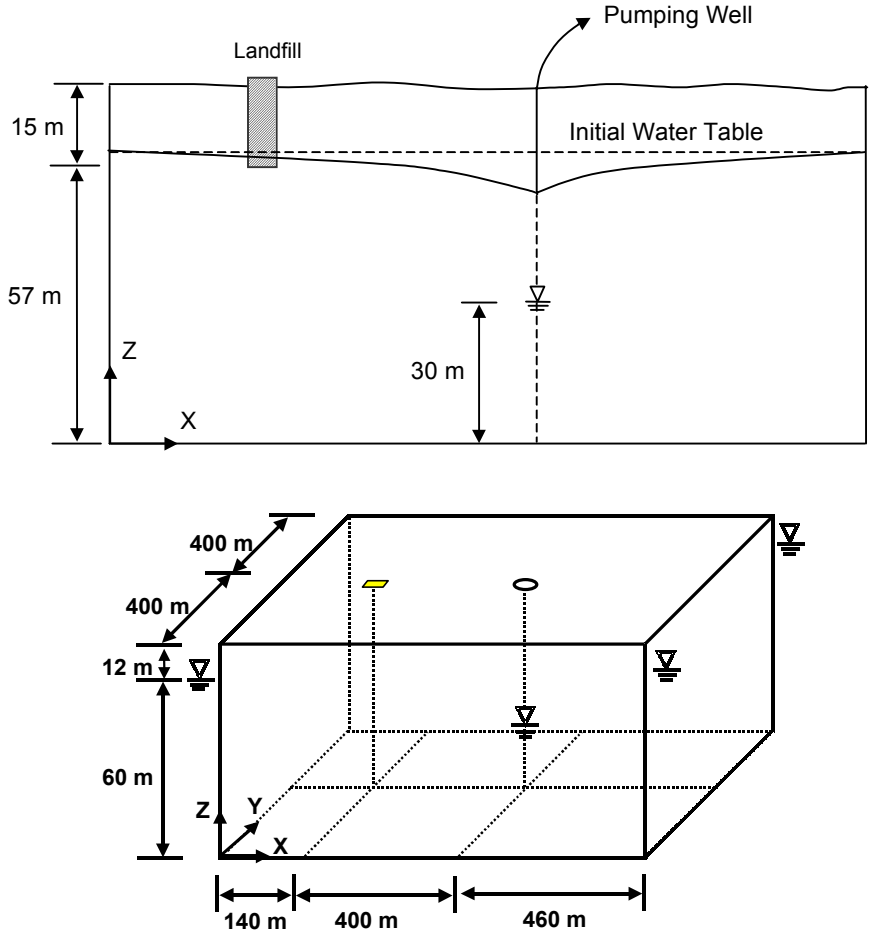

Fig. 3.14 Problem definition for three-dimensional Steady-State flow in pumped unconfined aquifer.

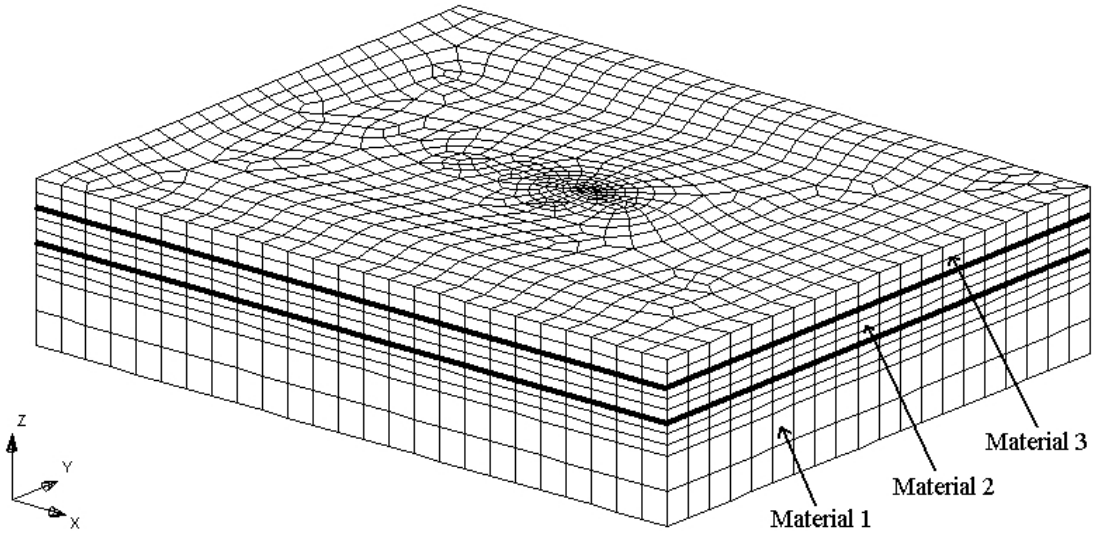

Fig. 3.15 Finite element discretization for three-dimensional steady state flow in a pumped unconfined aquifer.

The unsaturated characteristic hydraulic properties of the medium are given as Eqs. (3.5) to (3.9).

Restrictions on the multivariate structure of the input required a rank correlation between input variables x_3, x_4, x_6, and x_7. The correlation is specified on ranks since this correlation measure is meaningful for both normal and non-normal distribution. The variables x_3, x_4, x_6, and x_7 each had a lognormal distribution (table 3.10). The manner in which these correlations were implemented is explained in the next section.

This portion was then automatically discretized using a nonuniform quadrilateral element by Argus ONE's automatic mesh generation (e.g. an irregular finite element mesh containing elements of about 40 size), resulting 7,950 prism elements and 9,262 nodes (fig. 3.15).

Table 3.10 Parameter distributions used in application 3.

Input Var.	Parameter	Mat.*	Distribution	Mean	Std. Dev.
x_1	Saturated K_{xx} [m day^{-1}]	1	Lognormal	0.3144	0.6576
x_2	Saturated K_{yy} [m day^{-1}]	1	Lognormal	0.3144	0.6576
x_3	Saturated K_{zz} [m day^{-1}]	1	Lognormal	0.3144	0.6576
x_4	Res. Water Content (θ_r)	1	Normal	0.1	0.01
x_5	Sat. Water Content (θ_s)	1	Normal	0.39	0.07
x_6	Van Genuchten α [m^{-1}]	1	Normal	5.8	3.8
x_7	Van Genuchten β	1	Normal	1.48	0.13
x_8	Saturated K_{xx} [m day^{-1}]	2	Lognormal	1.0608	1.3512
x_9	Saturated K_{yy} [m day^{-1}]	2	Lognormal	1.0608	1.3512
x_{10}	Saturated K_{zz} [m day^{-1}]	2	Lognormal	1.0608	1.3512
x_{11}	Res. Water Content (θ_r)	2	Normal	0.065	0.02
x_{12}	Sat. Water Content (θ_s)	2	Normal	0.41	0.09
x_{13}	Van Genuchten α [m^{-1}]	2	Normal	7.5	3.7
x_{14}	Van Genuchten β	2	Normal	1.89	0.17
x_{15}	Saturated K_{xx} [m day^{-1}]	3	Lognormal	7.128	3.744
x_{16}	Saturated K_{yy} [m day^{-1}]	3	Lognormal	7.128	3.744
x_{17}	Saturated K_{zz} [m day^{-1}]	3	Lognormal	7.128	3.744
x_{18}	Res. Water Content (θ_r)	3	Normal	0.045	0.01
x_{19}	Sat. Water Content (θ_s)	3	Normal	0.43	0.06
x_{20}	Van Genuchten α [m^{-1}]	3	Normal	14.5	2.9
x_{21}	Van Genuchten β	3	Normal	2.68	0.29

Material type (1 = Sandy Clay Loam, 2 = Sandy Loam and 3 = Sand)

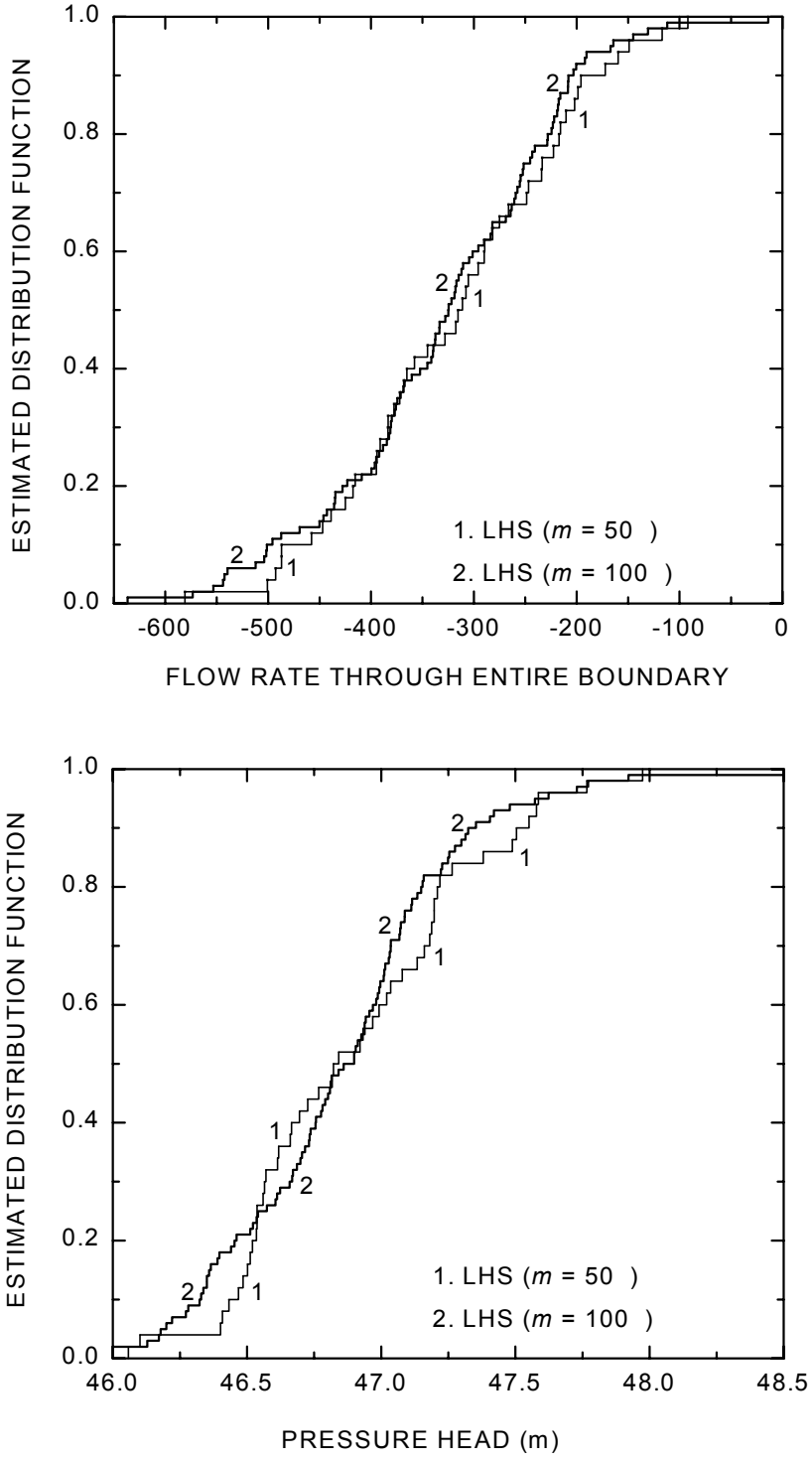

Fig. 3.16 LHS estimates of the CDF's (Cumulative Distribution Functions) for Y_1 (flow rate through the entire boundary) and Y_2 (pressure head) in application 3.

The nodal layers are located at z = 0, 15, 30, 35, 40, 45, 50,55, 60, 66, and 72 m in the z-direction. as reported by Huyakorn et al. (1986). The refinement of mesh according to Argus ONE's automatic mesh generation with a new element size, is responsible for higher number of elements and nodes than what was reported by Huyakorn et al. (1986).

3.2.3.2 Uncertainty Analysis for Application 3.

The required correlations in this application are induced by generating a LHS in the usual sense and then controlling the individual pairing of variables to produce specific rank correlations as explained in section 2.1.1 (Iman and Conover, 1984). A LHS size m = 50 was used with the 21 input variables and produced rank correlations for variables x_3, x_4, x_6, and x_7. The results of the rank correlation for these variables are presented in Table 3.11. These target

Table 3.11 Rank correlation values between input variables x_3, x_4, x_6, and x_7 for application 3.

Input Variable Pair	Target Value	Results
(x_3,x_4)	0.261	0.2434
(x_3,x_6)	0.952	0.9497
(x_3,x_7)	0.909	0.8489
(x_4,x_6)	0.392	0.4272
(x_4,x_7)	-0.113	-0.2598
(x_6,x_7)	0.787	0.7139

correlation values were taken from Carsel and Parrish (1988) (Table 3.6). At the same time, of the 204 remaining pairs of variables in rank correlation matrix, only one pair had correlation coefficients larger than 0.09. Thus, the 6 results of the input variable pairs have good matching with the target values, nevertheless the others pairs which have weak correlation should have values close to zero.

The output variables used in this investigation are the net flow rate through the entire boundary (Y_1) and pressure head at (x, y, z) = (540,400,0) (Y_2). The resulting estimated CDFs for output variable Y_1 and Y_2 appear in fig. 3.16. For ease in making comparison, there are actually two CDF estimates based on LHS. One is based on 50 runs and the other is based on 100 runs. The close agreement of the LHS estimates within figure 3.16 provides an indication of precision associated with estimates arising from LHS.

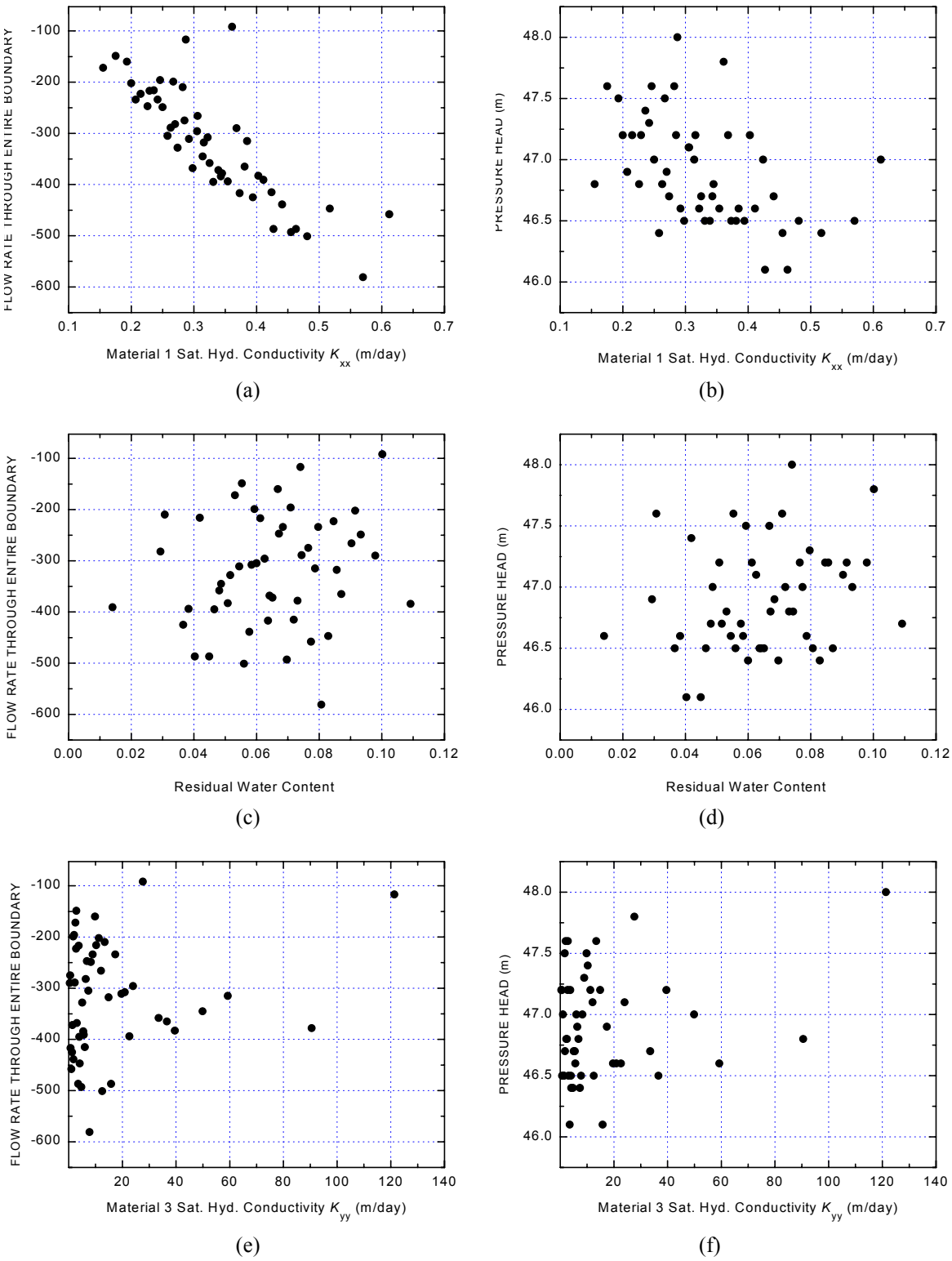

Fig. 3.17 Scatterplots of x_1, x_{11} and x_{16} versus Y_1 (flow rate through the entire boundary) and Y_2 (pressure head) in application 3.

3.2.1.3 Sensitivity Analysis for Application 3

Scatterplots of output variables Y_1 and Y_2 as function of parameter values are shown in Fig. 3.17. The parameters chosen for plotting are the most sensitive parameters as measured by partial rank correlation coefficient. The graphs on the left side show a scatterplot of x_1, x_{11} and x_{16} versus Y_1. The graphs on the right side show x_1, x_{11} and x_{16} versus Y_2. The dependence of Y_1 and Y_2 on x_1 are clear fig. 3.17 (a). Reverse linear relationships are implied. From the remaining plots in Fig. 3.17 it does not appear that Y_1 and Y_2 are very sensitive to x_{11} and x_{16}. Fig. 3.17 shows that the saturated hydraulic conductivity K_{xx}. for material 1 x_1 is the only parameter in this application, that has a strong effect on Y_1. The relationship between head and conductivity is less significant. Thus, conductivity play a main roll for model sensitivity. On contrary, porosity becomes sensitive with time dependent simulations and in case of transport modeling.

3.2.4 Application 4: Seawater Intrusion in Confined Aquifer

3.2.4.1 Problem Description

This application concerns groundwater flow and salt transport in coastal confined aquifer. The problem is described schematically in Section 3.1.4 (Fig. 3.8). Molecular diffusion was assumed and transient analyses was performed. For the constant dispersion case, the longitudinal dispersivities α_L and α_T were set to zero. As shown in Fig. 3.8, fresh water enters the aquifer on the left face, and the coastal side corresponds to the right face. The boundary conditions employed in this simulation are also shown.

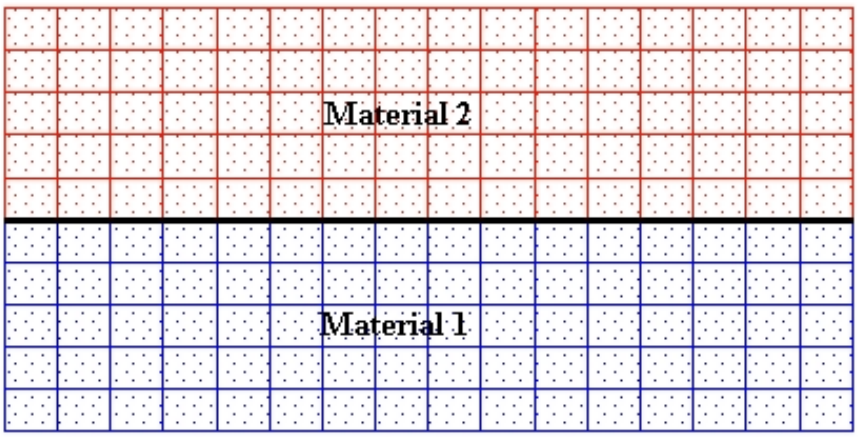

Fig. 3.18 A two-material simulated domain in application 4.

The aquifer region was represented by a three-dimensional rectanguler grid consisting of 160 (10 × 16) elements and 374 nodes. Two materials are included to compose the simulated domain as pictured in Fig. 3.18 Values of the media parameters and probability distributions used in this analysis are shown in Table 3.12. The ranges chosen of each variables are also shown. Further, the restricted pairing technique was used to force the rank correlations between variables to be close to zero.

Table 3.12 Parameter distributions used in application 4.

Input Var.	Parameter	Mat.	Distribution	Min.	Max.
x_1	Saturated K_{xx} [m day^{-1}]	1	Lognormal	0.8	1.1
x_2	Saturated K_{zz} [m day^{-1}]	1	Lognormal	0.8	1.1
x_3	Sat. Water Content (θ_s)	1	Normal	0.315	0.385
x_4	Bulk density ρ_b [kg/m^3]	1	Normal	1080	1320
x_5	Mol. Diffusion Coeff. α_m [m^{2}day^{-1}]	1	Normal	0.0594	0.0726
x_6	Saturated K_{xx} [m day^{-1}]	2	Lognormal	0.45	0.55
x_7	Saturated K_{zz} [m day^{-1}]	2	Lognormal	0.45	0.55
x_8	Sat. Water Content (θ_s)	2	Normal	0.198	0.22
x_9	Bulk density ρ_b [kg/m^3]	2	Normal	1080	1320
x_{10}	Mol. Diffusion Coeff. α_m [m^{2}day^{-1}]	2	Normal	0.0297	0.0363

A transient simulation based on the assumption of zero initial concentration was performed. An initial step of 5 days was used with a time multiplier of 1.17169 and the maximum allowable time step of 500 days. 15 time-steps were performed in this simulation.

3.2.4.2 Uncertainty Analysis for Application 4.

The output variables used in this investigation are the total net of contamination load through the entire boundary (Y_1) and concentrations as a function of location (Y_2). Y_2 is examined at y = 0, z = 0 and 0 < x < 200. The variable Y_1 is integrated over time (4943.4 day), while Y_2 is examined only at day 2443.4.

The 20 observations on the output Y_1 are summarized in Fig. 3.19, which presents the estimated CDFs of output variable Y_1. Also appearing in Fig. 3.19 is an estimate of CDF's obtained by running the model on LHS with m = 40 and 80. Once again there is a slight but definite improvement in the quality of the estimators as the sample size increases. The estimates seem to improve between m = 20 and 80.

Examination of the rank correlation matrix for the LHS indicated that 28 of the 45 pairwise entries were < 0.1 in absolute value, 35 of 45 were < 0.15, and the largest element was 0.184. The associated correlation matrix for the LHS had a variance inflation factor of 1.15.

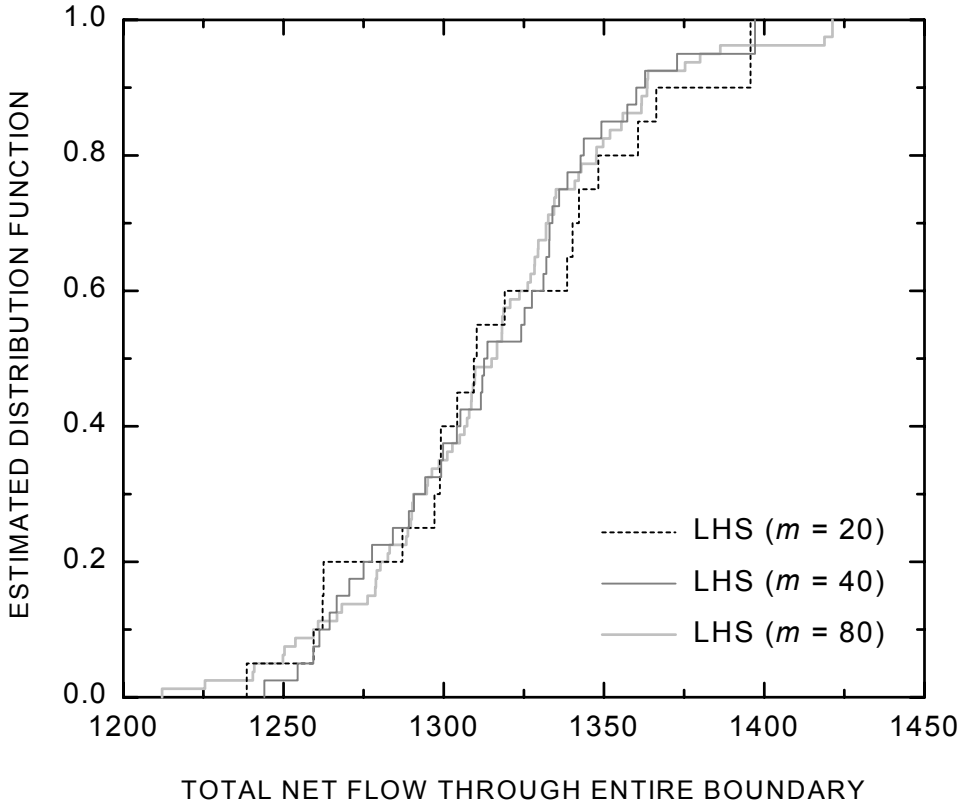

Fig. 3.19 LHS estimates of the CDF's (Cumulative Distribution Function) for Y_1 (mass flow through entire boundary) in application 4 with different sample size.

3.2.4.3 Sensitivity Analysis for Application 4

A useful way to present sensitivity results for variable Y_2 is with plots of partial correlation coefficients or standardized regression coefficients. Fig. 3.20 displays two sets of graphs. The upper set contains standardized rank regression coefficients plotted as a function of transport distance. The lower set contains partial correlation coefficients as a function of transport distance.

For both sets of graphs, the dependent variable Y_2 is the concentration at day 2443.4 in a fixed distance along the bottom face, and each graphs displays the values of the standardized rank

regression coefficient or partial rank correlation coefficient regarding this concentration to single input variable as function of distance. Fig. 3.20 displays graphs for selected variables that had a partial rank correlation coefficient of at least 0.5 in absolute value.

The saturated water content θ_s (x_3) or porosity in material 1 is shown to have the largest sensitivity to Y_2. The saturated hydraulic conductivity K_{zz} (x_2) is shown to have the smallest

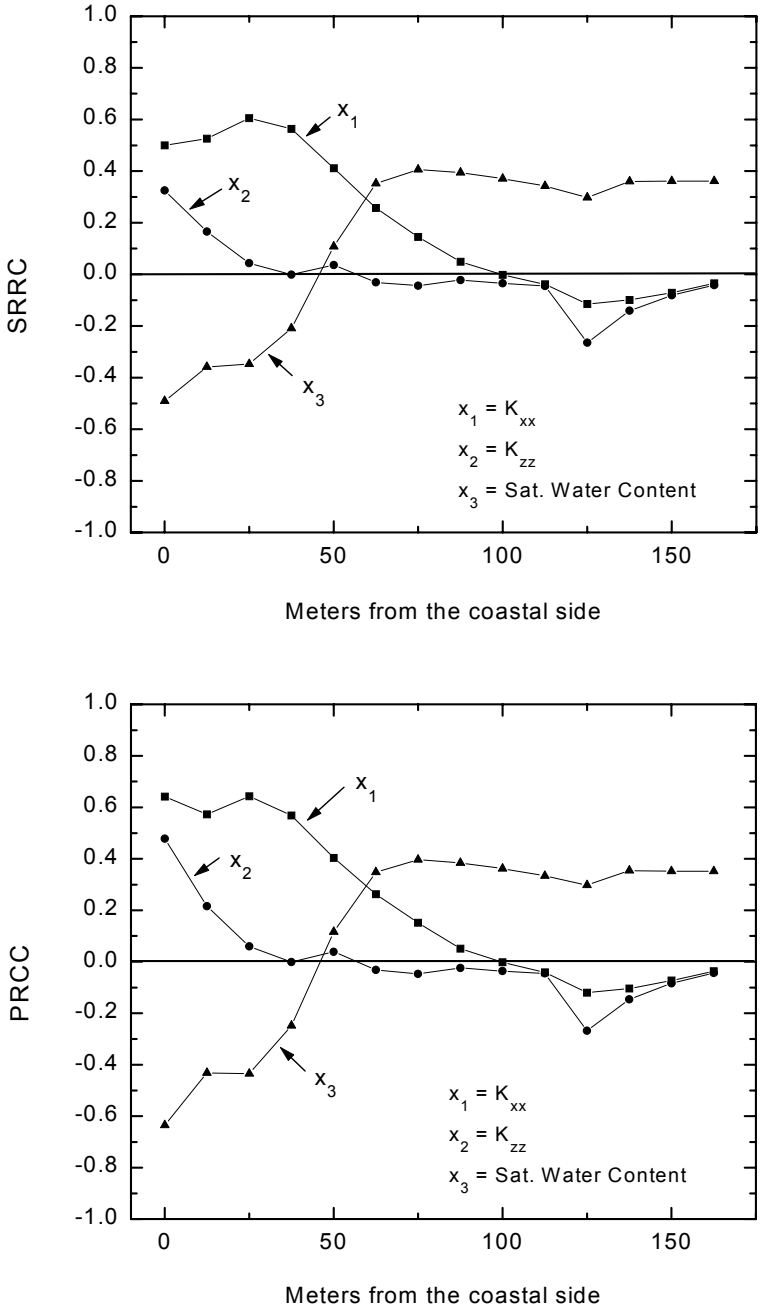

Fig. 3.20 Standardized rank regression coefficients and partial rank correlation coefficients for Y_2 (concentration at day 2443.4) in application 4.

effect on model predictions. The saturated hydraulic conductivity K_{xx} (x_1) and the saturated water content θ_s (x_3) have similar sensitivities to the model output Y_2, but x_1 is insignificant for more than 100 m distance from the coastal side. Fig. 3.20 shows a negative influence developing between the saturated water content θ_s (x_3) and Y_2 out to 50 m and then changes to constant positive influence.

4. SUMMARY AND CONCLUSIONS

The basic objective of this work was to develop a groundwater modeling code FEMWATER-LHS for saturated-unsaturated porous media by combining and modifying three existing codes: groundwater flow, solute transport and probabilistic Latin Hypercube Sampling (LHS). This was done by the development of the model called FEMWATER-LHS which comes with an Argus ONE™ GUI (Argus Open Numerical Environments Graphical User Interfaces). The GUI for FEMWATER-LHS is based on a public-domain Plug-In Extension (PIE) to Argus ONE that permits the use of Argus ONE to automatically create the appropriate geospatial information coverages (information layers); provide menus and dialogs for inputting geospatial information and simulation control parameters, and allow visualization of FEMWATER-LHS simulation results.

The flexibility and versatility of the developed model permits the application of a wide range of real-world problems, including the simulation of unsaturated and saturated subsurface flow and density-dependent groundwater flow problems. The LHS mode provided for FEMWATER-LHS allows the analyst to specify distributions, control correlation sampling, perform a simple Monte Carlo uncertainty analyses, and the more advanced LHS, as well as performing both using either random or restricted pairing techniques.

To demonstrate FEMWATER-LHS, four problems including the probabilistic analysis (i.e. LHS) were employed for verification by comparing numerical results from the model and from other models. Simulation for verification of the model showed the correctness of the model in mastering a variety geological information.

To demonstrate the applicability of the model capabilities of uncertainty and sensitivity analysis using LHS, four example problems were presented. LHS was used with all the example problems and good estimates of the CDF (Cumulative Distribution Function) in comparisons with results from large random or LHS samples were obtained. For example, for both applications one and two, the LHS estimates with m = 50 and m = 25 showed good agreement with random sample estimates with m = 500 and m = 100. In the case of the application three, the LHS estimate with m = 50 was compared against a LHS with m = 100 in order to illustrate the small variability associated with LHS estimates. Also in application four, the LHS estimates seem to improve slightly between m = 20 and 80.

Several measures of sensitivity based on probabilistic results were also discussed. These included scatter plots of output variable versus input parameter values. Statistical sensitivity were calculated by PRSRC to clarify the relationship between output variable and critical input parameter values. For the first two applications the analyses indicated that the saturated hydraulic conductivity K_{xx} was the most important parameter contributing to the uncertainty in pressure head at the fixed point. For the case of application three, the saturated hydraulic conductivity K_{xx} in material one was also the most sensitive parameter in both net flow rate through the entire boundary and pressure head. But in the case of application four, the saturated water content θ_s or porosity in material one was the most sensitive parameter followed by the saturated hydraulic conductivity K_{xx} contributing to the uncertainty in concentration.

The implementation of LHS is similar to that of simple Monte Carlo in that both have a probabilistic basis. In fact, for large sample sizes there is little difference between LHS and random sample. However, the original intent of LHS was to make more efficient use of computer runs than random sample for smaller sample sizes. Two important points can be draw as conclusions from this work. The first is the fact that LHS stratifies fully incorporate the range of every input variable. The second is that restricted pairing utilized with the generation of the LHS forces the pairwise correlations between the independent variables to be very near to zero. This is an important consideration because it eliminates the possibility of spurious correlations clouding the results of the analysis.

Many applications considered in practice are far more complex than the four applications used in this work. Therefore, further research is necessary to establish the reliability and capability of FEMWATER-LHS.

5. REFERENCES

Anderson, M. P., and Woessner, W. W., 1992, Applied Groundwater Modeling (Simulation of Flow and Advective Transport), Academic Press, Inc., London, 381p

Argus Interware, 1997a, Argus Numerical Environments and MeshMaker User's Guide, 463p.

Argus Interware, 1997b, Argus Numerical Environments PIE Technical Notes, 31 p.

Argus Interware, Inc., 1997c, User's guide Argus ONE™, Argus Open Numerical Environments . A GIS modeling system, version 4.0: Jericho, NY, Argus Holdings, Limited, 506 p.

Bear, J. and Vermijt, A., 1998, Modeling Groundwater Flow and Pollution. D. Reidel Publishing Company, Dordrecht, Holland. 414p

Bratley, P., Fox, B. L. and Schrage, L. E., 1987, A Guide to Simulation, Springer-Verlag, New York, 397p

Carsel, R. F., and Parrish R. S., 1988, Developing Joint Probability Distributions of Soil-Water Retention Characteristics. Water Resources Research, 24(5):755-769.

Cheng, J. R., Yeh, G. T., Lin, H. C., 1996, Development of a two-dimensional overland flow model using the Lagrangian-Eulerian finite element method, Computational Methods in Water Resources XI, Volume 2, 183-190

Cheng, J. R., Strobl, R. O., Yeh, G. T., Lin, H. C., and Choi, W. H., 1998, Modeling of 2D Density-Dependent Flow and Transport in Subsurface, Journal of Hydrologic Engineering, ASCE, Volume 3, Number 4, 248-257

Cheng, R. T., Casulli, V., Milford, S. N., 1984, Eulerian-Lagrangian solution of the convection-dispersion equation in natural coordinates. Water Resources Research, 20(7), 944-952

Dagan, Gedeon, 1986, Statistical theory of ground water flow and transport: Pore to laboratory to formation, and formation to regional scale. Water Resources Research, 22, no. 9:120S-134S

Domenico, P. A., Schwartz, F. W., 1990, Physical and Chemical Hydrogeology, John Wiley & Sons, Inc.

Draper, N. R., Smith, H., 1998, Aplied Regression Analysis (Third Edition), John Wiley & Sons, Inc., 706p

Ekberg, C., 1999, Sensitivity Analysis and Simulation Uncertainties in Predictive Geochemical Modeling, Freiberg On-line Geoscience, vol. 2 (http://www.geo.tu-freiberg.de/fog).

Fetter, C. W.,1993, Contaminant Hydrogeology, Macmillan Publishing Company, New York, 458p

Galeati, G., Gambolati, G., and Neuman, S. P., 1992, Coupled and partially coupled Eulerian-Langrangian model of freshwater-seawater mixing, Water Resources Research 28(1), 149-165.

Häfner, F., Sames, D. and Voigt, H. D., 1992, Wärme- und Stofftransport. Springer Verlag, Berlin.

Häfner, F., Boy, S., Wagner, S.,Behr, A., Piskarev, V. & Palatnik, B.M., 1997, The "front limitation" algorithm - A new and fast finite-difference method for groundwater pollution problems. Journal of Contaminant Hydrology 27, 43-61.

Hardyanto, W., 2001, Implementation of Latin Hypercube Sampling Algorithm for groundwater flow modelling, Freiberg Wissenschatliche Mitteilungen, 16, 195-204

Helton, J. C., 1993, Uncertainty and Sensitivity Analysis Techniques for use in Performance assessment for radioactive waste Disposal, Reliability Engineering and System Safety, 42, 327-367

Henry, H. R., 1964, Effects of dispertion on salt encroachment in coastal aquifers, seawater in coastal aquifers., U.S. Geological Survey Water Supply Paper No. 1613-C, U.S. Geological Survey, Washington D.C., 35-69.

Holzbecher, E. O., 1998, Modeling Density-Driven Flow in Porous Media: Principles, numerics, software., Springer-Verlag, Berlin, 286p.

Huyakorn, P. S., Andersen, P. F., Mercer J. W., and White, JR., H. O., 1987, Saltwater Intrusion in Aquifers: Development and Testing of a Three-Dimensional Finite Element Model, Water Resour. Res. 23(2):293-312.

Huyakorn, P. S., Pinder, G. F., 1983, Computational Methods in Subsurface Flow, Academic Press, New York, 473p.

Huyakorn, P. S., Springer E. P., Guvanasen V., and Wadsworth T. P., 1986b, A Three-Dimensional Finite-Element Model for Simulating Water Flow in Variably Saturated Porous Media. Water Resour. Res. 22(13):1790-1808.

Huyakorn, P.S. and Pinder, G.F., 1983, Computational Methods in Subsurface Flow, Academic, San Diego, CA.

Iman, R. L. & Devenport, J. M., 1982, Rank Correlation Plots for Use with Correlated Input Variables., Communications in Statistics, B11, 355-60

Iman, R. L. and Conover, W. J., 1980, Small Sample Sensitivity Analysis Techniques for Computer Models, With an Application to Risk Assessment., Communications in Statistics, Part A - Theory and Methods,9,1749-1874.

Iman, R. L. and Conover, W. J., 1982, A Distribution Free Approach to Inducing Rank Correlations Among Input Variables., Communications in Statistics, Part B - Simulation and Computation, 11, 311-334.

Iman, R. L. and Helton, J. C., 1988, An Investigation of Uncertainty and Sensitivity Analysis Techniques for Computer Models, Risk Analysis, Vol. 8, No. 1, 71-90

Iman, R. L. and Helton, J. C., 1991, The Repeatability of Uncertainty and Sensitivity Analyses for Complex Probabilistic Risk Assessment, Risk Analysis, Vol. 11, No. 4, 591-606

Iman, R. L. and Shortencarier, M. J., 1984, A FORTRAN 77 program and user's guide for the generation of Latin Hypercube and random samples for use with computer models. NUREG/CR-3624, SAND83-2365, Sandia National Laboratories, Albuquerque, NM.

Iman, R. L., Shortencarier, M. J. and Johnson, 1985, FORTRAN 77 Program and user's Guide for the Calculation of Partial Correlation and standardized Regression Coefficient. NUREG/CR-4122, SAND85-0044. Sandia National Laboratories, Albuquerque, NM

Iman, R. L., 1992, Uncertainty and Sensitivity Analysis for Computer Modeling Applications, Releability Technology, AD-Vol. 28, 153-168

Iman, R. L., Devenport, J. M., Frost, E. L. & Shortencarier, M. J., 1980, Stepwise Regression with PRESS and Rank Regression (Program User's Guide), SAND79-1472, Sandia National Laboratories, Albuquerque, NM

Istok, J. D., 1989, Groundwater modeling by the finite element method. American Geophysical Union, Washington, DC., 495p.

Kinzelbach, W., 1986, Groundwater Modeling: An Introduction with Sample Programs in BASIC, Elsevier Scientific Publishers, Amsterdam, The Netherlands, 333p.

Kinzelbach, W., 1987, Numerische Methoden zur Modellierung des Transportes von Schadstoffen im Grundwasser. Oldenbourg Verlag, Muenchen.

Lin, H. C., Richards, D. R., Yeh, G. T., Cheng, J. R., Cheng, H. P. and Jones, N. L., 1997, FEMWATER: A three dimensional finite element computer model for simulating density-dependent flow and transport in variably saturated media, Report CHL-97-12, U.S. Army Corps of Engineer, 3909 Halls Ferry Road, Vicksburg, MS 39180-6199

Mckay, M. D., Conover W.J. and Beckman R.J., 1979, A Comparison of Three Methods for Selectiong Values of Input Variables in the Analysis of Output From a Computer Code. Technometrics, 21,239-245.

Meinrath, G., 2000, Robust spectral analysis by moving block bootstrap designs, Analytica Chimica Acta 415, 105-115

Meinrath, G., Ekberg, C., Landgren, A. and Liljenzin, J.O., 2000, Assessment of uncertainty in parameter evaluation and prediction, Talanta 51, 231-246

Merkel, B. & Sperling, B. ,1990, Statistik für Mikro-Computer. Gustav Fischer Verlag, Stuttgart - New York

Merkel, B., Grossmann, J. & Faust, A., 1988, Simulation of Groundwater Transport taking into account Thermodynamical Reactions. Proc. VII Inter. Conf. on Computational Methods in Water Resources, Boston, Juni 1988. 281-286

Merkel, B. & Nemeth, G., 1984, Interaction between Soil-Gas and Seepage Water. Proc. of the Int. Symposium RIZA, Vol.2, 537-546

Nitzsche, O., Meinrath, G. and Merkel, B., 2000, Database uncertainty as a limiting factor in reactive transport prognosis, Contaminant Hydrology 44, 223-237

Reilly, T. E., and Goodman, A. S., 1985, Quantitative analysis of saltwater-freshwater relationships in groundwater systems --- A hystorical prespective., J. Hydro., Amsterdam, The Netherlands, 80, 125-160.

Shapiro, A. M., Margolin, J., Dolev, S., and Ben-Israel, Y., 1997, A graphical-user interface for the U.S. Geological Survey modular three-dimensional finite-difference ground-water flow model (MODFLOW-96) using Argus Numerical Environments: U.S. Geological Survey Open-File Report 97-121, 53p.

Stein, M., 1987, Large Sample Properties of Simulations Using Latin Hypercube Sampling. Technometrics, Volume 29, No. 2, 143-151.

van Genuchten, M. T., 1980, A closed-form equation for predicting the hydraulic conductivity of unsaturated soils, Soil Sci. Soc. J. 44, 892-898.

Voss, C. I., 1984, SUTRA: A finite-element simulation model for saturated-unsaturated, fluid density dependent ground-water flow with energy transport or chemically-reactive single-species solute transport: U.S. Geological Survey Water-Resources Investigations Report 84-4369, 409 p.

Voss, C. I., Boldt, David, and Shapiro, A.M., 1997, A graphical-user interface for the U.S. Geological Survey SUTRA code using Argus ONE: U.S. Geological Survey, Open-File Report 97-421, 106 p.

Voss, C. I., Souza, W. R., 1987, Variable density flow solute transport simulation of regional aquifers containing a narrow freshwater-saltwater transition zone, Water Resources Research 23(10), 1851-1866.

Winston, R. B., 1999, Upgrade to MODFLOW-GUI: Addition of MODPATH, ZONEBDGT, and additional MODFLOW packages to the U.S. Geological Survey MODFLOW-96 graphical-user interface: U.S. Geological Survey Open-File Report 99-184, 63p.

Winston, R. B., 2001, Programs for Simplifying the Analysis of Geographic Information in U.S. Geological Survey Ground-Water Models : U.S. Geological Survey Open-File Report 01-392, 67p.

Yeh, G. T., 1999, Computational Subsurface Hydrology: Fluid Flows, Kluwer Academic Publishers, Boston, 277p.

Yeh, G. T., 2000, Computational Subsurface Hydrology: Reactions, Transport, and Fate, Kluwer Academic Publishers, Boston, 344p.

Yeh, G. T., Chang, J. R., and Short, T. E., 1992, An exact peak capturing the oscillation free scheme to solve advection-dispersion transport equations, Water Resources Research, 28(11), 2937-2951.

Yeh, G. T., Chang, J. R., Cheng, H. P., and Sung, C. H., 1995, An adaptive local grid refinement based on the exact peak capture and oscillation free scheme to solve transport equations., Comp. And Fluids, 24(3), 293-332.

Yeh, G. T., Cheng, J. R. and Cheng, H. P., 1994, 3DFEMFAT: User's Manual of a 3-Dimensional Finite Element Model of Flow and Transport through Saturated-Unsaturated Media, technical report, Department of Civil and Environmental Engineering, the Pennsylvania State University, University Park, PA 16802.

Yeh, G. T., Cheng, J. R., and Short, T. E., 1997, 3DFATMIC: User's Manual of a Three-Dimensional Model of Subsurface Flow, Fat and Transport of Microbes and Chemicals. EPA/600/R-97-053. National Risk Management Research Laboratory, U.S. E.P.A., Ada, OK 74820

Yeh, G. T., Hansen, S. S, Lester, B., Strobl, R. and Scarbrough, J., 1992, 3DFEMWATER/3DLEWASTE: Numerical Codes for Delineating Wellhead Protection Areas in Agricultural Regions Based on the Assimilative Capacity Criterion, U.S. Environmental Protection Agency.

APPENDIX A

CD-ROM - SYSTEM REQUIREMENTS AND INSTALLATION

System Requirements

The FEMWATER-GUI has been developed only for computers operating under Windows 98 and Windows NT. The user must have the Windows version of Argus Open Numerical Environments (Argus ONE). However, the evaluation mode edition is included on CD-ROM allowing the user to install it on PC. This mode is fully functional but the user can not save or print the projects and export is limited to 625 elements. Additional information about Argus ONE and FEMWATER-GUI can be found on the WWW site http://www.argusint.com and http://www.geo.tu-freiberg.de/~hardy/fwgui.html.

Operation of Argus ONE requires at least CPU Pentium, Pentium Pro recommended with 32 MB of RAM, 7 MB of free disk space and an SVGA video card capable of displaying 65,000 colors. In addition, the FEMWATER-GUI requires a display with a resolution of at least 632 × 590.

Installation

The CD-ROM contains the following programs for use in conjunction with FEMWATER-LHS model.

Files required for installation	Location to install
FWGUI30.dll	<Argus directory>\ArgusPIE\FWGUI30
femwater_lewaste_lhs.met	<Argus directory>\ArgusPIE\FWGUI30
FEMWATER_List.dll	<Argus directory>\ArgusPIE\List
FEMWATER_GetMyDirectory.dll	<Argus directory>\ArgusPIE\GetMyDirectory
BIN2ASC.exe	<Argus directory>\ArgusPIE\GetMyDirectory
CALSTATS.exe	<Argus directory>\ArgusPIE\GetMyDirectory
PCCSRCP.exe	<Argus directory>\ArgusPIE\GetMyDirectory
EditContoursPie.dll	<Argus directory>\ArgusPIE\EditContours

All the files used by the PIE should be placed in the ArgusPIE directory or in subdirectories under the ArgusPIE directory. Unless otherwise noted, it is generally a good idea to place each PIE in its own subdirectories under the ArgusPIE directory.

The export templates used by the PIE (femwater_lewaste_lhs.met) should be placed in the same directory as the FEMWATER PIE (FWGUI30.dll).

The executable version of FEMWATER-LHS (FEMWLHS.EXE) is assumed to be located in a directory with the pathname C:\FEMWATER\; the full pathname of the executable for FEMWATER-LHS is assumed to be C:\FEMWATER\FEMWLHS.EXE.

The source code is also included in the CD-ROM in two main directories FEMWLHS_CODE and FWGUI30_CODE which contains the following files FEMWATER-LHS and FEMWATER-GUI files, respectively.

APPENDIX B

STEP-BY-STEP APPLICATIONS OF THE FEMWATER-LHS

Steady Two-Dimensional Drainage Problem

1. Double-click on the Argus ONE icon to open Argus ONE.
2. From the PIEs menu found along the top of the window, select, **New FEMWATER Project....** This brings up the *FEMWATER-LHS Type of Simulation Problem* window.
3. Here, the type of problem to be simulated is chosen. To select the type of **CROSS-SECTIONAL** click on check box and then click **Continue.** The *FEMWATER-LHS Model* dialog appears.
4. This window allows the user to specify values for the FEMWATER simulation that are not spatially variable. This dialog can be get again at any time by selecting **PIEs|Edit Project Info**. Rather than making changes here now, accept the default values by clicking **OK**. This brings up a new *Argus* ONE *window,* called "untitled1".
5. This is the window in which the model will be designed, run, and evaluated. It contains many layers in a stack; each layer will hold either model or mesh information. Additionally, another window (Fig. B.1), the *Layer List window* (also called "Layer Floater") appears, in which the user can see which layers are available. This window may be resized to display the full layer names.

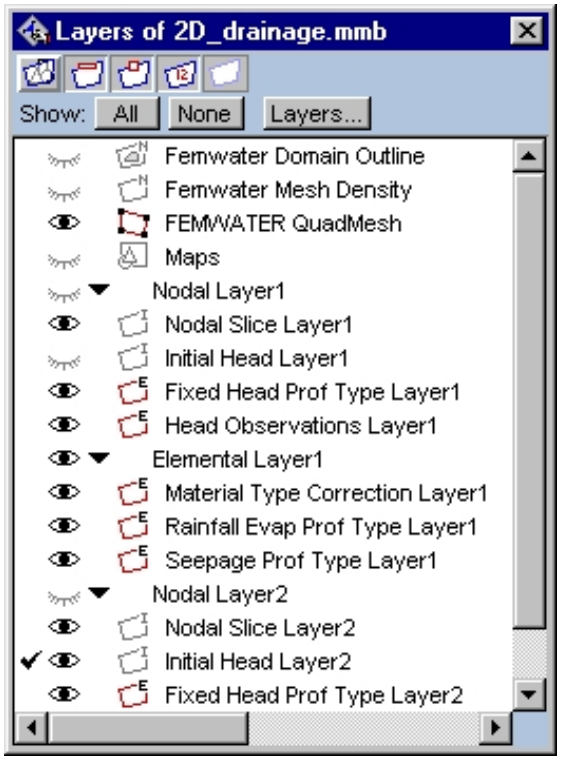

Fig. B.1 *Layer List Window*

The *Layer List window* shows which information layers are available for the particular problemtype, i.e. **Nodal Elevation Layer[i] or Nodal Slice Layer[i], Initial Head Layer[i], Material Type Correction Layer[i]**, etc. The window allows the user to control which of the layers will be visible (those with the open eye) and which layer is on top of the stack and thus available for input from the screen. Clicking on an 'eye' toggles the layer visibility, and clicking to the left of an 'eye' makes the layer 'active' (i.e. brings the layer to the top of the stack) and puts a 'check mark' next to the active layer.

6. To create a rectangular uniform elements. It is possible to read a ***Grid*** (rectangular uniform elements) into ***FEMWATER Quadmesh*** directly. However, mesh BandWidth can be minimized once the mesh is imported. A text file (e.g. *2D_drainage_mesh.exp*) containing 100 elements and 121 nodes was used to represent the flow region. Activate the ***FEMWATER Quadmesh*** by clicking to the left of its 'eye' in the *Layer List window.* Import *2D_drainage_mesh.exp* into the project by selecting **File|Import FEMWATER QuadMesh...|Text File**. In CD-ROM, the *2D_drainage_mesh.exp* file is located in a directory with the pathname examples\application_1\app1_import_files\.

7. To specify a constant slice position, or default slice position for the nodal of layer, the **Layers dialog** must be used. Moving the cursor to the *Layers...* button in the floating layers window and clicking, opens the Layers dialog. The list at the top of the dialog is the list of layers. Highlighting the layer under consideration, in this case **Nodal Slice Layer2**, in that list by clicking it with the cursor shows the parameters associated with that information layer in the table at the bottom of the dialog box. Moving the cursor to the **Value** column and clicking ***fx*** the *expression* box to appear. Just type 10 in the *expression* box and clicking **OK** exits the *expression* dialog.

8. To modify the non-spatial data (i.e. boundary conditions profile types and material correction types) in this project. Select **PIEs|Edit Project Info**, the *FEMWATER-LHS Model* dialog will appear.

9. Click on *Material and Soil Properties* tab to activate material correction by clicking *Material type correction* check box and set the following parameters:

   On *Correction Cond/Perm* tab, set

N	xx	yy	Zz	xy	xz	yz
1	0.06	0.0	0.06	0.0	0.0	0.0

   On *Correction Soil Prop* tab, set

N	Res MC	Sat MC	P Head	VG Alpha	VG Beta
1	0.034	0.046	0.0	1.6	1.37

10. Click on the *Boundary Conditions|Dirichlet* tab to activate fixed head profile type by clicking *Fixed Head* check box. Enter the values of the profile. Specify 2 m for the head in unlimited time, enter the same values of **Head 1** and **Head 2** with 2, **Time 1** with 0 and **Time 2** with the 1.0e38.

11. Click on the *Boundary Conditions|Variable Composite* tab to activate rain fall and seepage profile type by clicking *Rainfall/Evap-Seepage* check box. Enter the values of the first profile. Specify 0.006 m/day for the rain fall in unlimited time, enter the same values of **Rf/Evap 1** and **Rf/Evap 2** with 0.006, **Time 1** with 0 and **Time 2** with the 1.0e38. Add the number of profiles by clicking on the **Add Rows** button. Enter the values of the second profile. There are the same values of **Rf/Evap 1** and **Rf/Evap 2** with 0.0 in

unlimited time (**Time 1** with 0 and **Time 2** with the 1.0e38). Thus, there are two types (number 1 and number 2) rain fall and see-page boundary conditions. Finally clicking **OK** to finish the changes.

12. To enter the Dirichlet boundary conditions into the model, activate the ***Fixed Head Prof Type Layer1***, by clicking on its 'eye' in the *Layer List window*.
13. Draw a line by first activating the contour-drawing tool. To do this, click on the small quadrilateral just below the arrow along the left side of the *Argus* ONE *window* and select the Open Contour Tool from the pop-up menu. It is the middle item. Now draw a vertical line through the nodes in bottom left of the model and assign it a **Fixed Head Prof Type** to 1.
14. To set the precise node positions using *EditContours*. Select **File|Import Femwater Domain Outline|Edit Contours**. Then select the ***Fixed Head Prof Type Layer1*** from the list of layers. The objects on the ***Fixed Head Prof Type Layer1*** will be imported into the *EditContours* PIE. Click on any node there to select it and edit it's position (Fig. B.2).

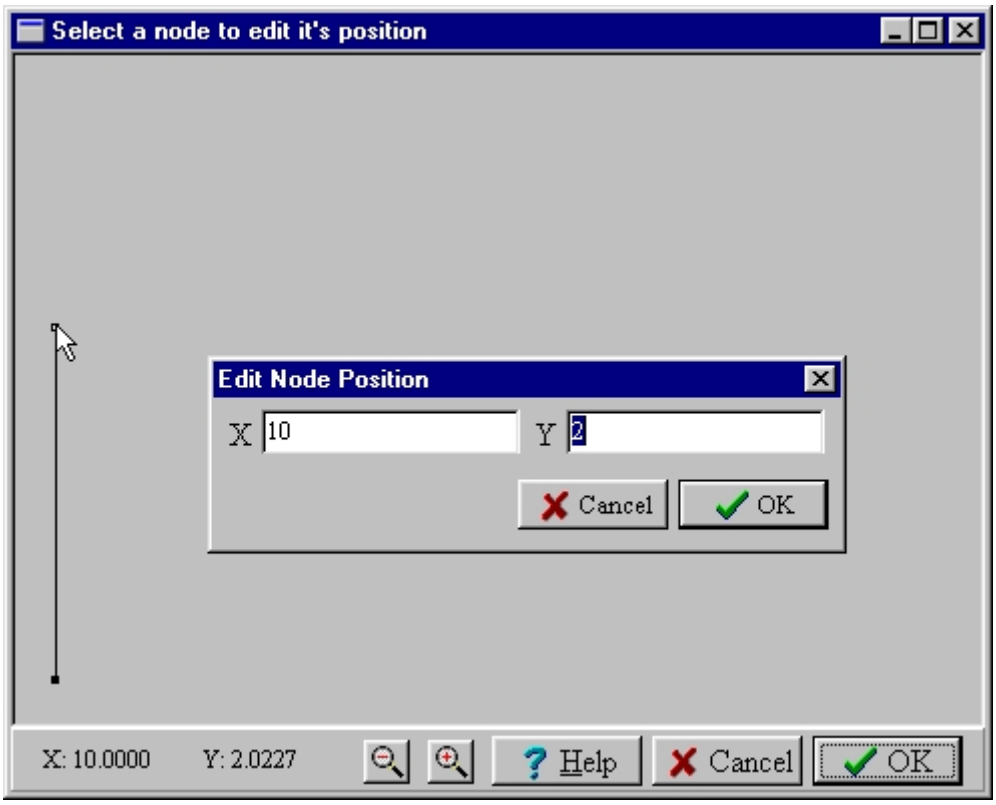

Fig. B.2 *EditContours* dialog

15. Copy this contour by pressing **Ctrl+C** or select **Edit|Copy.**
16. Activate the ***Fixed Head Prof Type Layer2***, by clicking on its 'eye' in the *Layer List window*. Select **Edit|Paste** to create this contour. Paste in the copied object by pressing **Ctrl+V** (or select **Edit|Paste**).
17. To enter the Rainfall/Evaporation boundary conditions into the model, activate the ***Rainfall Evap Prof Type Layer1***, by clicking on its 'eye' in the *Layer List window*.

18. Click on the small quadrilateral just below the arrow along the left side of the *Argus* ONE *window* and select the Open Contour Tool from the pop-up menu. It is the middle item. Draw a horizontal line through the top row elements and set:

    Rainfall Evap Prof Type = 1
    Ponding Depth = 0
    Min Pressure Head = -9000

    and click **OK**.

19. To enter the Seepage boundary conditions into the model, activate the ***Seepage Prof Type Layer1***, by clicking on its 'eye' in the *Layer List window*.
20. Draw a vertical line through the 8 elements on the left edge of the model and set:

    Seepage Prof Type = 2
    Ponding Depth = 0
    Min Pressure Head = -9000

    and click **OK**.

21. To enter the material correction type into the model, activate the ***Material Type Correction Layer1***, by clicking on its 'eye' in the *Layer List window*.
22. Click on the small quadrilateral just below the arrow along the left side of the *Argus* ONE *window* and select the Close Contour Tool from the pop-up menu. It is the first item. Draw a polygon through the 3 rows of element on the top of the model and assign it a **Material Type** to 1.
23. Save the project so far by clicking **File**, and then **Save As...**. Select the desired directory and type in the desired name (e.g. *2D_drainage*) and then click on **Save**. A project file called *2D_drainage.mmb* is created in the directory you chose, and the window name becomes the same, as shown in Fig. B.3.
24. The model information entered now needs to be exported from Argus ONE creating input files that FEMWATER-LHS requires, and the simulation can then be run. (Note that the ***FEMWATER QuadMesh*** layer must be active in order to export.) In the **PIEs** menu, select **Run FEMWATER**. The **Run FEMWATER** dialog box appears.

    The full paths to the executables should be displayed in edit-boxes on the FEMWATER Path the **Run FEMWATER** dialog box. If the executable for the chosen model is not at the location specified in the edit-box, the background of the edit-box and the status bar will change to red and a warning message will be displayed in the status bar to indicate that the path is incorrect. Normally, the user should correct the path before attempting to create the input files. Although it is possible to export the input files using an incorrect path. *Argus* ONE will not be able to start the model if the path is incorrect. Type the correct path or click on the Browse button to set the correct path. When a model is saved, the paths for all of the models will be saved in a file named *Femwater_lewaste_lhs.ini* in the directory containing the FEMWATER PIE. *Femwater_lewaste_lhs.ini* will be read whenever a new FEMWATER project is created or an old one is read so that the model paths do not need to be reset frequently. In this windows also allows the user to choose only creation of FEMWATER-LHS input files, or both creation of files and running of FEMWATER-LHS (which is already selected). Click **OK** to proceed. An *Enter export file name window* appears.

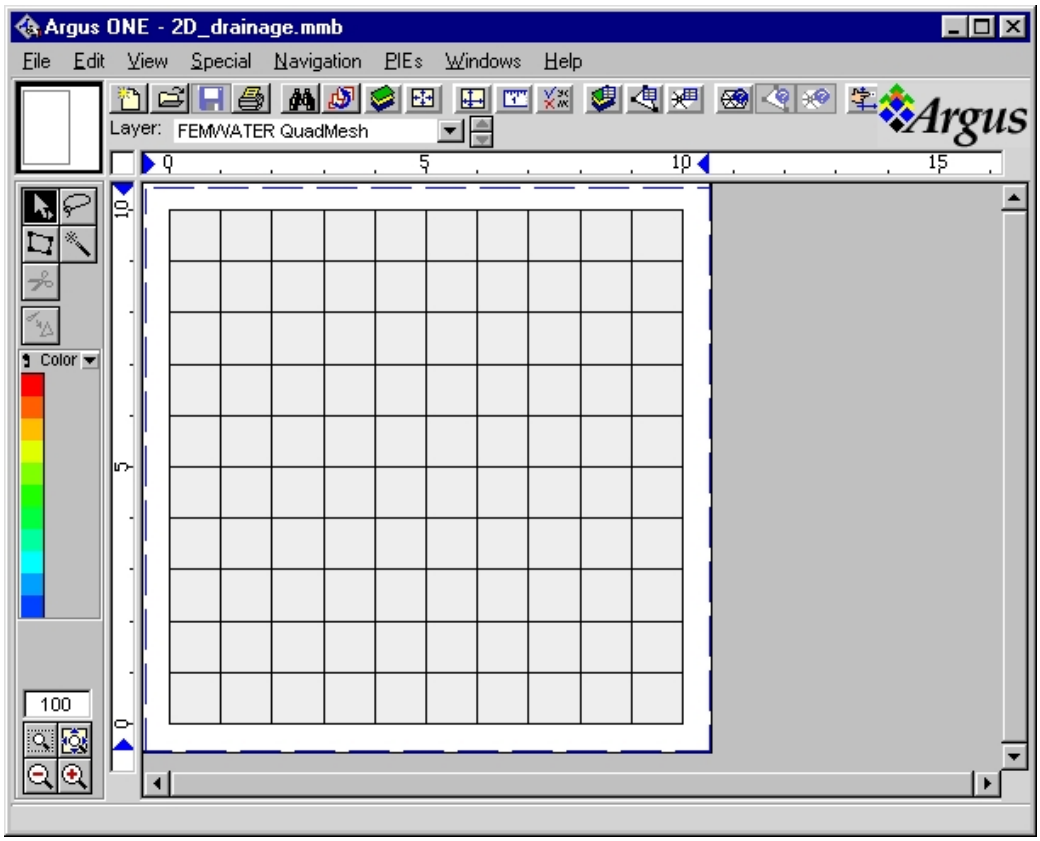

Fig. B.3 FEMWATER Mesh in Steady Two-Dimensional Drainage Problem

25. Select the directory into which the FEMWATER-LHS input files will be placed by Argus ONE. Then select the name of the files by typing in the space next to **File Name** (e.g. *2D_drainage*). The files created will all begin with the name entered here. Note, ignore the **Save as type** box.

26. Click on **Save** and the export takes place while the barber pole is visible, and then the FEMWATER-LHS simulation is run while the DOS window is visible.

27. To visualize the results, select **PIEs|FEMWATER Post Processing**. The Select Data Set window appears (Fig. B.4). Chose the type of FEMWATER output file to be read by clicking on *FEMWATER (Head)* check box, and click **Select Data Set**. Find the directory selected above for the FEMWATER files and double-click the appropriate "*.hef" file (e.g. *2D_drainage.hef*). This brings up the *FEMWATER Post-Processing* window (Fig. B.5). This window contains a list of all results available from FEMWATER simulation for visualization. Because the simulation was steady-state conditions, only one time step appears, select **Contour Map** from the list of chart types. Then click **OK** and the plots are created.

28. Because the ***FEMWATER QuadMesh*** layer was active, the plots appear below the mesh. Bring the plots to the top of the stack by activating the ***FEMWATER Post Processing Charts*** layer click left of the 'eye' in the *Layer List window*).

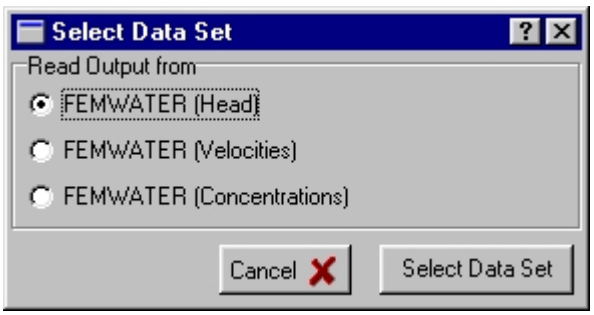

Fig. B.4 Select Data Set dialog.

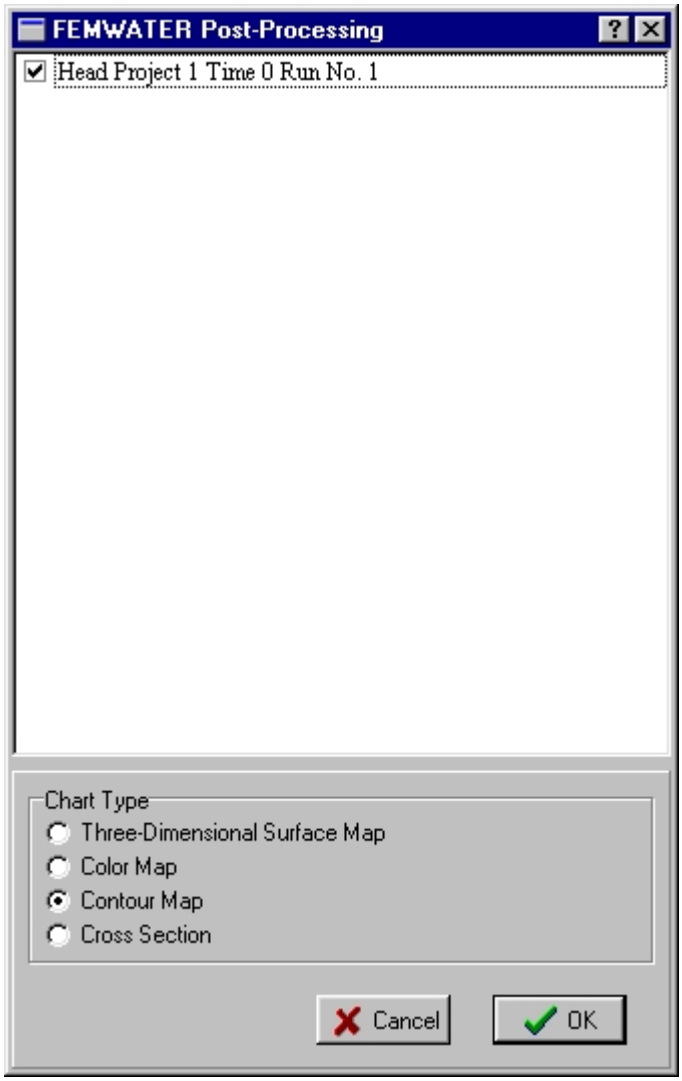

Fig. B.5 FEMWATER Post Processing dialog.

29. The plot appears, but is too cluttered because the mesh is also visible. Make the mesh invisible by clicking on the 'eye' next to ***FEMWATER QuadMesh*** in the *Layer List window.* A plot of head contours, similar to that in Fig. B.6 is visible.
30. Save the current state of the project by selecting **File**, and then **Save**.

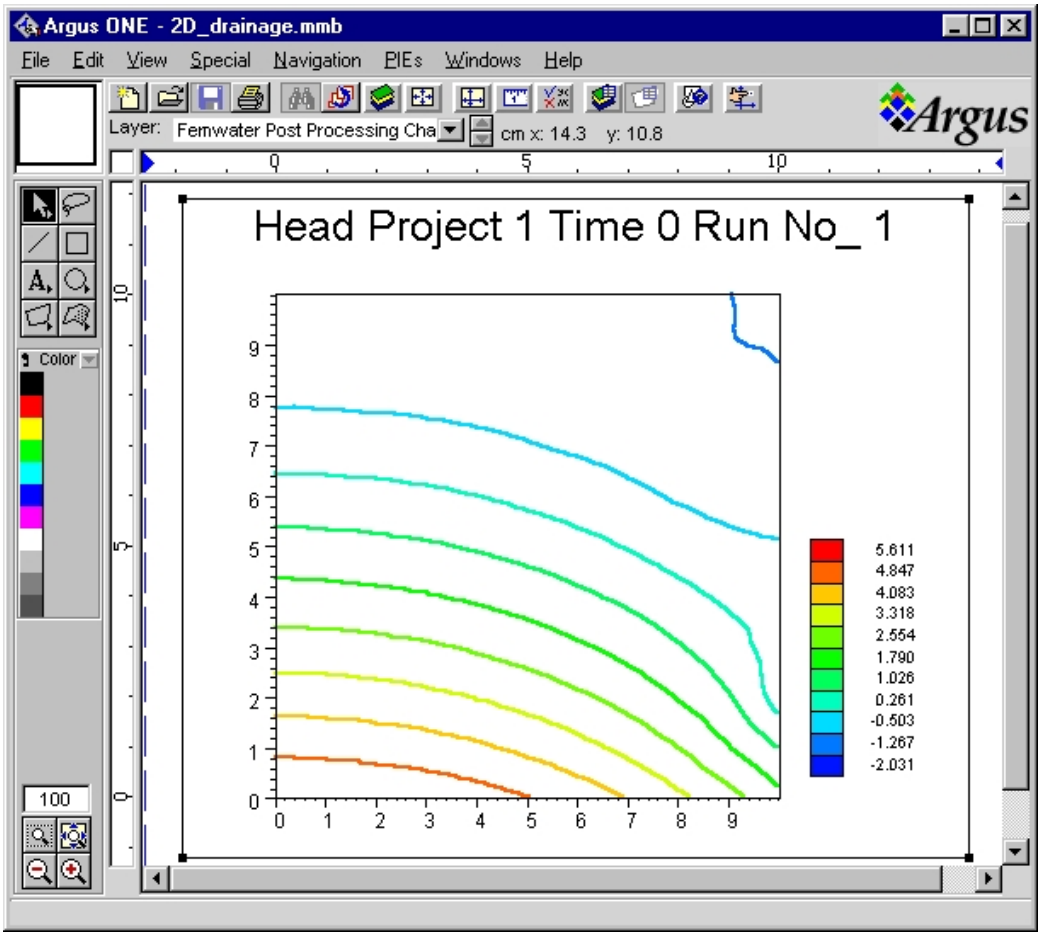

Fig. B.6 Head Plot in Steady Two-Dimensional Drainage Problem

31. The Argus ONE application may now be closed by selecting **File**, and then **Quit**. The same state that the project was left in will be reproduced when the project is reopened in Argus ONE at any later time.

Steady Two-Dimensional Drainage Problem (LHS mode)

1. Double-click on the Argus ONE icon to open Argus ONE.
2. Select **File**, then **Open...,** to bring back the project that was saved in the above case. In the *Choose file to open: window* that appears, move to the appropriate directory and double click on the ".mmb" project file that was saved in the above case (e.g. *2D_drainage.mmb*). This returns the user environment to the same state as when the project was previously saved (Fig. B.6).
3. To set this simulation, the FEMWATER-LHS Non-Spatial Information must be modified. Brings up this dialog by using **PIEs**, then **Edit Project Info ...**.
4. On *Model Title and Type* tab, change the Project Number by setting **NPROB** = 2 and click on *Latin Hypercube Sampling Simulation* check box, to change the type of simulation.
5. Click on the tab along the top of dialog that read, *Latin Hypercube Sampling*. Set the **Number of Runs** to 50. In order that the simulation will be run 50 times with the 50 sets of variable.

6. To enter the data directly in the table, click on the *Variables* tab (Fig. B.7). For *Variable Name, Correlated, Material Type* and *Distribution Type* select a cell and then click in it or press the **Enter** key on the keyboard to display a list of choices. For the other columns, just select the cell and type the data. The **Add** button can be used to add a new variable to the end of the list of variables. To delete a variable from the list, the cursor is moved to the table listing the variables. Clicking the row in the table highlights the information and then clicking the **Delete** button removes the variable from the list. Clicking the **Insert** button adds a variable below the highlighted variable. In this case assume that all soil hydraulic parameters for the two material types (e.g. default and correction(1)) have a

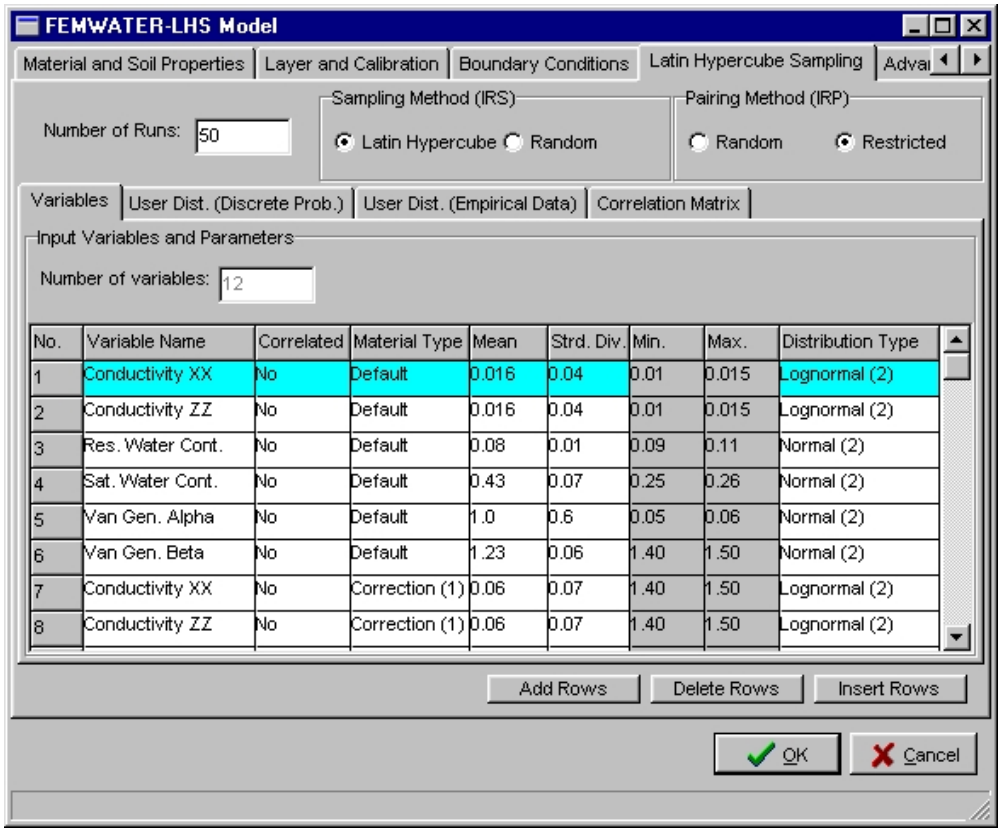

Fig. B.7 *Latin Hypercube Sampling* tab dialog

probabilistic distributions. Set the following parameters:

N	**Variable Name**	**Correlated**	**Mat. Type**	**Mean**	**Std Dev**	**Distribution Type**
1	Conductivity XX	No	Default	0.0168	0.0456	Lognormal (2)
2	Conductivity YY	No	Default	0.0168	0.0456	Lognormal (2)
3	Res. Water Cont.	No	Default	0.089	0.01	Normal (2)
4	Sat. Water Cont.	No	Default	0.43	0.07	Normal (2)
5	V. G. Alpha	No	Default	1	0.6	Normal (2)
6	V. G. Beta	No	Default	1.23	0.06	Normal (2)
7	Conductivity XX	No	Correction (1)	0.06	0.0792	Lognormal (2)
8	Conductivity YY	No	Correction (1)	0.06	0.0792	Lognormal (2)
9	Res. Water Cont.	No	Correction (1)	0.034	0.01	Normal (2)
10	Sat. Water Cont.	No	Correction (1)	0.46	0.11	Normal (2)
11	V. G. Alpha	No	Correction (1)	1.6	0.7	Normal (2)
12	V. G. Beta	No	Correction (1)	1.37	0.05	Normal (2)

7. Click **OK** to exit the dialog. Save the project (e.g. to 2D_drainage_lhs.mmb).
8. To export and run, activate the ***FEMWATER QuadMesh*** layer again bringing the mesh to the top of the stack. Select **PIEs**, and then **Run FEMWATER**.
9. Click **OK** in the *Run FEMWATER window*, and Select the directory into which the FEMWATER-LHS input files will be placed and select the name of the new files that will run the LHS mode simulation (e.g. *2D_drainage_lhs*). Note, ignore the **Save as type** box. Click on **Save** to export and run.
10. The results can be analyzed in statistically. However, the results can be visulaized. From the **PIEs** menu select **FEMWATER Post Processing**. Click on **FEMWATER (Head)** check box in the select data file dialog and click **Select Data Set**. Find the directory selected above for the FEMWATER files and double-click the appropriate "*.hef" file (e.g. *2D_drainage_lhs.hef*). The *FEMWATER Post-Processing* window will be appear. Select the data file and select *Contour Map* from the list of chart types. Then click **OK** and the plots are created.

Transient Two-Dimensional Drainage Problem

1. Double-click on the Argus ONE icon to open Argus ONE.
2. Select **File**, then **Open...,** to bring back the project that was saved in the above case. In the *Choose file to open: window* that appears, move to the appropriate directory and double click on the ".mmb" project file that was saved in the above case (e.g. *2D_drainage.mmb*). This returns the user environment to the same state as when the project was previously saved.
3. In this case the region consist only one material type. There is no material correction exist. To modify this information, brings up the FEMWATER-LHS Non-Spatial Information dialog by using **PIEs**, then **Edit Project Info ...**.
4. On *Model Title and Type* tab, set **NPROB =** 3.
5. To change the type of solution, click on *Run Control* tab and click *Transient State Solution* check box.
6. The transient simulation will be performed for 50 time steps. The initial time step size is 0.25 day and each subsequent time step size is increased with a multiplier of 2.0 with the maximum time step size of less than or equal to 32 days. The pressure head tolerance for nonlinear iteration is 2×10^{-3} m. The relaxation factor for the nonlinear iteration is set equal to 0.5. To input this information, click on *Time Control* tab and set:

   NTI = 50
   TMAX = 2000
   DELT = 0.25
   CHNG = 2.0
   DELMAX = 32

   and click **OK**.

7. To delete or inactivate the material correction, click on *Material and Soil Properties* tab and then clicking *Material type correction* check box.
8. In this simulation the initial conditions were used the steady state solution resulting from zero flux on the top. However, this solution is already done that so it can be just import those contours. Activate the ***Initial Head Layer1***, by clicking on its 'eye' in the *Layer List*

window. Import *2D_drainage_init.exp* into the project by selecting **File|Import Initial Head Layer1|Text File**, and then select *2D_drainage_init.exp*.

9. Copy this contour by pressing **Ctrl+C** or select **Edit|Copy.**
10. Activate the ***Initial Head Layer2***, by clicking on its 'eye' in the *Layer List window*. Select **Edit|Paste** to create this contour. Paste in the copied object by pressing **Ctrl+V** (or select **Edit|Paste**).
11. Save the project (e.g. to *T_2D_drainage.mmb*).
12. Export and run FEMWATER-LHS.
13. Then, from the **PIEs** menu, select **FEMWATER Post Processing** and then reselect the "hef" file (e.g. *T_2D_drainage.hef*). There are 50 time steps, but choose only the last time step, Time 2852.4 Select **Contour Map** and click the **OK**. A plot of head contours, similar to that in Fig. B.8 is visible.

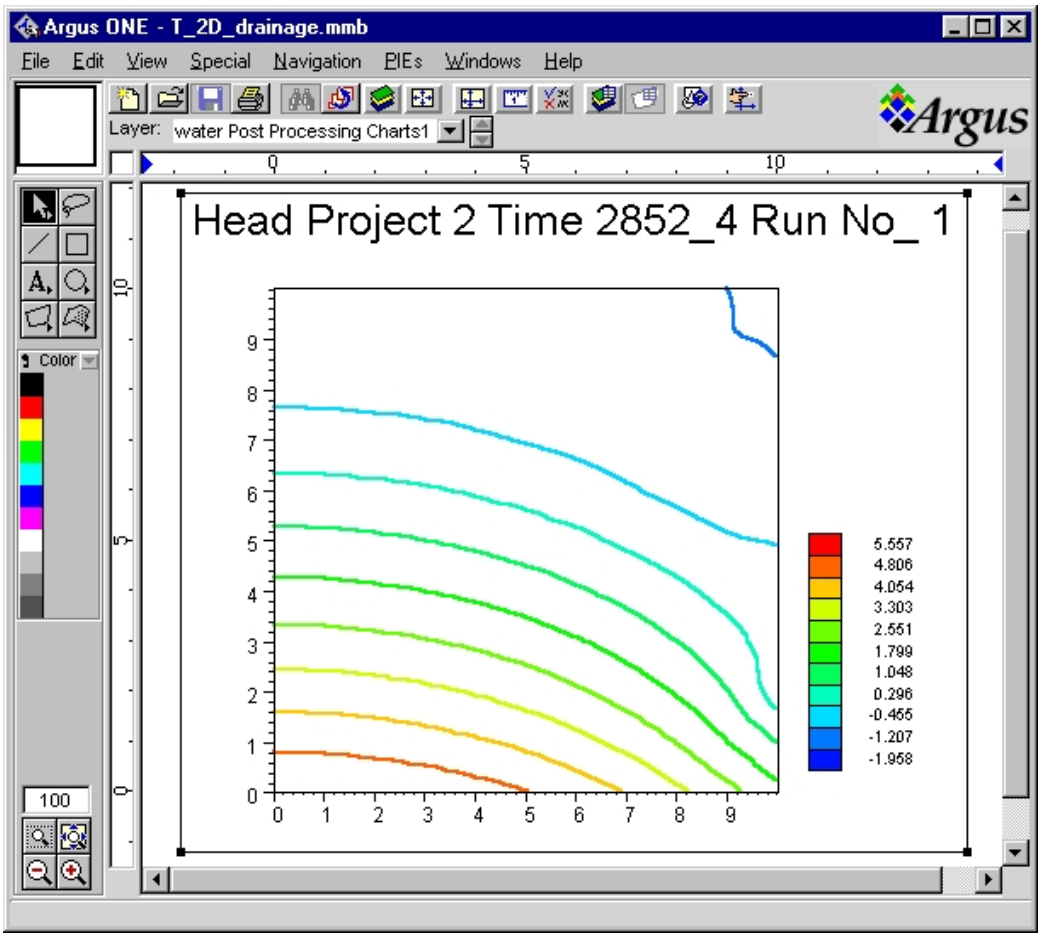

Fig. B.8 Head Plot in Transient Two-Dimensional Drainage Problem

Transient Two-Dimensional Drainage Problem (LHS mode)

1. Start Argus ONE. Open the ".mmb" project file that was saved in the above case (e.g. *T_2D_drainage.mmb*).

2. Select **PIEs**, then **Edit Project Info ...** to modify the the FEMWATER-LHS Non-Spatial Information.

   On *Model Title and Type* tab, set **NPROB** = 4 and click *Latin Hypercube Sampling Simulation* check box

   On *Latin Hypercube Sampling* tab, set the **Number of Runs** to 32

   On *Latin Hypercube Sampling|Variables* tab, set the following parameters:

N	**Variable Name**	**Correlated**	**Mat. Type**	**Mean**	**Std Dev**	**Distribution Type**
1	Conductivity XX	No	Default	0.0168	0.0456	Lognormal (2)
2	Conductivity YY	No	Default	0.0168	0.0456	Lognormal (2)
3	Res. Water Cont.	No	Default	0.089	0.01	Normal (2)
4	Sat. Water Cont.	No	Default	0.43	0.07	Normal (2)
5	V. G. Alpha	No	Default	1	0.6	Normal (2)
6	V. G. Beta	No	Default	1.23	0.06	Normal (2)

   Then click **OK**.

3. Save the project (e.g. to T_2D_drainage_LHS.mmb).
4. Export and run FEMWATER-LHS.
5. Uncertainty and sensitivity analysis of the input and the output variables.

Steady Three-Dimensional Pumping Problem

1. Start Argus ONE. In the *FEMWATER-LHS Type of Simulation Problem* window, select a **Areal** orientation. Then click **Continue**.
2. In the FEMWATER-LHS dialog, a number of changes to the initial default values are required.

   On *Model Title and Type* tab, set **NPROB** = 5

   On *Material and Soil Properties* tab, click *Material type correction* check box and click *Add Rows* button to add the number of correction material. Set the following parameters:

   On *Cond/Perm* tab, set

xx	**yy**	**zz**	**xy**	**xz**	**yz**
0.3144	0.3144	0.3144	0.0	0.0	0.0

   On *Soil Prop* tab, set

Res MC	**Sat MC**	**P Head**	**VG Alpha**	**VG Beta**
0.1	0.39	0.0	5.8	1.48

   On *Correction Cond/Perm* tab, set

N	**xx**	**yy**	**zz**	**xy**	**xz**	**yz**
1	1.0608	1.0608	1.0608	0.0	0.0	0.0
2	7.128	7.128	7.128	0.0	0.0	0.0

On *Correction Soil Prop* tab, set

N	**Res MC**	**Sat MC**	**P Head**	**VG Alpha**	**VG Beta**
1	0.065	0.41	0.0	7.5	1.89
2	0.045	0.43	0.0	14.5	2.68

On *Layer and* Calibration tab, click **Add** button 9 times to set the number of elemental layers to 10 or the number of nodal layers to 11.

On the *Boundary Conditions*|*Dirichlet* tab, click *Fixed Head* check box and then click **Add Rows** button to add the number of profile. Set the profiles as follows:

N	**Time 1**	**Head 1**	**Time 2**	**Head 2**
1	0.0	60.0	1.0e38	60.0
2	0.0	30.0	1.0e38	30.0

3. In the *Argus* ONE *window*, select **Special|Scale and Units...** and set **Uniform Scale:** = 50. That it reads "Every 1 cm on the screen represents 50 units in the real world in both the x and y direction".
4. Activate the ***Femwater Domain Outline*** layer and draw a model boundary with the contour-drawing tool. Try to create a square outline with 1000 m wide and 400 m high. Then, double-click on the location desired for the last vertex. The *Contour Information dialog* appears. Here the desired typical size of finite elements to be created by the mesh generator is specified. Type 40 in the space below the label, **Value**. This sets the desired width of an element to 40 in the units shown in the rulers around the periphery of the workspace. Click **OK** to exit the window.
5. To set the precise node positions using *EditContours*. Select **File|Import Femwater Domain Outline|Edit Contours**. Then select the ***Femwater Domain Outline*** layer from the list of layers. The objects on the ***Femwater Domain Outline*** layer will be imported into the *EditContours* PIE. Click on any node there to select it and edit it's position.
6. To copy the boundary and to convert it to an open contour. Activate the ***Femwater Domain Outline*** layer. Then use the lasso tool to outline all the cells that define where the constant head boundary ought to be (i.e. the left two cells). The selected cells will change from black squares to hollow squares. Copy them to the clipboard (**Edit|Copy**). Activate the ***Fixed Head Prof Type Layer1*** and paste the copied object by select **Edit|Paste**. A single open contour where the constant head boundary should be. Double click on it to bring up the *Contour Information dialog*. Set **Fixed Head Prof Type** = 1. Click **OK**.
7. Repeat step 6 to copy the other open contour (i.e. the right two cells) in ***Fixed Head Prof Type Layer1***.
8. To copy all open contours in constant head boundary layers (i.e. ***Fixed Head Prof Type Layer2*** through ***Fixed Head Prof Type Layer11***). Select **Edit|Select All** and then select **Edit|Copy**. Activate the ***Fixed Head Prof Type Layer2*** and select **Edit|Paste**. Paste the copied object to the remaining layers (i.e. ***Fixed Head Prof Type Layer3*** through ***Fixed Head Prof Type Layer11***).

9. Copy object in ***Femwater Domain Outline*** layer into ***Material Type Correction Layer6***. Double click on it to bring up the *Contour Information dialog*. Set **Material Type** = 1. Click **OK**.
10. Copy this object into ***Material Type Correction Layer7*** and ***Material Type Correction Layer8***.
11. Again copy this object into ***Material Type Correction Layer9*** and ***Material Type Correction Layer10***. But set those **Material Type** = 2.
12. Activate the ***Fixed Head Prof Type Layer1***. Click on the **Closed Contour** button and hold the mouse button down until a pop-up menu appears. Select the bottom selection which is the point tool. Click in the center of the model. A *Contour Information dialog* will appear. Set **Fixed Head Prof Type** = 2. Click **OK**.
13. Set the precise node positions of this point (i.e. **X** = 540 and **Y** = 400) using *EditContours*.
14. Copy this point into ***Fixed Head Prof Type Layer2*** and ***Fixed Head Prof Type Layer3.***
15. To force this point on the node, copy it into ***Femwater Domain Outline*** layer. Double click on it to bring up the *Contour Information dialog*. Set **elemen_size** = 40. This sets the desired width of an element to 40 in the units shown in the rulers around the point. Click **OK**.
16. Activate the ***FEMWATER QuadMesh*** layer. Click on the 'magic wand' found along the left side of the *Argus* ONE *window* near the arrow, and then click the magic-wand cursor inside the model boundary just drawn. An irregular finite element mesh containing elements of about 40 size is generated and displayed. Fig. B.9 shows the type of mesh that may be expected.

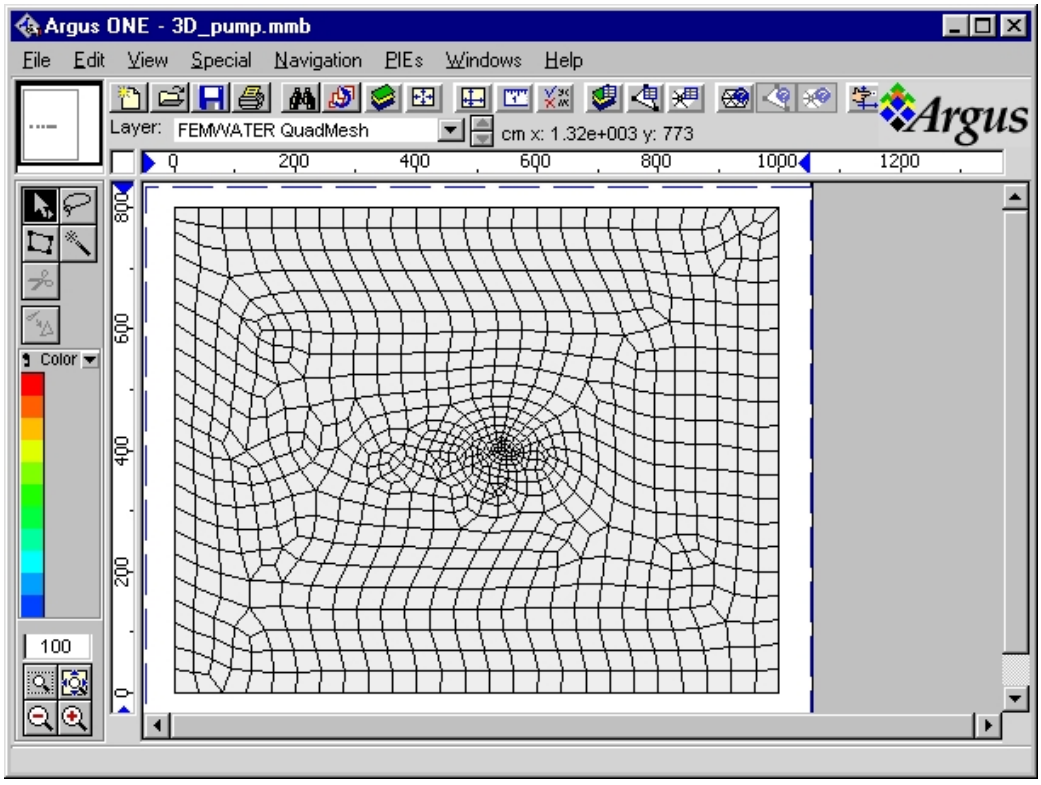

Fig. B.9 FEMWATER Mesh in Steady Three-Dimensional Pumping Problem

17. The band-width of a newly-generated mesh always needs to be reduced. Select the **Special** menu long the top of the *Argus* ONE *window*, then select **Renumber...**. This brings up the **Renumber window**. In this window click on **Optimize Bandwidth** and then **OK**. The mesh numbering is then optimized for the matrix solver currently used by FEMWATER-LHS.
18. Specify a constant elevation, or default elevation using the **Layers dialog**. In this case, enter 15, 30, 35, 40, 45, 50, 55, 60, 66, 72 in the **Expression dialog** for **Nodal Elevation Layer2** through **Nodal Elevation Layer11** respectively.
19. Specify a constant initial head, using the **Layers dialog**. In this case, enter 60, 45, 30, 25, 20, 15, 10, 5, 0, -6, -12 in the **Expression dialog** for ***Initial Head Layer1*** through ***Initial Head Layer11*** respectively.
20. Save the project (e.g. to *3D_pump.mmb*).
21. Export and run FEMWATER-LHS.
22. Using **FEMWATER Post Processing** in **PIEs** menu, plot pressure head for *Three-Dimensional Surface Map* type (Fig. B.10).

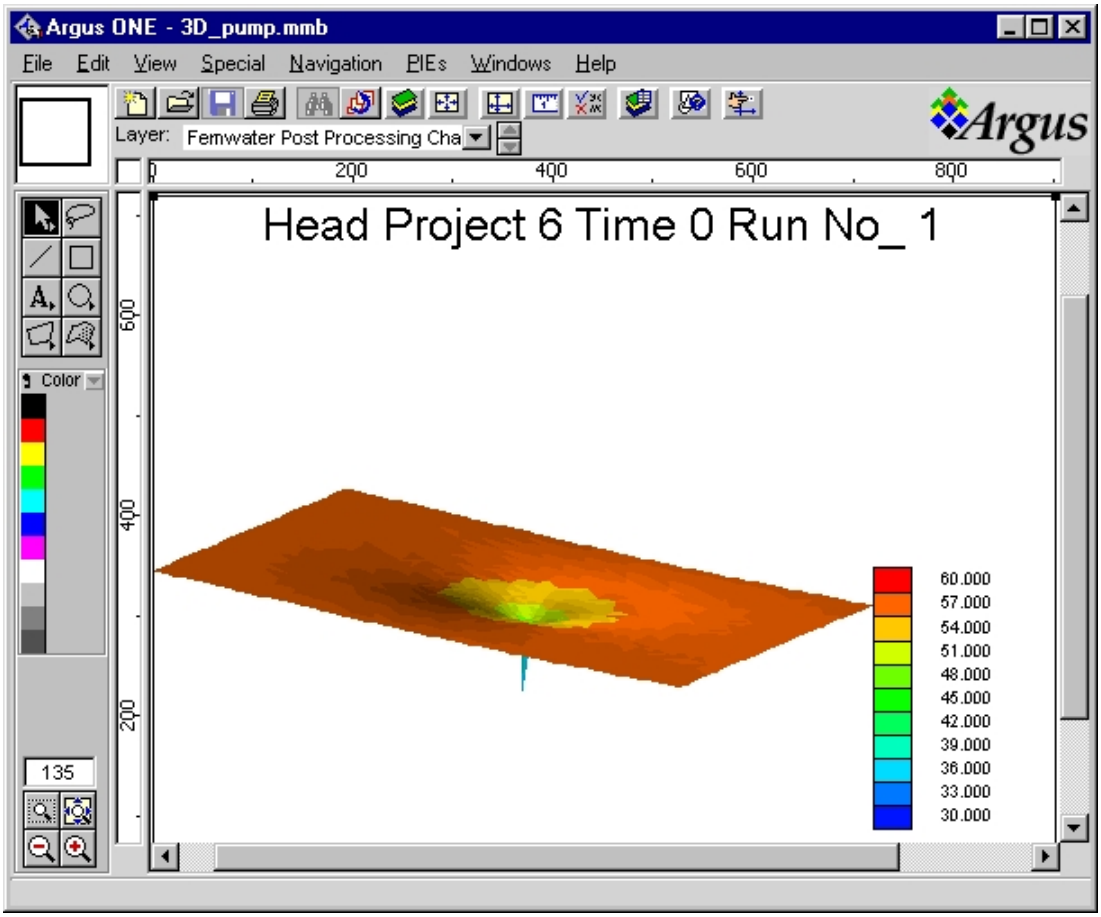

Fig. B.10 Head Surface Map in Steady Three-Dimensional Pumping Problem

Steady Three-Dimensional Pumping Problem (LHS mode)

1. Start Argus ONE. Open the ".mmb" project file that was saved in the above case (e.g. *3D_pump.mmb*).
2. Select **PIEs**, then **Edit Project Info ...** to modify the the FEMWATER-LHS Non-Spatial Information.

   On *Model Title and Type* tab, set **NPROB** = 6 and click *Latin Hypercube Sampling Simulation* check box

   On *Latin Hypercube Sampling* tab, set the *Number of Runs* to 50

   On *Latin Hypercube Sampling|Variables* tab, set the following parameters:

N	**Variable Name**	**Correlated**	**Mat. Type**	**Mean**	**Std Dev**	**Distribution Type**
1	Conductivity XX	No	Default	0.3144	0.6576	Lognormal (2)
2	Conductivity YY	No	Default	0.3144	0.6576	Lognormal (2)
3	Conductivity ZZ	Yes	Default	0.3144	0.6576	Lognormal (2)
4	Res. Water Cont.	Yes	Default	0.1	0.01	Normal (2)
5	Sat. Water Cont.	No	Default	0.39	0.07	Normal (2)
6	V. G. Alpha	Yes	Default	5.8	3.8	Normal (2)
7	V. G. Beta	Yes	Default	1.48	0.13	Normal (2)
8	Conductivity XX	No	Correction (1)	1.0608	1.3512	Lognormal (2)
9	Conductivity YY	No	Correction (1)	1.0608	1.3512	Lognormal (2)
10	Conductivity ZZ	No	Correction (1)	1.0608	1.3512	Lognormal (2)
11	Res. Water Cont.	No	Correction (1)	0.065	0.02	Normal (2)
12	Sat. Water Cont.	No	Correction (1)	0.41	0.09	Normal (2)
13	V. G. Alpha	No	Correction (1)	7.5	3.7	Normal (2)
14	V. G. Beta	No	Correction (1)	1.89	0.17	Normal (2)
15	Conductivity XX	No	Correction (2)	7.128	3.744	Lognormal (2)
16	Conductivity YY	No	Correction (2)	7.128	3.744	Lognormal (2)
17	Conductivity ZZ	No	Correction (2)	7.128	3.744	Lognormal (2)
18	Res. Water Cont.	No	Correction (2)	0.045	0.01	Normal (2)
19	Sat. Water Cont.	No	Correction (2)	0.43	0.06	Normal (2)
20	V. G. Alpha	No	Correction (2)	14.5	2.9	Normal (2)
21	V. G. Beta	No	Correction (2)	2.68	0.29	Normal (2)

   On *Latin Hypercube Sampling|Correlation Matrix* tab, set the following parameters :

	3	**4**	**6**	**7**
3				
4	0.261			
6	0.952	0.392		
7	0.909	-0.113	0.787	

Then click **OK**.

3. Save the project (e.g. to *3D_pump_LHS.mmb*).
4. Export and run FEMWATER-LHS.
5. Uncertainty and sensitivity analysis of the input and the output variables.

Seawater Intrusion in Confined Aquifer

1. Start Argus ONE. In the *FEMWATER-LHS Type of Simulation Problem* window, select a **CROSS-SECTIONAL** orientation. Then click **Continue**.
2. In the FEMWATER-LHS dialog, a number of changes to the initial default values are required.

   On *Model Title and Type* tab, set **NPROB =** 7

   On *Time Control* tab, set:

   NTI = 15
   TMAX = 5000.75
   DELT = 5
   CHNG = 1.17169
   DELMAX = 500

   On *Fluid Properties* tab, set the coefficients for computing density and viscosity:

coeff. A1	Coeff. A2	coeff. A3	coeff. A4	coeff. A5	coeff. A6	coeff. A7	coeff. A8
1.0	0.0245	0.0	0.0	1.0	0.0	0.0	0.0

   On *Material and Soil Properties* tab, click *Material type correction* check box to add the correction material. Set the following parameters:

   On *Cond/Perm* tab, set

xx	yy	zz	xy	xz	yz
1.0	0.0	1.0	0.0	0.0	0.0

   On *Soil Prop* tab, set

Res MC	Sat MC	P Head	VG Alpha	VG Beta
0.1	0.35	0.0	5.8	1.48

   On *Disp/Diff* tab, set

Dist coeff.	Bulk density	Long disper.	Trans disper.	Mol diff coeff.	Turtuosity	Decay const.	Fr N/Lang SMAX
0.0	1200	0.0	0.0	0.066.	1.0	0.0	0.0

   On *Correction Cond/Perm* tab, set

N	xx	yy	zz	xy	xz	yz
1	0.5	0.0	0.5	0.0	0.0	0.0

On *Correction Soil Prop* tab, set

N	**Res MC**	**Sat MC**	**P Head**	**VG Alpha**	**VG Beta**
1	0.1	0.22	0.0	5.8	1.48

On *Correction Disp/Diff* tab, set

N	**Dist coeff.**	**Bulk density**	**Long disper.**	**Trans disper.**	**Mol diff coeff.**	**Turtuosity**	**Decay const.**	**Fr N/Lang SMAX**
1	0.0	1200	0.0	0.0	0.033.	1.0	0.0	0.0

On the *Boundary Conditions*|*Dirichlet*|*Fixed Head* tab, click *Fixed Head* check box and then click **Add Rows** button to add the number of profile. Set the profiles as follows:

N	**Time 1**	**Head 1**	**Time 2**	**Head 2**
1	0.0	100.49	1.0e38	100.49
2	0.0	100.735	1.0e38	100.735
3	0.0	100.98	1.0e38	100.98
4	0.0	101.225	1.0e38	101.225
5	0.0	101.47	1.0e38	101.47
6	0.0	101.715	1.0e38	101.715
7	0.0	101.96	1.0e38	101.96
8	0.0	102.205	1.0e38	102.205
9	0.0	102.45	1.0e38	102.45

On the *Boundary Conditions*|*Dirichlet*|*Precribed-Concentration* tab, click *Prescr-Concentration* and set the profile:

N	**Time 1**	**Conctr 1**	**Time 2**	**Conctr 2**
1	0.0	1.0	1.0e38	1.0

On the *Boundary Conditions*|*Cauchy*|*Specified-Flux* tab, click *Specified-Flux* and set the profile:

N	**Time 1**	**S-flux 1**	**Time 2**	**S-flux 2**
1	0.0	-6.6e-3	1.0e38	-6.6e-3

On the *Boundary Conditions*|*Cauchy*|*Concentration* tab, click *Concentration* and set the profile:

N	**Time 1**	**Conctr 1**	**Time 2**	**Conctr 2**
1	0.0	0.0	1.0e38	0.0

On the *Boundary Conditions*|*Variable Composite*|*Rainfall/Evap.-Seepage* tab, click *Rainfall/Evap.-Seepage* and set the profile:

N	**Time 1**	**Rf/Evap 1**	**Time 2**	**Rf/Evap 2**
1	0.0	0.0	1.0e38	0.0

On the Boundary *Conditions*|*Variable Composite*|*Rainfall/Evap*.-Seepage tab, click Concentration and set the profile:

N	**Time 1**	**Conctr 1**	**Time 2**	**Conctr 2**
1	0.0	0.0	1.0e38	0.0

Click **OK**.

3. Activate the ***FEMWATER Quadmesh*** and import *seawater_intr_mesh.exp* into the project by selecting **File|Import FEMWATER QuadMesh...|Text File**. In CD-ROM, the *seawater_intr_mesh.exp* file is located in a directory with the pathname examples\application_4\app4_import_files\
4. Activate the ***Fixed Head Prof Type Layer1*** and import *Fixed Head Prof Type Layer1.exp* into the project by selecting **File|Import Fixed Head Prof Type Layer1...|Text File**.
5. Copy this object into ***Fixed Head Prof Type Layer2***.
6. Activate the ***Material Type Correction Layer1*** and import *Material Type Correction Layer1.exp* into the project by selecting **File|Import Material Type Correction Layer1...|Text File.**
7. Activate the ***Seepage Prof Type Layer1*** and import *Fixed Head Prof Type Layer1.exp* into the project by selecting **File|Import *Seepage* Prof Type Layer1...|Text File**.
8. Copy this object into ***Seepage Prof Type Layer2***.
9. Specify a constant slice, or default nodal slice using the **Layers dialog**. In this case, enter 0 and 1 in the **Expression dialog** for **Nodal Slice Layer1** and **Nodal Slice Layer2** respectively.
10. Save the project (e.g. to *seawater_intr.mmb*).
11. Export and run FEMWATER-LHS.
12. Using **FEMWATER Post Processing** in **PIEs** menu, plot concentration at day 4943.4 for *Contour Map* type (Fig. B.11).

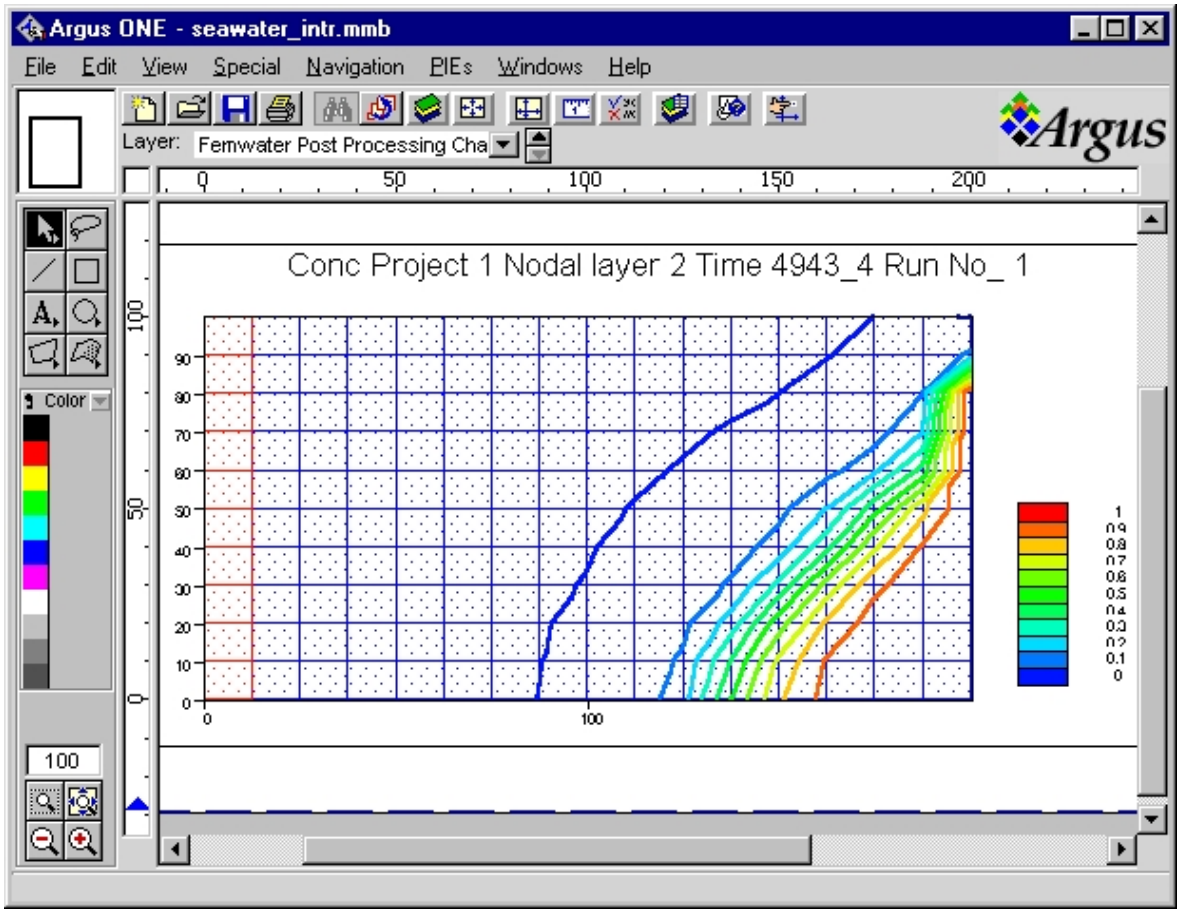

Fig. B.11 The concentration contours at the simulation time of 4943.4 days.

Seawater Intrusion in Confined Aquifer (LHS Mode)

1. Start Argus ONE. Open the ".mmb" project file that was saved in the above case (e.g. *seawater_intr.mmb*
2. Select **PIEs**, then **Edit Project Info ...** to modify the FEMWATER-LHS Non-Spatial Information.

   On *Model Title and Type* tab, set **NPROB** = 8 and click *Latin Hypercube Sampling Simulation* check box

   On *Latin Hypercube Sampling* tab, set the *Number of Runs* to 20

   On *Latin Hypercube Sampling*|*Variables* tab, set the following parameters:

N	**Variable Name**	**Correlated**	**Mat. Type**	**Min**	**Max**	**Distribution Type**
1	Conductivity XX	No	Default	0.8	1.1	Lognormal (1)
2	Conductivity ZZ	No	Default	0.8	1.1	Lognormal (1)
3	Sat. Water Cont.	No	Default	0.315	0.385	Normal (1)
4	Bulk density	No	Default	1080	1320	Normal (1)
5	Mol diff coeff.	No	Default	0.0594	0.0726	Normal (1)
6	Conductivity XX	No	Correction (1)	0.45	0.55	Lognormal (1)
7	Conductivity ZZ	No	Correction (1)	0.45	0.55	Lognormal (1)
8	Sat. Water Cont.	No	Correction (1)	0.198	0.22	Normal (1)
9	Bulk density	No	Correction (2)	1080	1320	Normal (1)
10	Mol diff coeff.	No	Correction (2)	0.0297	0.0363	Normal (1)

Then click **OK**.

3. Save the project (e.g. to *seawater_intr _LHS.mmb*).
4. Export and run FEMWATER-LHS.
5. Uncertainty and sensitivity analysis of the input and the output variables.